JPRS L/10150

1 December 1981

Translation

CHANNEL NUCLEAR ENERGY REACTOR

By

N.A. Dollezhal' and I. Ya. Yemel'yanov

FBIS FOREIGN BROADCAST INFORMATION SERVICE

NOTE

JPRS publications contain information primarily from foreign newspapers, periodicals and books, but also from news agency transmissions and broadcasts. Materials from foreign-language sources are translated; those from English-language sources are transcribed or reprinted, with the original phrasing and other characteristics retained.

Headlines, editorial reports, and material enclosed in brackets [] are supplied by JPRS. Processing indicators such as [Text] or [Excerpt] in the first line of each item, or following the last line of a brief, indicate how the original information was processed. Where no processing indicator is given, the information was summarized or extracted.

Unfamiliar names rendered phonetically or transliterated are enclosed in parentheses. Words or names preceded by a question mark and enclosed in parentheses were not clear in the original but have been supplied as appropriate in context. Other unattributed parenthetical notes within the body of an item originate with the source. Times within items are as given by source.

The contents of this publication in no way represent the policies, views or attitudes of the U.S. Government.

APPROVED FOR RELEASE: 2007/02/09: CIA-RDP82-00850R000400080004-5

JPRS L/10150

1 December 1981

CHANNEL NUCLEAR ENERGY REACTOR

Moscow KANAL'NYY YADERNYY ENERGETICHESKIY REAKTOR in Russian 1980 (signed to press 27 Mar 80) pp 11-78, 95-102, 119-123, 131-137, 182-203

[Chapters 2, 3, 5, 10, 11 and excerpts from chapter 6 from book "Channel Nuclear Energy Reactor" by N.A. Dollezhal' and I. Ya. Yemel'yanov, Izdatel'stvo Atomizdat, 2,500 copies, 208 pages]

CONTENTS

PHYSICAL CHARACTERISTICS OF THE CORE

Moscow KANAL'NYY YADERNYY ENERGETICHESKIY REAKTOR in Russian 1980 (signed to press 27 Mar 80) pp 11-47

[Chapter 2 from the book "Channel-Type Nuclear Power Reactor", by Nikolay Antonovich Dollezhal' and Ivan Yakovlevich Yemel'yanov, Scientific Research and Design Institute of Power Engineering, Atomizdat, 2,550 copies, 208 pages]

2.1. Structure of the Core

The RBMK nuclear power reactor is a heterogeneous thermal neutron channel-type reactor in which graphite is used as the moderator. The coolant-boiling light water--circulates through vertical channels that penetrate the lining of the core. This type of reactor is the latest development of uranium-graphite reactors in the USSR.

The core has the shape of a vertical cylinder 11.8 meters in diameter and 7 meters high. It is surrounded by a lateral reflector 1 meter thick and end reflectors 0.5 meter thick. The core contains the fuel elements, moderator, coolant, fuel channels and neutron absorber rods (control rods) (Figure 2.1).

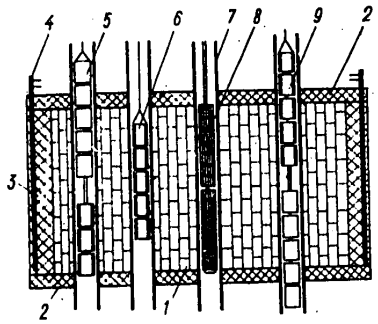

Figure 2.1. Structure of Core: 1--graphite stacking; 2--end reflector; 3--side reflector; 4--reflector cooling channel; 5--shortened absorbing rod (USP); 6--automatic regulator (AR) rod; 7--fuel channel; 8--fuel assembly; 9--manual control (RR) and safety system (AZ) rod

The graphite stacking of the reactor is 2,488 vertical columns which were assembled from blocks 250 X 250 mm in cross section with graphite density of 1.65 g/cm^3. The blocks have oblique openings 114 mm in diameter along the vertical axis that are designed for location of the fuel channels and the monitoring and control channels. Graphite rods are installed in the openings of four rows of the peripheral columns (the side reflector).

The fuel channels are located in 1,693 cells of the square lattice of the core. Part of the channel located in the core is made of a zirconium alloy and is a pipe 88 mm in diameter with wall thickness of 4 mm. Graphite rings are placed on the pipe to ensure thermal contact with the stacking blocks. The fuel assembly, which is two series-connected fuel assemblies (TVS) 3.5 meters long each, is installed inside the channel. The design gap between the TVS comprises approximately 20 mm. The TVS consists of 18 fuel rods which are attached by steel spacing lattices on a central pipe manufactured of zirconium alloy measuring 15 X 1.25 mm. Either a carrier rod 12 mm in diameter or a carrier pipe of zirconium alloy measuring 12 X 2.5 mm passes inside it. The fuel element is a pipe with outer diameter of 13.5 mm with wall thickness of 0.9 mm of zirconium alloy filled with pellets 11.5 mm in diameter of uranium dioxide with density up to 10.5 g/cm^3 and with enrichment of 1.8 or 2 percent U-235. The inner cavity of the fuel element is filled during manufacture with a mixture of argon and helium and is sealed by cathode-ray welding. Additional absorbers (DP) are installed in part of the fuel channels in the initial state.

The coolant is delivered to the bottom to each fuel channel. The economizer section of the channel in which water is heated to saturation temperature is approximately 2.5 meters high from the bottom of the core. The active boiling process occurs in its remaining part wherein the mass steam content of the coolant increases along the flow and comprises an average of 14.5 percent throughout the reactor at the output from the core.

The monitoring and control system channels are located identically to the fuel channels in the central openings of the graphite stacking columns. The square lattice for location of the 179 rods has spacing of 700 mm and is rotated by 45° with respect to the lattice of the fuel channels. The SUZ rods are functionally divided into groups that ensure radial control of the energy release field (the RR rods), automatic regulation of the mean power level (AR), scramming of a chain reaction (AZ) and regulation of the energy release field in height (USP). The rods of the first three groups are removed upward from the core and the shortened absorbing rods of the fourth group are removed downward.

The channel for the SUZ rods is made of the same zirconium alloy as the fuel channel but has diameter of 88 mm with wall thickness of 3 mm. Graphite rings are also placed on the outside of the channel. The absorbing rods are assembled from sections of the same type, articulately connected to each other. The absorbing section has a sleeve design. Boron carbide sleeves measuring 65 X 7.5 mm and with total thickness of 984 mm are enclosed in a sealed annular cavity formed by the outer pipe measuring 70 X 2 mm and by the inner pipe measuring 50 X 2 mm, the latter of which is manufactured from aluminum alloy. The RR, AR and AZ rods are assembled from five absorbing sections and have a total length of 5,120 mm; the USP are assembled from three sections with total length of 3,050 mm.

A self-contained water circuit with pump-heat exchange unit is used to cool the channels and the rods. Water moves in the channels from top to bottom and flows around the outer and inner surfaces of the absorbing rod jackets, being heated from 40 to 60°C. The inner cavity of the channels in an operating reactor is filled with water regardless of the location of the rods. With the exception of the AR rods, all the rods have displacers consisting of five sections articulately connected to each other with total length of 5,000 mm. The displacer section is a pipe measuring 74 X 2.5 mm of aluminum alloy with sealed end caps. One section is hollow and the remaining sections are filled with sleeves and cylindrical graphite blocks. When the absorbing rod is removed from the effective zone of the core, the displacer is introduced into this zone and the neutron balance is improved due to displacement of part of the water which is a strong absorbent. The AR rod differs from the RR and AZ rods by the fact that it has no displacer and a plate 20 mm in diameter is installed in the lower part of the absorbing assembly to distribute the flow rate of the cooling water. One-third of the total coolant flow rate through the channel passes through the inner cavities of the AR rods, the same as in the RR and AZ rods.

The neutron fuel distribution through the core is monitored by a physical monitoring system (SFKRE). Seven-section β-emission monitoring sensors are located behind the energy release fields in height in 12 channels uniformly distributed in the central part of the core for this purpose. The β-emission sensors which are installed in sealed cavities of the central carrying pipes of the fuel assemblies of the 117 fuel channels are used to monitor the energy release distribution to the reactor radius. Fission chambers, which are used to monitor the neutron flow when the reactor is started up, are arranged in four channels located in the peripheral row of the core.

There are 20 vertical openings 45 mm in diameter, in which channels with three-zone thermocouples are installed to monitor the graphite temperature, in the reactor stacking in the assemblies where the graphite blocks are joined. A total of 156 channels is provided in the central openings of the peripheral row of the graphite columns to cool the reflector. Water of the self-contained control system circuit is used as a cooling medium in these channels and also in 12 channels with height energy release monitoring sensors and four channels with fission chambers.

2.2. The Method of Neutron Physical Calculation

The RBMK reactor was developed on the experience of design and many years of operation of channel-type uranium-graphite reactors of the world's first AES [Nuclear power plant], the Sibirskaya AES and the Beloyarskaya AES imeni I. V. Kurchatov. Therefore, the methods of neutron-physical calculation checked in existing reactors were the basis for developing the method of neutron-physical calculation of the RBMK reactor. At the same time, due to orientation toward continuous recharging of the working channels and some design features of the RBMK reactor, supplements to the existing methods and in some cases development of new methodical solutions were required. One can distinguish three main phases in development of the methods of calculating the RBMK reactor:

a) working out the physical concept of the reactor and analyzing its main neutron-physical characteristics on the basis of traditional methods of calculating uranium-graphite reactors;

b) determining the main physical design characteristics of the reactor and working out specialized programs for calculating the cells and lattices of the channels of RBMK type reactors;

c) refining the physical characteristics of the reactor and making calculations for starting it up.

Program for calculating fuel burnup in the cell. The main program which was used to carry out a large part of the physical design calculations of the reactor and which was used to make preparatory calculations for other programs is the VRM program for calculating fuel burnup in the cell of a channel-type reactor operating on thermal neutrons with rod-type TVS with the geometrical dimensions and physical composition of the cell assigned. The extent of uranium burnup and the neutron balance in the continuous or partial recharging mode, the isotope composition of the fuel and the output of the channel as a function of time with given geometric dimensions, the initial enrichment of the uranium, the average output of the channel and neutron leakage beyond the cell are determined in the program. The fuel and moderator temperature is determined in the corresponding program blocks. Besides the main version, the program has several modificatons: calculation of a single-row lattice, claculation of reactivity effects and calculation of input data for heterogeneous programs and two-group constants.

The requirements of speed and simplicity of the algorithm determined the selection of simplified calculating methods. A channel with coolant temperature and density averaged in height is considered. Neutron breeding in the high-energy zone and absorption on U-238 resonances are calculated by ordinary methods for a homogeneous lattice. A Wigner-Zeitz cell is distinguished when considering the processes in the thermal energy zone, but neutron overflow is introduced on its boundary, which has different signs for fresh and burnt-up channels and provides an integral balance of neutron generation and absorption during the run. It is assumed that only thermal neutrons leak beyond the cell. Neutron capture in the epithermal energy zone is assumed to be low. The neutron spectrum in the thermal and epithermal zones is represented in the form of the sum of the Maxwell spectrum with effective neutron temperature dependent on coordinates and the Fermi spectrum and the Westcott cross-section system is used in this case. Neutron flow is calculated in P_1-approximation for the model of a two-zone cell. The thermal neutron flux distribution through inidividual fuel elements of the assembly is also calculated in P_1-approximation. The presence of non-breeding channels in the reactor is taken into account by introduction of effective spacing (graphite "smearing").

The GE heterogeneous program that takes into account epithermal effects. The most common method of calculating the characteristics of a heterogeneous lattice of working channels is the heterogeneous method [1, 2]. In the classical heterogeneous method the reactor is regarded as a system of working channels placed into a moderating medium, while channels of finite dimensions are regarded as filamentary sources of fast neutrons and sinks for thermal and resonance neutrons. The elementary diffusion equation is used to describe diffusion of thermal neutrons between channels. The absorbing properties of the channels are characterized by the logarithm derivative of the thermal neutron flux to the channel surface.

Application of the classical heterogeneous method to calculations of modern power reactors is very difficult. First, the channel volume comprises a significant part of the cell volume so that the assumption of their filamentary nature leads to an appreciable error. Second, a considerable number of neutrons is slowed down inside the channel, as a result of which it is a source not only of fast, but of thermal neutrons as well. Moreover, a considerable part of the neutrons is absorbed and generated in the epithermal energy zone in power reactors with high uranium burnup with accumulation of isotopes having cross-sections with high resonance integrals. Modification of the heterogeneous method, that permits one to take into account the indicated characteristics of the channel lattice, has the arbitrary name GE. The breeding coefficient and the neutron flux distribution through the cell channels with periodicity having a maximum of 16 heterogeneous channels can be calculated by the GE program. The GE program is used as a block in the program for calculating the fuel burnup of the channel lattice with regard to the height heterogeneity of properties.

The heterogeneous burnup calculating program. The method of calculating fuel burnup in a channel-type reactor operating in the continuous recharging mode (with heterogeneous core) is based on two assumptions. First, the structure of the core charge and the sequence of recharging the working channels are assumed such that the core is a periodic lattice of fuel channels with different fuel burnup, the main repeating element of which is the feed-rate cell (or macrocell). A macrocell consisting of 14 fuel channels and two control channels is usually considered when calculating an RBMK reactor. This assumption simplifies calculation of the neutron fields through the macrocell, but it is suspected in this case that the considered macrocells are located in an energy release distribution plateau (or the reactor is infinitely large in radius). Second, it is assumed that the macroscopic constants of the fuel channels are determined only by the extent of fuel burnup in a given channel and are not dependent on the properties of adjacent channels. In this case calculation of burnup in a heterogeneous system is broken down into two independent parts:

a) calculation of the macroscopic properties of fuel channels as a function of the degree of fuel burnup;

b) calculation of power distribution through the macrocell, consisting of different channels whose properties are determined in the first part of the calculation.

The GE program is used in the latter part as the main block. The power distribution obtained in this manner is assumed to be fixed during a given time step, which can be selected as sufficiently small. This separation of burnup calculation permits one to significantly reduce the calculating time since the channel properties are not calculated directly in the second part but only a sample is taken from the properties.

The capability of distinguishing up to eight zones in height (the HINDI program) is provided in the program to take into account the inhomogeneity of the fuel channel properties in height that results from variation of the coolant density, nonuniform fuel burnup or variable fuel charge through the length of the channel. The neutron flux distribution is calculated in single-group approximation. The program takes

into account variation of the core charge structure according to one of the channel recharging schemes and the determined reactor operating modes, for example, when the multiplication factor decreases below a given value or when other conditions are fulfilled: upon reaching a given degree of burnup and with channel output. It is sufficiently universal and permits one to investigate different fuel charges of channel-type reactors. Unlike the VRM program, the real structure of the reactor feed-rate cell and the presence of nonmultiplying channels in the lattice are taken into account in it. The limitations of the program capabilities are related to representation of the core in the form of a set of identical macrocells and with the assumption of constant coolant density distribution during the run through the height of the channel, although the nature of the energy release distribution varies considerably, especially during the initial period of reactor operation.

Programs for two-dimensional calculation of a reactor. The development of computer technology considerably expanded the capabilities of realizing calculating methods which could not be accomplished previously. Attention was primarily devoted to those problems of reactor calculation which had been hardly investigated, specifically, on calculation of the energy release distribution through the entire reactor. The experience of operating the reactors of the Beloyarskaya AES indicates that, unlike uranium-graphite reactors operating on natural uranium, local surges of energy release determined by the local inhomogeneities of the core structure can occur in reactors with slightly enriched fuel. A program for two-dimensional calculation (in x-y configuration) of the energy release fields was developed for the M-220 computer for reactors of the Beloyarskaya AES with approximately 1,000 channels [3]. The numerical method of calculating the criticality and the energy release distribution used in it was realized in two-dimensional programs for up to 3,000 channels with the appearance of the BESM-6 computer. The BOKR program was used extensively to process the results of physical startup of the reactor and to form a full charge. The BOKR-COBZ program [4] is now used as the operating program for calculating the energy release fields after introduction of additional units into the program that take into account nonuniform contamination of the fuel with xenon and fuel burnup.

Solution of a system of two-group diffusion equations for a reactor consisting of various types of square cells is realized in the BOLR program. The physical properties are constant inside each cell. The assemblies of the calculating grid coincide with the centers of the channels. Upon comparison of the calculated and experimental data, it was shown that this arrangement of assemblies was more preferable than in the angles of elementary cells of the reactor as was used in [3]. The iteration process, in which the neutron source distribution and the new neutron flux distribution of the first and second groups are taken into account as a result of sequential bypass of all the assemblies of the calculating grid on the basis of given initial single neutron flux distribution in each energy group and for the initial value of the multiplication factor equal to one, was used to solve the system of diffusion equations. The next iteration was then carried out using the neutron fluxes found as a result of the previous iteration. The new value of the multiplication factor is calculated after each iteration.

This iteration scheme is one with "mixed" iterations in which, unlike the classical scheme with external and internal iterations, the neutron sources are corrected after each iteration rather than after some approximation of the neutron flux

for them. This scheme was convergent and convenient by the rate of calculation. The method of sequential Young and Frankel overrelaxation used to accelerate the convergence of internal iterations in the classical scheme, was used to reduce the calculating time.

The presence of control rods and other nonbreeding channels in the core is taken into account by assigning the corresponding homogenized properties of cells in which these absorbers are located. Partially inserted rods are replaced by fully inserted rods equivalent to the first ones in efficiency.

A method of heterogeneous calculation of a reactor that extends the classical heterogeneous method to reactor systems having a large number of cells (up to 2,500) was developed in [5, 6]. A heterogeneous reactor is represented in the form of a finite lattice of thin rods (channels) in a infinite moderator. Neutron transport in the moderator is described by two-group diffusion equations of the Galinin-Feinberg type using the quasi-albedo method. Two-dimensional diffusion equations with filamentary sources--sinks--are approximately rewritten in a form similar to the finite-difference method. To do this, the reactor is covered with a square grid equal to the spacing of the lattice so that the sink-sources are located only at its points.

The QUAM program (its subsequent modifications are NEWQUAM and QUAM-2), which permits calculation of the energy release distribution to the channels of a reactor whose core is inscribed into a square with side of not more than 48 cells, was compiled by the indicated method. The number of different varieties of rods (channels) does not exceed 99. There is the capability of assigning individual characteristics for each channel; linear interpolation is made for all channel parameters when determining the dependence of properties on burnup.

It was shown upon comparison of the results of calculation by the BOKR and QUAM programs that both programs yields sufficiently close energy release distribution through the reactor channels.

The programs used in physical calculations. Without dwelling on the characteristics of the programs, let us present a list of the names and designation of programs used in making physical calculations of the RBMK reactor and intended for making traditional reactor calculations.

The SI-5, P3-15 and P3-50 are programs for solving the single-speed kinetic equation in P3-approximation. They are used to calculate the thermal neutron flux distribution through the elementary cell.

The DOP and MOV are programs for solving single-dimensional two-group diffusion equations. They are used when calculating the energy release fields in height and radius of the homogenized reactor model.

POIS is a program for calculating transient poisoning. It is used to calculate reactor poisoning in transient modes.

VOR is a program for calculating fuel burnup "at the point." It is used when calculating the physical properties of cells with channels differing from the model used in the VRM program.

DSP is a two-group synthetic program for two-dimensional calculation of a reactor by the separation of variables method. Two-dimensional calculation is replaced by sequential one-dimensional calculations.

GRIM is a program to determine the physical characteristics of nonbreeding channels.

"FUGA" is a modernized heterogeneous program for calculation of channels with regard to fast, resonance and epithermal neutron effects determined by the presence of nonbreeding channels in the charge.

"FIALKA" is a program for calculation of corrections to heterogeneous constants of working channels determined by the presence of nonbreeding channels near them.

2.3. Physical Experiments

The complexity of the core structure of a reactor operating in the continuous recharging mode, the presence of channels with significantly different breeding, absorbing and moderating properties and the large dimensions of the core made full-scale experiments essentially impossible due to their high cost and mainly due to the long periods required to conduct them--development of a full-scale bench, manufacture of channels, assemblies and so on. However, the need for an experimental check and refinement of the methods of calculating complex lattices was clear. Therefore, experiments were conducted during the period of working out the design on an insert of an already existing graphite bench; the spacing of the channel lattice in the insert was equal to the design spacing and comprised 25 cm and the number of channels was 81; the height of the investigated systems was 3.5 meters, i.e., it was one-half the design height. The experimental data were used to correct the calculating methods and to analyze the characteristics of the reactor.

Experiments to determine the characteristics of complex lattices were conducted in phases--from simple to complex. Homogeneous lattices of RMBK-type TVS consisting of rod fuel elements of uranium dioxide with natural U-235 content were investigated during the first phase. The lattice multiplication parameters and also the neutron fields in the cell were measured. It was shown in these experiments that the system cannot be critical for an RBMK-type lattice when using uranium dioxide of natural enrichment. Therefore, further experiments with natural uranium were conducted in a subcritical assembly surrounded by a seed region. The experiments were conducted at 25°C with a dry zone and one filled with water. The positive nature of reactivity upon dehydration of the TVS channel lattice was shown.

The neutron distribution through the channel height in the rupture zone was measured and the degree of increase of neutron flux density was determined due to the structural rupture of fuel through the core height between TVS. It was shown that this surge drops rapidly as the distance from the channel axis increases so that introduction of a displacer in the center of the TVS leads to appreciable equalization of the neutron field through the channel radius. The results of measurements made with assemblies of 18 fuel elements with two percent fuel enrichment are presented in Table 2.1. The gap between the fuel in the fuel elements comprised 41 mm along the vertical and the material of the end parts was SAV alloy. Analysis of experimental data made it possible to conclude that the surge of energy release on the peripheral fuel elements of fresh TVS of the RBMK reactor comprises 35-40

percent in the operating state and decreases exponentially as the distance from the gap increases with relaxation length of 1.3 cm^{-1}.

Table 2.1. Relative Surge of Neutron Flux Density in Region of TVS Rupture

	Material Between Fuel Elements			
	SAV and H_2O		SAV	
Point of Measurement	Inner Ring	Outer Ring	Inner Ring	Outer Ring
In center of rupture	1.83	1.58	1.51	1.39
At fuel boundary	1.53	1.37	1.35	1.25
Far from rupture	1.0	1.26	1.0	1.13

Besides experiments with homogeneous lattices, experiments were conducted with mixed lattices which were assembled from assemblies of two percent and natural enrichment. The mixed lattices were formed of polycells which were squares consisting of four channels. The types of investigated lattices and the results of determining their materials parameters $\varkappa^2$ with and without water in the fuel channels are presented in Table 2.2.

Comparison of the values of $\varkappa^2$ for the considered lattices with and without water in the fuel channels showed that the effect of variation of reactivity upon dehydration of the channels is negative for a lattice containing a two percent enrichment assembly and positive for the other investigated types of lattices. With average enrichment of 1.7-1.8 percent U-235 through the polycell, the effect of dehydration is close to zero. due to the dependence of $\varkappa^2$ on the average enrichment, it was concluded that the minimum enrichment at which a cold nonpoisoned reactor with water in the fuel channels can be made critical comprises approximately 1.2 percent.

Table 2.2. Values of Material Parameter $\varkappa^2$

Charge of Polycell	Average Enrichment Through Polycell, percent	$\varkappa^2$, 10^{-4} cm^{-2}		$\Delta^2 = \varkappa^2$ without water — $\varkappa^2$ with water, 10^{-4} cm^{-2}
		Without Water	With Water	
0:4	0.714	-0.712	-3.87	3.16
4:0	2	5.74	6.43	-0.69
3:1	1.67	4.57	4.07	0.5
2:2	1.35	4.07	1.67	1.41
1:3	~1	1.42	-1.03	2.45
2:1+ +1 empty**	1.57	3.12	2.12	1

*The ratio of the number of enriched assemblies to the number of assemblies with natural fuel composition is shown.

**The effective spacing was 33 cm

As one would expect, the neutron spectrum in lattices with enriched fuel is more rigid compared to that in a spectrum of assemblies containing natural uranium. Filling the fuel channels with water leads to significant spectrum softening and variation of the neutron field through the assembly, especially for fuel elements of the outer ring in which the neutron density increases by 15-20 percent. The excess of effective neutron temperature at the cell boundary over graphite temperature comprises 160 and 100°C, respectively, for assemblies with enriched fuel with and without water and comprises 110 and 80°C for assemblies with natural oxide fuel. The coefficient of nonuniformity of neutron density through the assembly, determined as the ratio of the maximum density in any fuel element to its average value through all fuel elements, increased by 3 and 5 percent when the channel was filled with water for channels with natural and enriched fuel, respectively, but did not exceed 1.1 in a single case. The dependence of DP effectiveness on the ratio of sleeves of two percent boride steel ("heavy" sleeve) and ordinary steel ("light" sleeves) was studied experimentally in different systems, but mainly with and without water in fuel channels having TVS and in DP channels. The fraction of epithermal absorption $\eta = \rho^{et}_{DP}/(\rho^{et}_{DP} + \rho^{t}_{DP})$ for DP in a channel without water was equal to 3.0 percent for a light DP, depending on the ratio of heavy and light sleeves; it was 1-5 percent for DP with ratio of heavy to light sleeves of 3 and was 8 percent for heavy DP. Here ρ^{et}_{DP} and ρ^{t}_{DP} are the effectiveness of absorption in the epithermal and thermal regions of the spectrum, respectively. Taking the sleeve design of the DP into account, the effect of internal water on the absorptivity of the DP was investigated, which showed that the internal water increases the efficiency of the DP. For example, the efficiency of a heavy DP increases by 13 percent with the presence of internal water. Thus, the experiments showed that efficiency decreases, all things being equal, when the DP is dehydrated and it confirmed the feasibility of introducing an internal aluminum displacer.

Experiments on the effect of an outer water layer on the compensating capability of a DP with internal aluminum displacer showed that a layer of water around the DP decreases its efficiency by 10 percent. This result is true of both a heavy DP and of a DP having boride and ordinary sleeve ratio of 1:1. However, if the channel with absorbent consisting only of light sleeves is filled with water, its efficiency is increased.

The same experiments were conducted with absorbing rods similar to reactor control rods having boron carbide as the absorbent. The experiments showed that the presence of water inside the rod increases its efficiency by approximately 5 percent, while the outer layer of water considerably reduces its compensating capability. Thus, the efficiency of the rod is reduced by approximately 5 percent with layer thickness of 2 mm, by 9 percent with thickness of 4 mm and by 13 percent with thickness of 6 mm. The fraction of epithermal absorption with water inside the rod comprises 18-20 percent.

It should be noted that all the experimental data were found in small critical assemblies which only simulated the different fragments of a full reactor charge and different conditions for a cold nonpoisoned reactor. Therefore, they were used to check and correct the calculating methods.

2.4. Neutron-Physical Calculating Characteristics

2.4.1. Main Periods of Reactor Operation

The neutron-physical characteristics of the RBMK reactor were calculated for three main operating periods: The first phase of reactor operation with initial charge, the so-called transient period which precedes the steady recharging mode and the steady continuous fuel recharging mode. Each of the indicated periods has its own specific direction. The reactor should have the best engineering and economic indicators that ensure competitiveness compared to electric power plants of other types in the steady fuel recharging mode. The initial reactor charge should provide dependable compensation of the initial excess reactivity of the fresh fuel with optimum engineering and economic indicators. The transient period is characterized by continuous variation of the core structure and its neutron-physical characteristics. The main calculated neutron-physical characteristics of the RBMK reactor and their variation as a function of the reactor operating period are considered below.

2.4.2. The Initial Reactor Charge

Versions of accomplishing the initial charge and the passage of the transient period were considered: reducing the fuel enrichment in the assemblies of the initial charge, using assemblies with different fuel enrichment, incomplete core charge and so on. One or another version was selected on the basis of the neutron-physical, heat engineering, economic and dynamic investigations of the core and of the installation as a whole. Problems of optimizing the initial fuel charge are considered in more detail in [7-9], the main results of which are presented in Table 2.3. Different compositions of the periodicity cell consisting of 16 cells, including two SUZ channels, are presented in it.

It follows from Table 2.3 that the local misalignment of channel output in the periodicity cell for all versions except version 2 appreciably exceeds the corresponding value equal to 1.25 for a steady reactor operating mode. This means that for the thermal loads not to exceed the values used for the steady mode the reactor should operate at reduced power for some time. The same thing can be noted with regard to nonuniformity of the field in height. The coefficient of axial energy release nonuniformity not exceeding the value in the steady mode, in which the energy release is equalized in height as a result of fuel burnup, can be provided only in versions 2 and 6 by selecting the corresponding properties of the DP in height.

The principle of an incomplete reactor charge and introduction of the DP into the freed cells was used on the basis of investigations when forming the initial fuel charge of the RBMK reactor. Selecting the length of the DP and of the distribution of its absorbing properties in height is determined by two factors. First, the DP rods should provide compensation of reactivity (together with rods of the control system) in all states of the reactor. Second, the DP rods should contribute to equalization of the energy release field through the reactor height to the required limits. The DP composition was corrected directly during physical startup of the RBMK reactor: the heavy and light absorbing rings were assembled in a ratio of 1/2 in the upper and lower sections 1 meter long each and in the ratio 3/1 in the central section 5 meters long.

Table 2.3. Main Characteristics of Some Versions of Initial Charge

Number of Charge Version	Composition of Periodicity Cell (except 2 SUZ channels)	Initial Load, tons		Consumption of Natural Uranium Over 10 Years of Operation, tons	
		Uranium	Natural Uranium	Without Regeneration of U-235	With Regeneration of U-235
1	14 channels with 1.14 percent enrichment	179.7	345	1,924	1,748
2	2 channels with DP and 12 channels with 1.8 percent enrichment	154	515	1,929	1,796
3	6 channels with 1.8 percent enrichment	77	360	1,882	1,767
	8 channels with natural uranium	102.7			
4	5 channels with 2 percent enrichment	64	356	1,872	1,758
	9 channels with natural uranium	115.7			
5	8 channels with 1.5 percent enrichment	102.7	354	1,896	1,776
	6 channels with natural uranium	77			
6	2 channels with DP and 12 channels with 1.5 percent enrichment	154	415	1,991	1,794

[Continued on following page]

Table 2.3 (Continued).

Number of Charge Version	Accumulation of U-239 and Pu-241 During 10 Years, kg	Extent of Fuel Burnup of Initial Charge, GW·day/t		Length of Run of Channels of Initial Charge, Eff. days	
		Maximum	Minimum	Maximum	Minimum
1	1,402	15.8	3.6	1,300	240
2	1,308	23.5	12.7	1,700	800
3	1,402	21.4	17.0	1,460	1,020
4	1,397	9.7	2.4	920	210
		23.7	19.4	1,460	1,100
		9.8	2.3	1,000	200
		19.2	12.8	1,430	810
5	1,417	7.7	2.6	700	230
6	1,400	16.8	6.3	1,340	390

[Table continued on following page]

Table 2.3 [Concluded].

Number of Charge Version	Coefficient of Nonuniformity Through Periodicity Cell		Average Reduced Expenditures Over 10 years, kop/(kW·hr)	Temperature Coefficient of Fuel, 10^{-5}°C^{-1}	Steam Coefficient Of Reactivity,* percent
	Maximum	Minimum			
1	1.015	1.35	0.8057	-1.8	1.8
2	1.17	1.25	0.8058	-1.1	-1.3
3	1.4	1.4	0.8048	-1.5	1.7
	1.53	1.53	0.8058	-1.5	1.8
5	1.24	1.33	0.8032	-1.4	1.85
6	1.19	1.38	0.8175	-1.04	-0.9

*The results of preliminary calculations of the steam coefficient of reactivity are presented.

Selecting the location of installing the DP in the core. Since the DP rod is interchangeable by design dimensions with the assembly, locating them in the core is not limited by any design solutions and different methods of locating the DP with respect to the SUZ channels in the periodicity cell can be considered. Calculations of the periodicity cells by the GE program with different arrangement of the DP and different content of SUZ channels showed that the multiplication factor may differ in this case by approximately one percent without rods and by 0.5 percent with SUZ rods, while the maximum output of the fuel channels may differ by approximately 2 percent. Of greatest interest is comparison of two symmetrical arrangements of the DP in the periodicity cell with respect to the SUZ channels, shown in Figure 2.2. The locations of the DP were compared with full initial charge of the reactor in the working state both with and without SUZ rods. With the standard arrangement of the DP, the control rods regulate the output of the freshly charged assembly more effectively than with checkerboard arrangement. This circumstance forces one to give preference to standard arrangement of the DP since both versions differ slightly in efficiency of the DP and the SUZ rods.

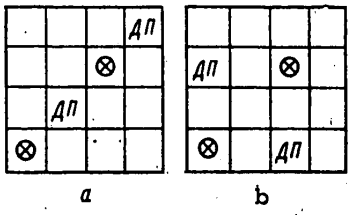

Figure 2.2. Arrangement of DP in Periodicity Cells: a--standard; b--checkerboard; the control channel is noted by the symbol

Energy release distribution through core height and radius. The distribution of the absorbing properties through the length of the DP have a significant effect on the shape of the axial energy release distribution during the initial moment of reactor operation; the SUZ rods may have the same effect. The actual arrangement of the control rods in the core in the absence of programs for three-dimensional calculation of the reactor can be taken into account only approximately. This type of analysis shows that the shape of the field may vary very slightly in height when the rods are shifted and the USP rods must be located below the center of the core to compensate for the field distortions of incompletely inserted RR rods. The nonuniformity coefficient in height can be maintained in the range of 1.25-1.50 with selected composition of the DP.

Calculated investigations of the energy release distribution through the reactor radius can be arbitrarily divided into three phases. The ratio of the number of DP in the central and peripheral homogenized regions of the reactor required for given equalization of energy release through the core radius is determined in the first phase. The specific cartogram of DP arrangement in the core is refined during the second phase by means of two-dimensional programs for calculating the reactor as a whole. The physical startup period of the reactor when a large number of calculations is made by two-dimensional programs, from the results of which the initial charge of the reactor is selected with regard to the data actually achieved in the reactor, should be taken into account by the third phase of

investigating the radial energy release fields. (The initial charge contains 1,450-1,440 assemblies and 230-240 DP for operating RBMK reactors as a function of the production tolerances on the charge and enrichment of the fuel and graphite density). It was shown by calculations that a position of SUZ rods can be selected in the hot poisoned state of the reactor in which the reactivity compensated for by them is approximately equal to the design operational reserve of reactivity, while nonuniform energy release distribution through the radius comprises 1.28.

Calculated investigations of a full charge and later the experience of operating the RBMK reactor showed that its characteristic feature is the high sensitivity of neutron fields to displacement of the control members. This is related to the fact that the high excess reactivity is compensated for by a large number of absorbers and when some of them are removed (especially the peripheral absorbers) a region occurs, sometimes close to criticality and containing 15-20 channels with TVS among which there is not a single absorber. In this regard the point of locating the rods and the RR rods to be removed should be selected very carefully, observing a specific sequence of removing the RR rods.

Based on numerous calculations to equalize the energy release fields in the reactor, it has been suggested that all 89 RR rods be divided into four groups as a function of their location in the reactor (Table 2.4). The fourth group combines the peripheral rods and the central rods are divided into three regular lattices embedded into each other. Operational compensation of the excess reactivity is accomplished at each moment of time by the RR rods of one of the central groups and by the peripheral rods which are shifted so as to equalize the currents of the side ionization chambers. The rods of each central group are shifted sequentially, occupying an approximately identical position in height with deviation of $\pm$ 0.5 meter from the mean position. The rods of the two other central groups occupy the extreme upper or lower positions depending on the reactivity reserve. The indicated procedure for removing the RR rods permits a radial nonuniformity coefficient of approximately 1.8 to be maintained.

Table 2.4. Division of RR Rods by Groups*

(1) I группа	II группа	III группа	IV группа	I группа	II группа	III группа	IV группа
22—21	16—25	22—25	12—31	42—41	36—45	42—35	36—65
22—31	16—35	22—35	12—35	42—51	36—55	42—45	42—11
22—41	16—45	22—45	12—41	42—61	46—15	42—55	42—65
22—51	26—15	22—55	12—45	52—21	46—25	52—25	46—11
32—21	26—25	32—15	16—21	52—31	46—35	52—35	46—65
32—31	26—35	32—25	16—55	52—41	46—45	52—45	52—15
32—41	26—45	32—35	22—15	52—51	46—55	52—55	56—21
32—51	26—55	32—45	22—61	52—61	56—25	62—35	56—61
32—61	36—15	32—55	32—11	62—31	56—35	62—45	62—25
42—21	36—25	42—15	32—65	62—41	56—45		62—55
42—31	36—35	42—25	36—11	62—51	56—55		66—31
							66—35
							66—41
							66—45

*Arrangement of the rods in the reactor is shown in Figure 2.3.

Key:
1. Group

When reactor power is reached at which the readings of the sensors of the physical monitoring system become reliable, the field is actually equalized from their readings by using rods of different groups.

Effects and coefficients of reactivity for initial reactor charge. Determination of the temperature and density effects of core reactivity of the RBMK reactor is one of the most complex calculations. This is largely determined by the complexity of the core composition and also by the essentially total absence of experimental data by the time of reactor startup which would make it possible to correct the methods of calculating the effects of reactivity. Experimental data were obtained on an insert of 81 channels and on critical assemblies having half the core height where rods 2 or 3 meters long were used rather than on a full-scale bench. In this regard the calculations of reactivity effects were corrected and were partially done again with regard to the experimental results obtained in the reactor.

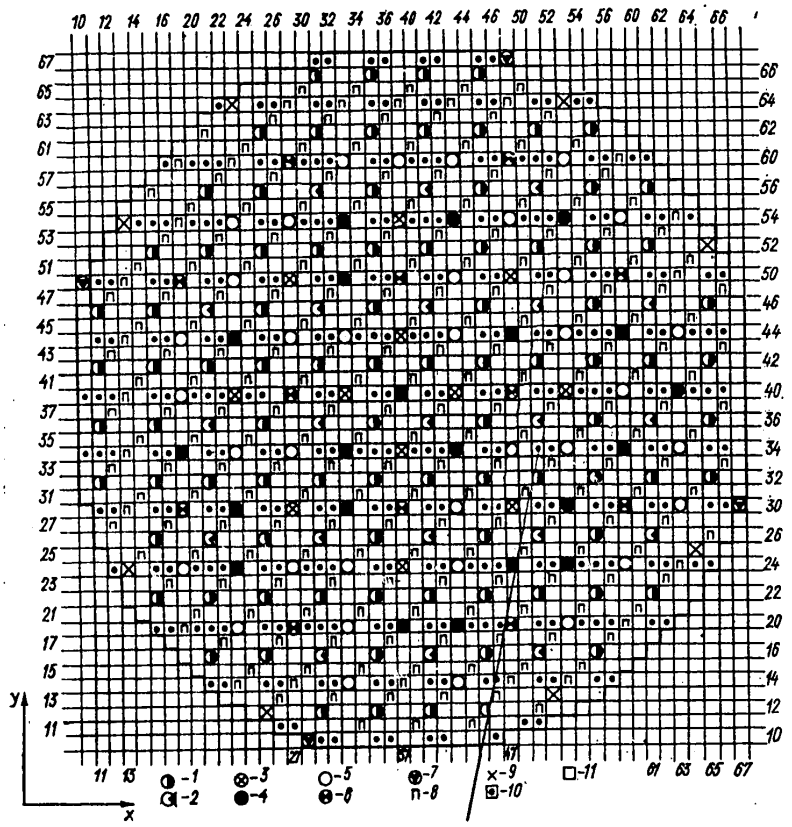

Figure 2.3. Initial Reactor Charge of Second Unit of Leningrad AES: 1--RR rod; 2--USP rod; 3--AR rod; 4--AZ rod; 5--AZ recompensating rod; 6--energy release sensor in height (DKE (h)); 7--starting fission chamber; 8--additional absorber; 9--uncharged channel; 10--fuel assembly with energy release sensor through radius (DKE (r)); 11--fuel assembly

Three main problems were considered for the initial charge: variation of reactivity upon dehydration of the core in the cold state, variation of reactivity upon heating of the core and determination of the reactivity coefficients in the working state. The calculated and experimental data on variation of reactivity with dehydration of the core of a cold unpoisoned reactor are presented in Table 2.5.

Table 2.5. Effect of Dehydration

Dehydrated Channels	Calculation	Experiment
With TVS	-0.00055	-0.001 ± 0.0005
With DP	-0.00726	-0.011 ± 0.0013
SUZ	0.0141	-0.010 ± 0.0013

Table 2.6. Calculated and Experimental Temperature Coefficients of Reactivity, $10^{-5}°C^{-1}$

Reactivity Coefficient	Calculation	Estimate from Experimental Data
α_Σ	-4.8	-5
α_C	3.4	3
$\alpha_{tv} + \alpha_t$	-8.5	-8

Study of the variation of reactivity with heating of the core made it possible to analyze such important reactor characteristics as the temperature coefficients of moderator reactivity α_C, water α_{tv}, fuel α_t and total temperature coefficient α_Σ The calculation was made for the temperature range of 100-200°C on the assumption that 90 control rods were inserted into the core (Table 2.6). The reactivity coefficients were calculated for nominal working values of heat engineering parameters of the reactor on the assumption that 30 fully charged rods were located in its core in this state. The calculated values of the reactivity coefficients were as follows: $\alpha_C = 0$, $\alpha_{tv} = -5.1 \cdot 10^{-5}°C^{-1}$, $\alpha_t = -1.0 \cdot 10^{-5}°C^{-1}$; the density coefficient of reactivity was $\alpha_\gamma = 1.44 \cdot 10^{-2}$ cm^3/g and the steam coefficient of reactivity was $\alpha_\phi = \Delta\rho/\Delta\phi = -1 \cdot 10^{-2}$.

Variation of the reactivity coefficients during reactor operation is considered below.

Neutron flux density distribution through the assembly and fuel elements. The thermal flux density distribution through the cell was calculated by the SI-5 program in P_3-approximation with regard to thermalization for a homogenized model of the channel. For conveience in making heat engineering calculations, the flux density distribution through each fuel element, according to [10], is reduced to the form

$$\Phi_i(r,0) = (p_i + q_i r \cos\theta) \exp(\xi_i r^2),$$

where p_i is the relative flux density level in the fuel element of the i-th row, q_i is the flux density gradient through fuel elements of the i-th row, ξ_i is the coefficient of corrosion of the flux density in the fuel element and θ and r are the polar coordinates of a point with respect to the center of the fuel element.

The neutron distribution through the microcell, consisting of a fuel element surrounded by an equivalent amount of water, was calculated to determine parameter in P_3-approximation. Parameter ξ, which was equal to 0.2 cm^{-2}, was determined by the neutron distribution inside the fuel element. It was assumed that the value of ξ is identical for all fuel elements. Parameters $p_1 = 0.611$, $q_1 = 0.0331$ cm^{-1}, $p_2 = 0.706$ and $q_2 = 0.0845$ cm^{-1} were determined for fuel elements of the inner (i = 1) and outer (k = 2) ring by the neutron flux density distribution through the cell. As a result the following expressions were found for energy release in relative units:

$$\Phi_1(r, \theta) = (0{,}611 + 0{,}0331\, r\cos\theta)\exp(0{,}2\, r^2);\ \bar{\Phi}_1 = 0{,}655;$$
$$\Phi_2(r, \theta) = (0{,}706 + 0{,}0845\, r\cos\theta)\exp(0{,}2\, r^2);\ \bar{\Phi}_2 = 0{,}765;\ \bar{\Phi} = 0{,}73,$$

where $\bar{\Phi}_1$, $\bar{\Phi}_2$ and $\bar{\Phi}$ are the mean values of the volumetric energy release in the fuel elements of the inner ring, the outer ring and in all the fuel elements, respectively.

According to the derived expressions, the coefficient of nonuniformity of energy release through the fuel elements was $K_{tv} = 1.05$, the coefficient of nonuniformity of the specific energy intensity of the fuel was $K_V = 1.11$ and the maximum coefficient of nonuniformity through the radius of the fuel element was $K_r^{tv} = 1.06$. The calculation corresponds to uniform distribution of fissionable isotopes through the radius of the fuel element. Accumulation of Pu-239, which will occur to a greater degree in the outer layers of the fuel element core, distorts the form of energy release in the fuel, but the considered distribution is the most dangerous for maximum fuel temperature.

2.4.3. The Transient Operating Period of the Reactor

The transient operating period of the reactor, i.e., the time from the initial charge to the stationary fuel recharging mode, is characterized by continuous variation of the reactor parameters and the composition of the core. One of the most significant problems during this period is that of organizing continuous recharging of the fuel assemblies that satisfy the conditions of maintaining the reactivity reserve and nonuniformity of energy release within given limits. Solution of this problem can be complicated by additional operating conditions, for example, delay of the deadlines for introducing the loading-unloading machine, the need to recharge specific channels and so on. Recommendation on the sequence of recharging the DP were presented for conditions of planned continuous recharging and the consumption of assemblies, the extent of burnup of removed fuel and other indicators of the reactor required to determine the economic characteristics of the plant during the transition period were determined.

For convenience in calculations, fuel recharging can be related to periodicity cells. In this case the core was divided into two radial zones: a central and peripheral and it was assumed that the periodicity cells in each zone are

identical and have their own constant total output determined by the number of cells in the zone and by the average output of the zone. The calculated periodicity cell in the central zone has a mean output of 28.9 MW and contains 12 fuel assemblies, 2 DP and 2 SUZ channels at the initial moment. The calculated cell in the peripheral zone has a mean output of 21.8 MW and contains 13 assemblies, 2 DP and 1 SUZ channel.

All the periodicity cells in each zone are recharged by an identical program with specific sequence of assembly replacement. This sequence of channel recharging is maintained throughout the entire operating life of the reactor. Channels arranged identically in the periodicity cells are recharged to maintain the charge symmetry and its periodicity in each reactor zone. It is obvious that under real conditions the recharging program can be corrected on the basis of the actual power generation of the channels and the energy release distribution through the reactor. Moreover, disruptions of the adopted sequence may occur on the periphery of the reactor where identical periodicity cells cannot be clearly determined.

Calculating the fuel recharging mode. The results of calculating the recharging mode by the HINDI program are presented in Tables 2.7-2.9. According to the calculation by this program, the average extent of fuel burnup in the steady recharging mode comprises 19 GW·day/t, which is in agreement with the planned value of 18.5 GW·day/t within several percent.

The data presented in Tables 2.7 and 2.8 permit one to estimate the operating conditions of the initial charge channels in the reactor and to find several values that characterize the transient operating period of the reactor, for example, the consumption of assemblies for the entire reactor during the transient operating period (Table 2.10). The consumption of fuel assemblies comprises 475 with the reactor generating 10^6 MW·day of thermal energy in the steady recharging mode.

Effects and coefficients of reactivity. Due to the complexity of the core structure and the nonuniform distribution of burnup through the core, calculation of the effects and coefficients of reactivity during transient operation of the reactor is a complex problem. Therefore, they were designed with average burnup of 5 and 10 GW·day/t of the charged channels initially since removal of the DP through one of each periodicity cell is completed with burnup of 5 GW·day/t and removal of all DP is completed with burnup of 10 GW·day/t. The calculated values of the reactivity coefficients and the indicated moments of the run are presented in Table 2.11.

The results indicated in Table 2.11 were found on the assumption that the reactor has nominal heat engineering characteristics and that 20 control rods are inserted into the core to compensate for the operational reserve of reactivity.

Misalignment of output during recharging of the DP. Calculations of a reactor in the DP recharging mode presented above and of replacement of the DP by fuel assemblies were made on the basis of the condition of simultaneous replacement of DP in all periodicity cells of the reactor. In this case only the power redistribution inside the periodicity cell is taken into account. In fact, periodicity cells with different number of DP are located in the reactor, which distorts the neutron flux distribution through the reactor.

Table 2.7. Main Characteristics of Recharging Mode in Central Zone

(1) Номер перегрузки в ячейке периодичности	Время до перегрузки, (2) эфф. сут		Глубина выгорания, (3) ГВт·сут/т			Перегрузочный коэффициент (7) $K_{пер}=\frac{N_{макс}}{\bar{N}}$
	(4) минимальное	(5) максимальное	минимальная	(6) средняя	максимальная	
(8) 1 (перегрузка ДП)	100	390	0	0	0	1,182
2 (перегрузка ДП)	390	630	0	0	0	1,085
3	630	670	11,8	12,2	12,6	1,193
4	670	720	12,6	13,0	13,4	1,193
5	720	770	13,4	13,8	14,2	1,193
6	770	820	14,3	14,7	15,3	1,192
7	820	890	15,0	15,5	16,0	1,192
8	890	950	16,1	16,6	17,1	1,193
9	950	1020	17,1	17,6	18,2	1,191
10	1020	1100	18,1	18,7	19,3	1,188
11	1100	1180	19,2	19,5	20,5	1,175
12	1180	1260	20,3	20,6	20,9	1,153
13	1260	1340	20,6	21,1	21,6	1,142
14	1340	1430	21,4	22,2	23,0	1,118
15	1430	1510	22,3	22,5	22,6	1,149
16	1510	1590	18,8	20,0	21,2	1,162
17	1590	1660	17,2	18,1	19,0	1,182
18	1660	1740	18,2	18,5	18,8	1,181
19	1740	1810	18,9	19,0	19,1	1,184
20	1810	1890	19,1	19,3	19,5	1,180
21	1890	1970	19,4	19,6	19,7	1,184
22	1970	2050	19,7	19,9	20,0	1,185
23	2050	2130	20,0	20,2	20,4	1,184
24	2130	2210	20,1	20,1	20,1	1,206
25	2210	2280	19,8	19,9	20,0	1,174
26	2280	2360	19,7	19,8	19,9	1,182
27	2360	2430	19,1	19,2	19,3	1,176
28	2430	2510	19,0	19,1	19,2	1,156
29	2510	—	—	19,5	—	1,141

Key:
1. Number of recharging and periodicity cell
2. Time to recharging, eff. days
3. Extent of burnup, GW·day/t
4. Minimum
5. Maximum
6. Average
7. Recharging factor $K_{per} = N_{maks}/\bar{N}$
8. Recharging of DP

The experience of calculating the reactor recharging by two-dimensional programs shows that first, the misalignment occurring upon replacement of DP by assemblies are greater than would follow from calculations of the periodicity cells (the coefficient of misalignment reaches 1.5) and second, moving the control rods permits a significant reduction of misaslignments, bringing them up to the accepted design values.

Table 2.8. Main Characteristics of Recharging Mode in Peripheral Zone

(1) Номер перегрузки в ячейке периодичности	Время до перегрузки, (2) эфф. сут		(3) Глубина выгорания, ГВт·сут/т			Перегрузочный коэффициент (7) $K_{пер}=\frac{N_{макс}}{\bar{N}}$
	(4) минимальное	(5) максимальное	минимальная	(6) средняя	максимальная	
(8) 1 (перегрузка ДП)	50	430	0	0	0	1,119
2 (перегрузка ДП)	430	790	0	0	0	1,073
3	790	840	10,6	11,0	11,4	1,198
4	840	900	11,4	11,7	12,0	1,197
5	900	960	12,0	12,4	12,8	1,199
6	960	1030	12,6	13,2	13,6	1,197
7	1030	1100	13,3	13,4	13,5	1,192
8	1100	1170	14,0	14,3	14,6	1,180
9	1170	1250	14,3	14,8	15,3	1,164
10	1250	1330	15,3	15,7	16,1	1,143
11	1330	1410	16,1	16,5	16,9	1,122
12	1410	1500	16,8	17,3	17,8	1,114
13	1500	1600	17,7	18,2	18,7	1,111
14	1600	1700	18,8	19,2	19,6	1,110
15	1700	1800	19,6	20,1	20,6	1,098
16	1800	1910	20,6	21,1	21,7	1,129
17	1910	2000	16,8	18,0	19,2	1,111
18	2000	2090	15,5	16,4	17,3	1,155
19	2090	2180	16,8	16,9	17,1	1,209
20	2180	2280	17,1	17,2	17,5	1,208
21	2280	2370	17,5	17,6	17,7	1,209
22	2370	2460	17,1	17,2	17,3	1,210
23	2460	2550	17,3	17,4	17,5	1,190

Key:
1. Number of recharging and periodicity cell
2. Time to recharging, eff. days
3. Extent of burnup, GW·day/t
4. Minimum
5. Maximum
6. Average
7. Recharging factor $K_{per} = N_{maks}/\bar{N}$
8. Recharging of DP

2.4.4. The Steady Fuel Recharging Mode

The extent of fuel burnup. The characteristics of the RBMK reactor in the steady continuous fuel recharging mode are presented in Table 2.12. A reactor with height-averaged properties is considered: average coolant density of 0.516 g/cm^3 and average coolant temperature of 284°C. The operational reserve of reactivity is equal to 1 percent and leakage to the height is 1 percent, which corresponds to a reactor model with unequalized power distribution by height. Correction for self-equalization of power by height during burnup is introduced into the average burnup of removed fuel to the reactor. With regard to the data presented in Table 2.12, the average fuel burnup through the reactor is equal to 18.5 GW·day/t and the average run of the channel is approximately 1,100 effective days. The fuel removed from the reactor contains on the average, kg/t:

Table 2.9. Isotope Composition of Fuel, kg/t

(1) Выгорание, ГВт·сут/т	^{235}U	^{239}Pu	^{241}Pu	^{238}U	^{236}U	^{240}Pu	^{242}Pu	(2) Шлаки
0	17,870	0	0	982,13	0	0	0	0
1,825	15,763	0,9216	0,0053	980,96	0,3432	0,0640	0,00012	1,9452
3,635	13,937	1,5393	0,0335	979,79	0,6374	0,2108	0,00185	3,8655
5,405	12,335	1,9094	0,0827	978,63	0,8913	0,3888	0,00760	5,7341
7,122	10,916	2,1703	0,1430	977,50	1,1122	0,5730	0,01899	7,5406
8,774	9,662	2,3357	0,2062	976,38	1,3037	0,7555	0,03668	9,2734
10,358	8,556	2,4314	0,2673	975,29	1,4692	0,9317	0,06060	10,9280
11,871	7,579	2,4795	0,3237	974,23	1,6124	1,0978	0,09058	12,506
13,320	6,714	2,4956	0,3743	973,19	1,7362	1,2518	0,12590	14,008
14,702	5,948	2,4906	0,4186	972,18	1,8432	1,3931	0,16600	15,438
16,023	5,270	2,4719	0,4567	971,19	1,9355	1,5217	0,21025	16,800
17,286	4,668	2,4448	0,4892	970,22	2,0150	1,6382	0,25806	18,098
18,495	4,136	2,4129	0,5166	969,27	2,0832	1,7433	0,30889	19,337
19,655	3,663	2,3786	0,5396	968,34	2,1415	1,8379	0,36225	20,521
20,768	3,244	2,3436	0,5586	967,43	2,1912	1,9227	0,41773	21,656

Key:

1. Burnup, GW·day/t

U-235	4.1
Pu-239	2.4
Pu-241	0.5
U-238	969.3

2. Poisons

U-236	2.1
Pu-240	1.7
Pu-242	0.3

Energy release distribution through the height and radius of the reactor. The energy release distribution through the height of the core was calculated by the HINDI program with regard to nonuniform water density through the length of the channel, nonuniform fuel burnup and the actual design of the control rod displacer. It was assumed that displacers are located in both SUZ channels in the periodicity cell. The nonuniform fuel burnup coefficient through the length of the channel is equal to approximately 1.4 and maximum burnup of approximately 22 GW·day/t is located at a height of approximately 5 meters from the bottom of the core. The nonuniform energy liberation coefficient through the height of the RBMK reactor is equal to 1.3 in the steady mode. The maximum field is located at a height of approximately 4 meters.

The energy release field through the core radius can be represented in some cases in the form of an equalized field having a plateau zone and a peripheral zone on which local misalignment from the SUZ rods and other inhomogeneities in the core are imposed. The equalized neutron flux density field through the reactor radius, calculated by the one-dimensional two-group program DOP for a reactor model with five radial zones, is shown in Figure 2.4. The coefficient of field nonuniformity through the radius is $K_r = 1.1$. Local distortions characterized by an irregularity factor K_{lok}, whose value, according to the experience of operating uranium-graphite reactors, is equal to 1.15, must be applied to this field. Thus, the maximum channel output (without regard to the recharging coefficient K_{per}) exceeds the average channel output in the reactor by a factor of approximately 1.27.

Table 2.10. Consumption of Fuel Assemblies During Transient Period as a Function of Power Generation

E, 10^6 MW·day	g	E, 10^6 MW·day	g	E, 10^6 MW·day	g
0	0	1.5	154	3.0	815
0.25	6	1.75	187	3.25	950
0.5	30	2.0	225	3.5	1,075
0.75	57	2.25	375	3.75	1,195
1.0	87	2.50	520	4.0	1,325
1.25	120	2.75	670		

Note. E = is the integral generation of thermal power by the reactor; N_T is the thermal output of the reactor; and g is the consumption of assemblies per charge of the reactor

Table 2.11. Calculated Values of Reactivity Coefficients

Coefficient	Average Fuel Burnup in Reactor, GW·day/t	
	5	10
α_C, 10^{-5} °C^{-1}	3.2	5.4
α_{tv}, 10^{-5} °C^{-1}	0.42	5.0
α_t, 10^{-5} °C^{-1}	-1.0	-1.1
α_γ, 10^{-2} cm^3/g	-0.22	-1.30
α_ϕ, 10^{-2}	0.15	0.92

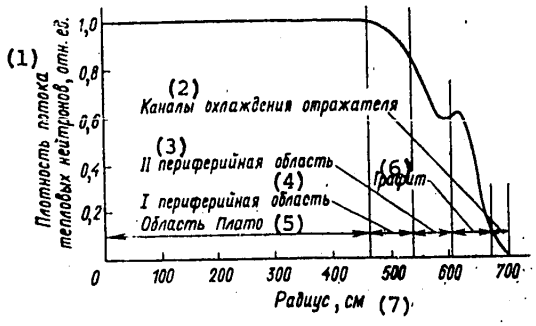

Figure 2.4. Neutron Flux Density Distribution Through Radius of Reactor (K_r = 1.1)

Key:
1. Neutron flux density, relative units
2. Reflector cooling channels
3. Second peripheral zone
4. First peripheral zone
5. Plateau zone
6. Graphite
7. Radius, cm

Table 2.12. Main Characteristics of Reactor in Steady Fuel Recharging Mode

(1) Характеристика	(2) Зона (см. рис. 2.4)		
	(3) плато	I периферийная (4)	II периферийная (5)
Радиус зоны, см (6)	465	541	612
Количество: (7)			
ячеек (8)	1087	384	413
ячеек периодичности (9)	68	24	26
загруженных каналов (10)	952	336	405
незагруженных каналов (11)	135	48	8
Средняя мощность канала, кВт (12)	1980	1940	1470
Средний коэффициент размножения (13)	1,02	1,05	1,07
Плотность потока тепловых нейтронов: (14)			
на границе ячейки, 10^{13} нейтр./(см^2·с) (15)	8,37	7,85	5,17
в топливе, отн. ед.: (16)			
в начале кампании (17)	0,591	0,585	0,580
в конце кампании (18)	0,570	0,564	0,559
в воде, отн. ед.: (19)			
в начале кампании	0,639	0,686	0,681
в конце кампании	0,661	0,656	0,652
в замедлителе, отн. ед.: (20)			
в начале кампании	0,973	0,969	0,967
в конце кампании	0,941	0,942	0,942
Коэффициент размножения: (21)			
в начале кампании	1,203	1,204	1,207
в конце кампании	0,832	0,885	0,920
Мощность канала, кВт: (22)			
в начале кампании	2540	2365	1745
в конце кампании	1405	1450	1140
Выгорание топлива*, ГВт·сут/т (23)	21,13	18,42	16,65
Кампания канала (24)	1160	1030	1230
Изотопный состав выгружаемого топлива, кг/т: (25)			
^{235}U	2,88	3,94	4,72
^{236}U	2,26	2,12	2,02
^{238}U	967,1	969,3	970,7
^{239}Pu	2,20	2,29	2,36
^{240}Pu	1,99	1,76	1,58
^{241}Pu	0,50	0,46	0,41
шлаки (26)	22,04	19,28	17,47

*The data are presented without regard to nonuniform burnup through the absorption height in SUZ channels and the heterogeneous effect.

Key:

1. Characteristic
2. Zone (see Figure 2.4)
3. Plateau
4. First peripheral
5. Second peripheral
6. Radius of zone, cm
7. Number
8. Of cells
9. Of periodicity cells
10. Of charged channels
11. Of uncharged channels
12. Average output of channel, kW
13. Average multiplication factor
14. Neutron flux density
15. At cell boundary, 10^{13} neutrons/(cm^2·s)
16. In fuel, relative units
17. At beginning of run
18. At end of run
19. In water, relative units
20. In moderator, relative units
21. Multiplication factor
22. Output of channel, kW
23. Fuel burnup, GW·day/t
24. Channel run
25. Isotope composition of removed fuel, kg/t
26. Poisons

The recharging coefficient K_{per} characterizes an increase of output of a freshly charged channel compared to the mean value. According to calculation $K_{per} = 1.21$ and the output of a freshly charged channel in the plateau zone of the RBMK reactor may reach approximately 3,000 kW with regard to the coefficients indicated above.

The output of each production channel in the reactor must be known to solve a number of design and operational problems, specifically to determine the reliability of the core and to select the distribution of coolant flow rates through the core channels. This calculation was possible with development of the BOKR and QUAM programs for two-dimensional calculation of the reactor. If they are used, it is no longer necessary to divide the core into zones, while the maximum output of the channel is determined by the actual state of the core and by the position of the control members. Calculations of the radial power distribution by two-dimensional programs confirmed the possibility of achieving an irregularity factor of $K_r = 1.27$.

Reactivity effects and coefficients. The reactivity effects and coefficients in the standard fuel recharging mode were calculated on the assumption that there are channels in each periodicity cell of the reactor with burnup of 0, 1, 2, 4, 5, 6, 8, 10, 12, 14, 16, 18 and 20 GW·day/t. The average fuel burnup is equal to 9 GW·day/t. Assuming that 20 SUZ rods are completely inserted into the core, the following reactivity coefficients were found: $\alpha_C = 5.2 \cdot 10^{-5} °C^{-1}$, $\alpha_{tv} = 4.9\ 10^{-5} °C^{-1}$, $\alpha_\gamma = -\ 2.14 \cdot 10^{-2} cm^3/g$, $\alpha_T = -1.15 \cdot 10^{-5} °C^{-1}$ and $\alpha_\phi = 1.52 \cdot 10^{-2}$. The effect of dehydrating the working channels in the cold state for a reactor with 25 rods removed was also determined for the steady fuel recharging mode and comprises 1.1 percent.

Natural indicators of the fuel cycle. The natural indicators of the fuel cycle such as consumption of enriched uranium, consumption of natural uranium, accumulation of secondary nuclear fuel and so on are usually considered to compare the engineering and economic parameters of the RBMK reactor to those of other types of reactors and to investigate fuel cycles. The natural indicators of the fuel cycle of the RBMK reactor are presented below:

Initial charging of reactor	
Mass of charged uranium, tons	165
Initial enrichment, percent	1.8*
Enclosure of natural uranium, tons	515
Transient operating mode	
Length of transient period, effective days	1,400
Average extent of uranium burnup of initial charge, GW·day/t	16.5
Average consumption of enriched uranium, t/year	38.0
Enrichment of uranium charged during transient period, percent	1.8
Average consumption of natural uranium, t/year	96.0
Average productivity of reactor in fissionable plutonium plutonium isotopes, kg/year	172
Average content in removed fuel, kg/t:	
U-235	5.0

Pu-239 and Pu-241	3.0
Steady recharging mode	
Mass of charged uranium, tons	192
Initial enrichment of loaded fuel, percent	1.8
Extent of burnup of unloaded fuel, GW·day/t	18.5
Consumption of enriched uranium, t/year	50.5
Consumption of natural uranium, t/year	136
Plutonium productivity of reactor, kg/year:	
all isotopes	253
fissionable isotopes	146
Content in unloaded fuel, kg/t:	
U-235	4.1
Pu-239 and Pu-241	2.9
Graphite mass in core, tons	2,000
Mass of zirconium pipes of channels, tons	103
Mass of zirconium in assemblies, tons	74
Consumption of zirconium, t/year	19.3

Note. Analyses of the operational data and additional calculations showed the possibility and feasibility of increasing the fuel enrichment. Conversion for enrichment of 2 percent is now carried out. Conversion to enrichment of 2.4 percent and higher is planned in the future.

The effective fraction of delayed neutrons A significant fraction of the output in the RBMK reactor is generated as a result of fission of Pu-239 nuclei accumulated during operation, the fraction of delayed neutrons of which is considerably lower than that of U-235: $\beta_{U-235} = 0.0065$ and $\beta_{Pu-239} = 0.0021$. The effective fraction of delayed neutrons β_{eff} decreases in this regard as the extent of fuel burnup increases (Table 2.13). For a reactor brought up to steady fuel recharging mode, $\beta_{eff} = 0.0045$.

Table 2.13. Variation of Effective Fraction of Delayed Neutrons

(1) Выгорание, ГВт·сут/т	β·ф	Выгорание, ГВт·сут/т	β·ф	Выгорание, ГВт·сут/т	β·ф
0	0,0065	7,13	0,0046	13,2	0,0040
1,00	0,0060	8,08	0,0045	14,0	0,0039
2,10	0,0056	9,00	0,0044	14,8	0,0038
3,15	0,0054	9,90	0,0043	15,5	0,0037
4,17	0,0051	10,80	0,0042	16,2	0,0037
5,18	0,0050	11,60	0,0041	16,9	0,0036
6,17	0,0047	12,4	0,0040	17,6	0,0036

Key:
1. Burnup, GW·day/t

Repoisoning of reactor upon variation of output. Variation of reactivity as a result of xenon poisoning during variation of output of a power reactor is of great interest. This is related to the fact that one or another reactivity reserve should be maintained as a function of the nature of load variation in the power

system and of the corresponding requirements placed on variation of reactor power, which has a direct effect on the extent of fuel burnup. All the characteristics of the RBMK reactor were calculated on the assumption that the operational reactivity reserve is equal to 1 percent. In this case a reduction of reactor power to 50 percent of the nominal level is possible without it falling into the iodine pit. The operational reactivity reserve must be increased to expand the range of permissible variation of power, which either reduces the extend of fuel burnup or requires an increase of the initial fuel enrichment to maintain the extent of burnup. The number of control rods that compensate for the operational reactivity reserve also varies. These functions are presented in Figure 2.5. The operational reactivity reserve also affects the permissible time of complete shutdown of the reactor or a reduction of power or on the time of scramming of the reactor if it falls into the iodine pit. Thus, if reactor power varies from the 100 percent level and if the operational reserve is 1 percent, the permissible time for complete shutdown of the reactor is approximately 1 hour and the forced shutdown time is approximately 24 hours; these times are equal to 3 and 18 hours, respectively, for an operational reserve of 2 percent.

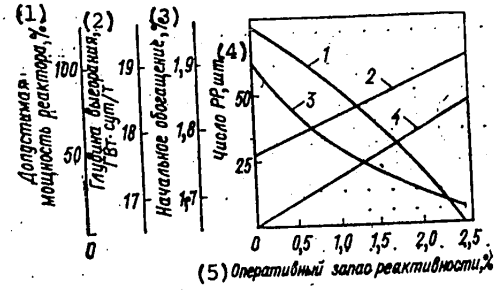

Figure 2.5. Dependence of Reactor Characteristics on Operational Reactivity Reserve: 1--extent of burnup with initial enrichment of 1.8 percent; 2--initial enrichment with burnup of 18.5 GW·days/t; 3--permissible output; 4--number of RR rods inserted into core

Key:
1. Permissible power of reactor, percent
2. Extent of burnup, GW·day/t
3. Initial enrichment, percent
4. Number of RR rods, units
5. Operational reactivity reserve, percent

Cases of cyclic variation of station load over 24 hours were also investigated: 16 hours at 100 percent power and 8 hours at reduced power (Figure 2.6). This operating mode was permissible for an operational reserve of 1 percent with dumping of load up to 50 percent, but reactivity over a period of 24 hours varies by approximately 1.2 percent (by approximately 0.8 percent toward a decrease and 0.4 percent toward an increase from the steady poisoning level during operation at constant nominal power). The operator should compensate for variation of reactivity by the RR rods, providing minimum power misalignments in this case.

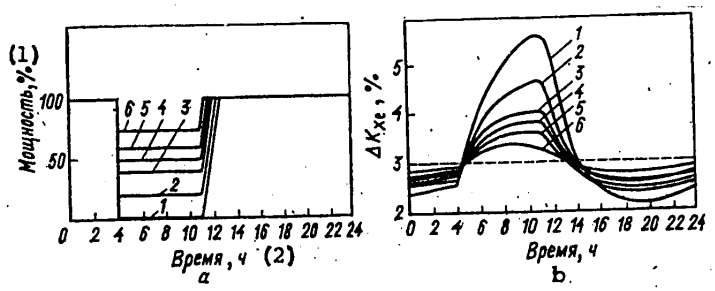

Figure 2.6. Daily Schedule of Reactor Power Variation (a) up to 0 (1), 20 percent (2), 40 percent (3), 50 percent (4), 60 percent (5), 75 percent (6) and the corresponding variation of the degree of xenon poisoning during cyclic operation (b)

Key:
1. Output, percent
2. Time, hr

Some functions of interest during operation, related to reactor poisoning, are presented in Tables 2.14-2.16.

Table 2.14. Variation of Degree of Xenon Poisoning ΔK_{Xe} on Time During Operation of Reactor at 100 Percent Power

(1) Время, ч	ΔK_{Xe}, %	Время, ч	ΔK_{Xe}, %	Время, ч	ΔK_{Xe}, %
0	0	12	1,93	24	2,68
2	0,27	14	2,13	26	2,74
4	0,66	16	2,29	28	2,79
6	1,05	18	2,42	30	2,82
8	1,40	20	2,53	∞	2,98
10	1,69	22	2,61		

Key:
1. Time, hr

Table 2.15. Variation of Xenon Poisoning With Total Reactor Shutdown, Percent

(1) Отравление	(2) Мощность реактора перед остановкой, %				
	100	75	50	40	25
Стационарное (3)	2,98	2,80	2,53	2,35	1,94
Максимальное, в иодной яме (4)	6,35	5,05	3,73	3,20	2,24
Глубина иодной ямы (5)	3,37	2,25	1,2	0,85	0,30

Key:
1. Poisoning
2. Reactor power prior to shutdown, percent

[Key continued on following page]

[Key continued from preceding page]:
3. Steady
4. Maximum, in iodine pit
5. Depth of iodine pit

Table 2.16 Steady Xenon Poisoning at Different Levels of Reactor Power N_p

N_p, %	ΔK_{Xe}, %	N_p, %	ΔK_{Xe}, %
10	1,15	60	2,66
20	1,74	70	2,77
30	2,11	80	2,85
40	2,35	90	2,92
50	2,53	100	2,98

The nature of variation of xenon poisoning in time with total shutdown of the reactor is presented in Figure 2.7 as a function of the previous power level.

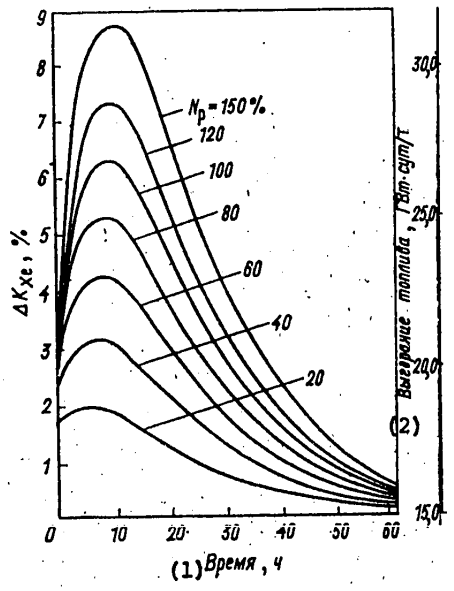

Figure 2.7. Variation of Xenon Poisoning After Shutdown of Reactor Operating at Different Power Levels

Key:
1. Time, hr
2. Fuel burnup, GW·day/t

Effect of deviations of production parameters on reactivity and extent of burnup. The dependence of burnup and of some other characteristics of a reactor on fuel density, coolant density, channel output and other parameters for the reactor plateau zone is presented in Table 2.17. The initial value of the mean multiplication factor of the core in the steady recharging mode is equal to 1.03 (1.01 is

the operational reactivity reserve and 0.02 is reactivity for leakage through the height of the reactor with regard to equalization of the neutron flux during burnup); fuel density is γ_t = 8.814 g/cm^3, water density is γ_v = 0.516 g/cm^3, graphite density is γ_C = 1.67 g/cm^3, average channel output is 2,100 kW and uranium enrichment is C_5^Q = 17.87 kg/t. The estimated dependence of the extent of burnup and the initial multiplication factor on fuel enrichment is presented in Figure 2.8.

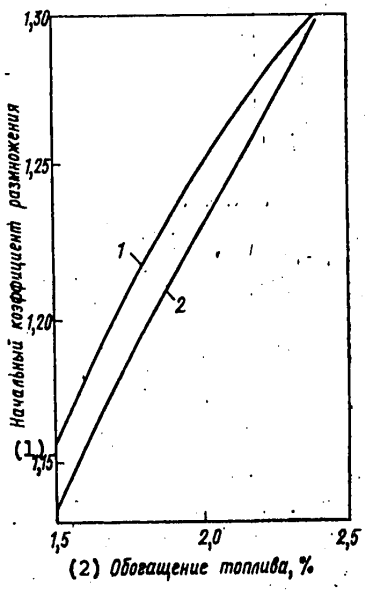

Figure 2.8. Dependence of Initial Multiplication Factor (1) and Extent of Burnup (2) on Fuel Enrichment (lattice spacing of 26.7 cm)

Key:
1. Initial multiplication factor
2. Fuel enrichment, percent

2.4.5. Efficiency of Control and Monitoring Members

The control and monitoring members of the RBMK reactor consist of 179 absorbing rods. They are functionally divided into 89 manual control rods (RR), 12 automatic control rods (AR), 21 emergency power reduction rods (AZ) and 21 shortened absorbing rods (USP). The SUZ channel has an outer diameter of 88 and inner diameter of 82 mm and is made of a zirconium alloy of mark 125. The absorbing material of the rod is B_4C with density of 1.65 g/cm^3. The parameters of the absorbent, mm, are:

Outer diameter of sleeve	65
Inner diameter	50
Outer diameter of jacket	70
Length of absorbing section:	
of RR, AZ and AR rods	5,120
of USP rods	3,000

Table 2.17. Effect of Production Deviations on Reactivity and Extent of Burnup

(1) Параметр	(2) Глубина выгорания, ГВт·сут/т	(3) Изменение глубины выгорания, ГВт·сут/т	(4) Начальный коэффициент размножения	(5) Изменение начального коэффициента размножения
(6) Основное состояние	21,017	—	1,211615	—
(7) Изменение плотности топлива до 8,914 г/см³	21,118	0,101	1,212293	0,00068
(8) Изменение плотности воды до 0,416 г/см³	21,640	0,623	1,215447	0,003832
(9) Изменение коэффициента размножения до 1,02	21,920	0,903	1,211468	—0,000147
(10) Изменение средней мощности канала до 1900 кВт	21,022	0,005	1,212628	0,001013
(11) Изменение плотности графита до 1,72 г/см³	20,912	—0,105	1,212645	0,001030
(12) Изменение обогащения урана до 18,37 кг/т	21,921	0,904	1,220405	0,00879
(13) Уменьшение наружного диаметра канальной трубы до $d_{нар}$=84 мм	22,240	1,223	1,231459	0,019844
(14) Увеличение массы стали в каждом канале на 1 кг	20,152	—0,865	1,198020	—0,013595
(15) Уменьшение толщины оболочки твэла на 0,1 мм при сохранении внутреннего диаметра оболочки	21,131	0,114	1,214540	0,002925
(16) Уменьшение толщины оболочки твэла на 0,1 мм при увеличении внутреннего диаметра оболочки	21,522	0,505	1,216661	0,005046

Key:
1. Parameter
2. Extent of burnup, GW·day/t
3. Variation of extent of burnup, GW·day/t
4. Initial multiplication factor
5. Variation of initial multiplication factor
6. Main state
7. Variation of fuel density to 8.914 g/cm^3
8. Variation of water density to 0.416 g/cm^3
9. Variation of multiplication factor to 1.02
10. Variation of average channel output to 1,900 kW
11. Variation of graphite density to 1.72 g/cm^3
12. Variation of uranium enrichment to 18.37 kg/t
13. Decrease of outer diameter of channel pipe to d_{nar} = 84 mm
14. Increase of mass of steel in each channel by 1 kg
15. Decrease of thickness of fuel jacket by 0.1 mm while maintaining inner diameter of jacket
16. Decrease of thickness of fuel jacket by 0.1 mm with increase of inner diameter of jacket

Structurally the rods are made of individual absorbing sections 967.5 mm long each with gap of 65 mm between sections. The rods are cooled by a special water circuit with temperature of 60-90°C. The RR, AZ and USP rods have displacers with outer diameter of 74 mm and length of 4,960 mm to reduce the harmful absorption of

neutrons in the cooling water. Thus, if these rods are completely removed from the core, a displacer is located in the channel symmetrically with respect to the center of the core while sections of the channel approximately 1 meter long from the top and bottom of the displacer are filled with water. The AR rods have no displacer and the channel is completely filled with water when they are removed.

The travel of the RR and AZ rods is 6,250 mm and that of the AR rods is 4,500 mm. Being located in the extreme upper position, these rods are completely removed from the core and are separated by 200 mm from its upper boundary. The USP rods have travel of 7,000 mm and are completely removed through the bottom of the core and in this position the upper end of the USP rod is located at the level of the lower boundary of the core.

The efficiency of the individual structural components of the SUZ channels in the reactor plateau zone are essentially independent of the reactor operating period--initial or steady. The efficiencies presented in Table 2.18 were calculated with respect to a solid graphite block for an absorber equal in length to the height of the core.

Table 2.18. Efficiency of Idealized SUZ Rod, 10^{-4}

Contents of SUZ Channel	State of Working Channels		
	Hot	Cold with Water	Cold Without Water
Absorbing rod	8.12	6.08	7.69
Displacer	0.45	0.75	0.69
Water column	2.64	3.31	3.36

The neutron flux distribution through the height for a steady recharging mode is taken into account to determine the efficiency of rods with regard to their real dimensions and arrangement through the height of the core. The curve of the relative effectiveness of the absorbent corresponding to this flux is shown in Figure 2.9 as a function of the depth of insertion. The reactivity introduced with complete displacement of the RR, AR and USP rods located in the reactor plateau zone is presented in Table 2.19. The distribution of reactivity through the rods of different types is presented in Table 2.20.

Table 2.19. Efficieny of Real SUZ Rods in Plateau Zone, 10^{-4}

Rod	State of Working Channels		
	Hot	Cold With Water	Cold Without Water
RR, AZ	6.27	4.34	5.50
AR	3.55	1.78	2.79
USP	4.49	3.54	4.53

The values of the total efficient of the rods in the reactor presented above were calculated for a two-zone reactor model through the radius (the periphery plateau). Therefore, the efficiency of the rods was also calculated by two-dimensional programs. The calculations show that if the peripheral rods whose efficiency is determined to a significant degree by the specific structure of the surrounding zone

are excluded from consideration, then the efficiency of the rods is proportional to the square of the neutron field in the region of insertion of the rod with accuracy up to 10 percent. Therefore, the efficiencies of the rods in the plateau zone may differ in the range of ± 30 percent according to deviations of the field from a uniform plateau in the zone in the range of ± 15 percent. Nevertheless, the experience of operating the RBMK reactor shows that in some cases, for example, when determining the effects of variation of reactivity at which shifting of a large number of rods occurs, the concept of average rod efficiency, which is equal to approximately $50 \cdot 10^{-5}$, can be introduced, which is less than the reactivity of the RR rod in the plateau zone since the peripheral rods are also taken into account.

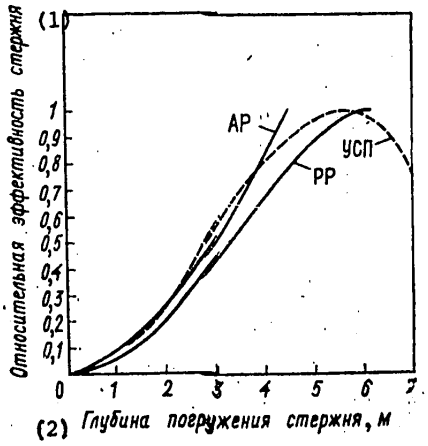

Figure 2.9. Relative Efficiency of Rod

Key:
1. Relative efficiency of rod
2. Depth of rod insertion, meters

The deformation of the neutron field through the reactor radius with shifting of the control rods was investigated from the results of the two-dimensional calculations made. Deformation of the neutron flux near the rod with total and partial insertion of it is shown in Figure 2.10. The degree of deformation was determined as the ratio of the mean flux density on a given radius after insertion of the rod to the flux density prior to insertion of the rod. Averaging was carried out for all cells located at the same distance from the rod. This ratio is less than 1 for all rods at a distance up to 12 spacings of the channel lattice from the rod and the ratio then becomes greater than 1 due to redistribution of the neutron field through the entire reactor.

Efficiency of rods with film cooling. The design of control rods with displacers in the RBMK reactor is not optimum in neutron balance. Actually, a considerable amount of water that absorbs neutrons remains in it after the rod is removed from the core. When all the rods are removed from the core, the harmful absorption in

Table 2.20. Total Efficiency of Rods

(1) Стержни	(2) Состояние реактора		
	(3) Горячее	(4) Холодное с водой	(5) Холодное без воды
(6) РР	0,0443	0,0309	0,0390
(7) АЗ	0,0360	0,0247	0,0314
(8) АР	0,0042	0,0021	0,0033
(9) УСП	0,0094	0,0074	0,0095
(10) Все стержни	0,094	0,065	0,083

Key:
1. Rods
2. State of reactor
3. Hot
4. Cold with water
5. Cold without water
6. RR
7. AZ
8. AR
9. USP
10. All rods

Table 2.21. Efficiency of SUZ Rods With Film Cooling, 10^{-4}

(1) Стержень	(2) Состояние реактора		
	(3) Горячее	(4) Холодное с водой	(5) Холодное без воды
РР, АЗ (6)	6,85	5,1	6,47
АР (7)	3,55	1,78	2,79
УСП (8)	4,49	3,54	4,53
Столб воды (9)	2,34	3,01	3,06

Key:
1. Rods
2. State of reactor
3. Hot
4. Cold with water
5. Cold without water
6. RR and AZ
7. AR
8. USP
9. Water column

the structural elements of the SUZ channels comprises 1.87 percent, including 0.34 percent in the zirconium channels, 0.53 percent in the displacers and 1.0 percent in the cooling water.

The water flowing around the displacer and filling the SUZ channel from the top and from the bottom makes the greatest contribution to harmful absorption. The so-called film cooling system of the SUZ channels in which the flow rate of cooling water decreases to the level required to create a surface film approximately 1 mm thick that cools the pipe of the production channel after removal of the rod from the core has the best neutron-physical characteristics in this respect. Besides

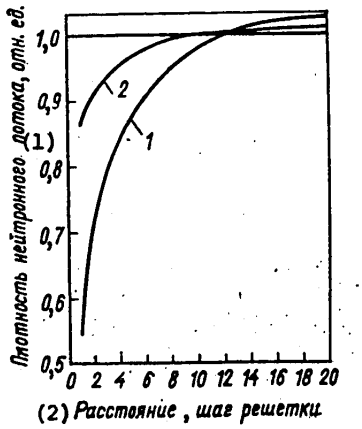

Figure 2.10. Deformation of Neutron Flux Density Distribution with Variation of Position of Control Rod: 1--total insertion of rod; 2--insertion of rod by 2.5 meters

Key:
1. Neutron flux density, relative units 2. Distance, lattice spacing

reducing the amount of water in the core, this cooling system has a number of other advantages. For example, the conditions of equalizing the energy release field through the reactor height are improved (the coefficient of field nonuniformity in height comprises approximately 1.2 in the steady mode) and the extent of fuel burnup increases by approximately 700 MW·day/t. It essentially becomes possible to control the neutron field by varying the height of the water column in the SUZ channel. Some characteristics of the RR and AZ rods with film cooling are presented in Table 2.21. The design and dimensions of the AR and USP rods do not change and the length of the RR and AZ rods is 6,130 mm. The channels of the RR and AZ rods operate in the film cooling mode. The efficiency of the rod increases by 9 percent in the hot state.

The fraction of absorbed neutrons in the SUZ channels is presented below with respect to a solid graphite block with different filling of cooling water, 10^{-4}:

Water layer with thickness, mm:	
0	0.21
1.0	0.30
1.5	0.32
2.0	0.34
2.5	0.36
3.0	0.38
Displacer 7 meters long	0.45
Water column	2.64

Harmful neutron absorption in the core with total removal of all RR and AZ rods with film cooling of the channels comprises 0.94 percent, including 0.34 percent in the zirconium channels, 0.05 percent in the USP displacers and 0.55 percent in the cooling water. The average heat release per unit of rod length is 80 W/cm^2. With RR rod length of 510 cm, heat release comprises 41 kW and the maximum specific heat release is 112 W/cm (at K_r = 1.4).

2.5. Nuclear Safety

The core of the RBMK reactor and the fuel assemblies and also the reactor control and safety system and its actuating members are made with regard to the main requirements of nuclear safety regulations of the reactor which is provided in all operating modes and states of the reactor and also during any possible emergency situations in the production circuit.

The efficiency of 21 AZ rods with minimum rod efficiency of $4.3 \cdot 10^{-4}$ in the cold state of the reactor comprises 0.9 percent, which exceeds the value of β in reactivity with a reserve sufficient with regard to possible "hanging" of part of the rods. The efficiency and number of AZ rods was selected on the basis of the maximum possible rapid variation of reactivity. Variation of reactivity upon "collapse" of steam in the core and cooling of the fuel elements to temperature at input into the reactor (265°C) and upon dehydration of the fuel channels in a cold reactor was considered. It was shown by calculations that the values and even the signs of these effects are considerably dependent on the composition of the core: on fuel burnup, the number of DP, SUZ rods, displacers and the water columns. Therefore, states more typical for different phases of reactor operation were selected to determine the effects of reactivity and the number of AZ rods. Of course, the conditional calculated representation of the core structure was taken into account in this case. The values of the considered fast-proceeding variations of reactivity used to determine the number of AZ rods are presented in Table 2.22.

Table 2.22. Fast-Occurring Variation of Reactivity as a Function of Extent of Fuel Burnup

Effect of Reactivity	State of Reactor: Initial load	Burnup of 5 GW·day/t	Burnup of 10 GW·day/t	Steady Mode
Dehydration of fuel channel in cold state	-0.0108	-0.0096	-0.0067	0.0093
"Collapse" of steam and "cooling" of fuel elements	0.0083	--	--	-0.0003

According to the calculated efficiency of SUZ rods in different states and according to the data of Table 2.21, the number of rods should be no less than 17. Taking into account that the error of calculating the efficiency of a rod may be estimated at $\pm$ 20 percent, the number of AZ rods was assumed equal to 21. The minimum efficiency of one group of AR, consisting of four rods, comprises $7.2 \cdot 10^{-4}$ and the efficiency of one AR group in the hot state comprises $14.4 \cdot 10^{-4}$. With a rate of displacement of the rods of 0.4 m/s, the minimum rate of input of reactivity by the AR rods comprises $0.75 \cdot 10^{-5}$ s^{-1} = 0.012 β/s (on the linear section of the graduated curve).

Table 2.23. Value of K_{eff} for Different States of Reactor with Charged SUZ Rods

Average Extent of Fuel Burnup, GW·day/t	State of Core		
	Working	Cold with Water	Cold without Water
0 (initial charge)	0.913	0.967	0.963
5	0.927	0.954	0.950
10	0.937	0.938	0.947
Steady recharging mode	0.917	0.922	0.926

A decrease of the compensating capability of both the SUZ and DP rods due to the difference of their actual design and arrangement through the core from the idealized calculated models used was taken into account in the calculations. The results of calculations for different states of the reactor and different moments with respect to the run are presented in Table 2.23, from which it is obvious that the SUZ system provides the required subcriticality of the reactor for all states. It should be noted that a core structure in which the inserted DP channels were partially replaced by fresh TVS was arbitrarily assumed for burnup of 10 GW·day/t. Specifically, the core was assumed to consist of 35 periodicity cells with 2 DP and two displacers, 20 cells with one DP, one displacer and one SUZ rod and 65 cells with one DP and two displacers for burnup of 5 GW·day/t; it consisted of 20 cells without DP and with two displacers, 20 cells without DP and with one displacer and one SUZ rod and 50 cells with one DP and two displacers for burnup of 10 GW·day/t. The actual state of the reactor will naturally differ from that assumed. Therefore, "instructions to ensure nuclear safety during recharging operations in the RBMK reactor" were worked out to observe the conditions of nuclear safety during operation of the reactor in the group DP recharging mode.

2.6. Physical and Power Startup of Reactor

Experiments during physical startup of the first unit of the RBMK reactor. Startup of the RBMK reactor is an important phase of checking the correctness of the calculated methods and of the applicability of the physical models and finding the final, most dependable neutron-physical characteristics of the reactor. Special attention should be devoted to obtaining information required for subsequent operation of the reactor.

The main problems of experiments conducted during physical startup of the reactor and assembly of full charge of the core reduce to the following. Several ever-increasing critical systems for estimating the characteristics of the fuel assemblies, DP, SUZ rods and graphite stacking are assembled for comparison with experimental data found on a bench or on previous reactors. The minimum critical system, including the assemblies located in the center of the core, are first assembled according to the charging cartogram; the critical systems with DP and with DP and SUZ rods are then assembled. The reactivity effects when the SUZ channels, channels with assemblies and with DP are filled with water are analyzed as full charge is approached. The neutron fields are measured in a full charge. The initial charge of the reactor is shaped with regard to the specific production characteristics of its components during the final phase by readjustment or removal of several DP. The results of calculations are corrected parallel to obtaining the

experimental data. The detailed order of experiments with calculated substantiation for each reactor is determined by the working program of physical startup.

A system without DP with standard SUZ rods removed with dehydrated MPTs circuits and cooling of SUZ reached criticality after charging of 23 fuel assemblies with two partially charged rods of the temporary SUZ).

A system with additional absorbers was then investigated, which made it possible to determine the critical mass with removed SUZ rods and to estimate the efficiency of the initially selected composition. A DP composition with ratio of 3:1 of heavy and light sleeves in the central part 5,000 mm long and ratio of 1:2 in the end sections 1,000 mm long each was taken and charging was continued up to 77 periodicity cells from the results of analyzing the experiment and calculation.

Reactivity effects related to filling the SUZ channels and channels with fuel assemblies and DP with water were investigated in a system consisting of 77 periodicity cells. The experiments were conducted in three phases:

1) study of the reactivity effects with SUZ channels filled with water with "dry" MPTs circuit;

2) investigating the variation of reactivity with the MPTs circuit filled with water with filled SUZ circuit;

3) determining the effect of dehydration of the SUZ circuit with MPTs circuit filled.

Each phase of the investigations was completed by bringing the reactor to the critical state.

The SUZ channel cooling circuit was filled separately for each group of rods. Positive reactivity was observed with the channels having charged rods filled with water, while the water in the channels with removed rods reduced the reactivity as a result of neutron absorption. The total effect of filling the SUZ circuit with water was negative and was compensated for by removing 16 standard SUZ rods and by inserting two RR rods of the temporary SUZ. Filling the MPTs circuit with water led to determination of positive reactivity of 1.75 β. Dehydration of the SUZ circuit with water in the MPTs circuit was compensated for by introduction of 19 standard SUZ rods.

It was established as a result of the experiments that a system with MPTs circuit filled with water and dehydrated SUZ circuit has the highest reactivity. However, further charging was continued in the completely dehydrated core with regard to the need of conducting production work in the MPTs circuit.

The effect of variation of reactivity with dehydration of channels containing fuel assemblies, which was negative and equal to 0.15 β, was determined in this system of 77 periodicity cells. Removal of water from DP channels decreased the reactivity of the system by 1.8 β.

One of the important integral parts of physical startup was measuring the energy release fields through the reactor. The purpose of these measurements was as follows:

selecting the final arrangement of the fuel assemblies and DP;

analysis of the capabilities of equalizing the energy release field with SUZ rods;

substantiation of using the physical calculation programs to predict the energy release fields;

determination of the effects of the field microstructure and other characteristics required to process the discrete measurements of the energy release fields during operation of the reactor.

The measurements were made by small fission chambers whose design was specially calculated for installation in the carrier tubes of the fuel assemblies with energy release monitors. The measurements were made at eight points through a height of 249 assemblies. The calculated distribution gives a good reflection of the microstructure of the energy release field, but yields exaggerated values of energy release on the reactor periphery. Analysis of the divergence of the experimental distribution of the energy release field with the calculated value found by the BOKR-COBZ program showed that the structure of the zone, specifically the extent of insertion of the rods, the presence of channels under the starting ionization chambers in the reflector and the axial distribution of the neutron field, must be taken into account in detail for more accurate calculation of the energy release field. Comparison of the experimental and calculated data found during physical startup of the reactor of the second unit showed that the mean square deviation of the calculated data found by the BOKR-COBZ program (with regard to the height distribution of neutrons) comprises 9.7 percent from the experimental values. This deviation was also found for calculations made by the QUAM-2 program.

Investigation of the physical characteristics during power startup. Measuring the reactivity effects and coefficients.

Determination of reactivity effects begins with determination of the integral effect of variation of reactivity upon heating of the reactor. Calibrated curves for "weighing" individual rods, obtained in the reactor during heating, are used to estimate the variation of reactivity compensated for by moving the SUZ rods.

The total temperature coefficient α_Σ that takes into account the simultaneous variation of temperature and water density, fuel and graphite temperature measured during first heating of the reactor in the temperature range of 100-220°C was negative and equal to $-(4 \pm 0.5)\cdot 10^{-5}°C^{-1}$. The total temperature coefficient determined upon heating of the reactor after operation for 25 effective days comprised $-(5 \pm 0.5)\cdot 10^{-5}°C^{-1}$ in the temperature range of 120-260°C. Comparison of the states of the reactor with the constants of water temperature and power, but differing graphite temperature, permits one to determine the temperature coefficient of the graphite α_C. The value of $\alpha_C = (3 \pm 1)\cdot 10^{-5}°C^{-1}$ upon heating for the initial charge of the reactor.

Precise determination of the reactivity coefficients, which however it is complicated to determine by calculation, is required to ensure reliable and safe operation of the reactor; therefore, a program of experiments to determine the steam and power coefficients is realized in the reactor. An estimate of the steam coefficient of reactivity, according to a mode with deviation of one power pump by 45 percent of nominal power, carried out with average fuel burnup of 500 MW·day/t in the first unit of the RBMK, yielded $\alpha_\phi = \Delta\rho/\Delta\phi = -0.22\beta$. A steam coefficient of reactivity α_ϕ was determined by deviation of two GNTs upon burnup of 3.5 GW·day/t. The experiment was conducted with reduction of power and low operational reserve of reactivity (6-8 rods). Processing of the experimental data showed that the steam void coefficient of reactivity became positive: $\alpha_\phi = +0.7\beta$.

The total power coefficient of reactivity (with time constant of the effect less than 100 seconds), measured at power of 2,060 MW (t) with burnup of 1 GW·day/t, was found to be negative: $\alpha_N = \Delta\rho/\Delta N = -2.5\cdot10^{-6}$ MW^{-1} (thermal); $\alpha_N = -3.2\cdot10^{-6}$ MW^{-1} with burnup of 2 GW·day/t and with power reduction from 1,540 to 1,240 MW (t).

The temperature coefficient of graphite $\alpha_C = 4\cdot10^{-5}{}^\circ C^{-1}$ was determined by replacing the helium purging of the graphite stacking with nitrogen purging with constant reactor power and burnup of 3.5 GW·day/t. Processing the graphite temperature by the readings of standard thermocouples with averaging through the reactor volume (without regard to the nonuniformity of the graphite block through the volume) showed that the increase of the mean graphite temperature through the reactor per MW of thermal power is equal to 0.05°C/MW for helium cooling of the stacking and was equal to 0.1°C/MW for nitrogen cooling. Accordingly, the power coefficient of reactivity through the graphite was equal to $0.2\cdot10^{-5}$ MW^{-1} for helium cooling and to $0.4\cdot10^{-5}$ MW^{-1} for nitrogen cooling. The error of determining the data can be estimated at $\pm$ 30 percent.

Experimental investigation of energy release fields. The distribution of the residual γ-activity of the TVS was measured repeatedly in the shutdown reactor during operation of the RBMK reactor. The purpose of these experiments was to calibrate the radial distribution sensors, to determine the error of discrete monitoring of the energy release fields and to estimate the error of calculating the energy release fields. According to the experimental results, the mean square errors of determining the output of the TVS comprise 9 percent forphysical calculation by the BOKR-COBZ program and 3 percent for γ-scanning.

Satisfactory agreement of the calculated and measured power distribution of the fuel assemblies made it possible to confidently use the calculated data for operational control of the energy release field in the core by using the Prizma program in the plant computer. Besides the Prizma program, the energy release fields were monitored and controlled through the reactor by using calculations by a complex of Bazis programs on an external BESM-6 computer. The complex of Bazis programs combines the program for physical calculation of the fields (BOKR-COBZ), the program of statistical interpolation of channel output from the readings of the energy release monitoring sensors (Atlas) and the program for thermohydraulic calculation of the channels and calculation of the heat engineering reliability (Zapas). The position of the control members, fuel burnup in the channels, currents of the intrareactor sensors and distribution of the coolant flow rates through the reactor channels are used as the input data. The power distribution

through all the operating channels of the reactor, the error of determining the output of each channel and the reserve to heat transfer crisis in each channel are determined as a result of calculation. The complex of Bazis programs is a means of monitoring the operation of the Prizma program.

Recharging the RBMK reactor during operation. A loss of reactivity due to fuel burnup is restored when the reactor is recharged. Recharging the channels during operation by means of an unloading-loading machine (RZM) is provided in RBMK reactors. If putting the RZM into operation is delayed, the channels can be recharged in groups (the DP is unloaded during the initial phase) in a shutdown reactor. The number and location of the removed DP is determined by the specific operating conditions of the reactor prior to shutdown (the reactivity reserve, the form of radial energy release and so on) and after shutdown (maximum power and proposed operating time). Calculated prediction of the next recharging is made by BOKR-COBZ and QUAM-2 programs, but a depoisoned reactor with dehydrated SUZ cooling circuit (a state with maximum reactivity) is periodically brought to the critical state after each recharging to check that nuclear safety conditions are fulfilled. The main characteristics of recharging carried out on the RBMK reactor of the first unit of the Leningrad AES are presented in Table 2.24 and the change of the core structure is shown.

All the DP were distributed on several lattices embedded one into the other, which were recharged in sequence, for convenience in selecting the DP during routine recharging. The peripheral DP are exceptions to this rule, which is related to the characteristic features of the SUZ rod lattice on the reactor periphery. The DP of the peripheral group are recharged as necessary with regard to equalization of the radial energy release field.

Physical startup of the second unit of the RBMK reactor. Physical startup of the second unit of the RBMK reactor was begun in May-June 1975. The most important problem of the experiments carried out during physical startup was comparison of the characteristics of the reactors of the first and second units. Systems investigated in the reactor of the first unit were brought to the critical state several times for this purpose during assembly of a full charge and a full charge completely similar to the initial charge of the reactor of the first unit was also assembled. It was established by experiments that all the investigated critical systems have lower reactivity than the corresponding systems of the reactor of the first unit. This difference comprised 0.5 percent for a full charge with water in the MPTs circuits and SUZ cooling.

Analysis of the calculated and experimental data showed that this divergence can be explained to a significant degree by the difference in the average graphite density in the reactors of both units (1.73 and 1.67 g/cm^3, respectively). The effect of dehydration of the fuel channels (0.65 β for the second unit compared to 0.5 β for the first unit) became somewhat more negative.

The number of DP was reduced to supplement the deficient reactivity in the reactor: the initial charge contains 1,455 TVS and 230 DP and eight channels (on the reactor periphery) remained uncharged. The initial reactor charge is presented in Figure 2.3. Physical startup of the reactor is an important phase of putting an AES into operation. The startups of the RBMK reactors showed that the difference of

Table 2.24. Main Recharging Characteristics

Number of Recharging	Date of Shutdown for PPR	Reactor Operating Time from Startup, effective days	Removed DP	Removed TVS	TVS Loaded	Composition of Core After Recharging FK	Composition of Core After Recharging DP	Composition of Core After Recharging Uncharged Channels	Number of RR Inserted prior to Shutdown	Increase of Reactivity Upon Recharging (calculation), percent
1	12 Jan 74	5.55	17	0	13	1,465	224	4	38	1.1
2	13 Mar 74	24.12	9	0	7	1,472	215	6	40	1.01
3	15 May 74	49.06	2	0	6	1,478	213	2	38	0.36
4	28 Aug 74	108.51	16	0	17	1,495	197	1	22	1.55
5	12 Dec 74	180.06	40	1	40	1,534	157	2	9	2.46
6	15 May 75	265	38	0	39	1,573	119	1	15	2.36
7	15 Aug 75	307	21	0	21	1,594	98	1	35	1.2

characteristics has a significant effect on the properties of the core for technical reasons of the core components. Therefore, physical startup should precede introduction of each reactor. The process of physical startup permits formation of a specific charge of each newly introduced reactor with regard to the actual characteristics of the core components and to ensure conditions of subsequent reactor operating safety.

BIBLIOGRAPHY

1. Feynberg, S. M., "Heterogeneous Methods of Reactor Calculation. Survey of Results and Comparison to Experiment," in "Materialy Mezhdunarodnoy konferentsii po mirnomu ispol'zovaniyu atomnoy energii" [Proceedings of an International Conference on Peaceful Uses of Atomic Ene gy], Geneva, 8-20 August 1955, Vol 5, "Fizika reaktorov" [Reactor Physics], Moscow, Izdatel'stvo AN SSSR, 1958.

2. Galinin, A. D., "Teoriya yadernykh reaktorov na teplovykh neytronakh" [The Theory of Nuclear Reactors Based on Thermal Neutrons], Moscow, Atomizdat, 1959.

3. Akimov, I. S., M. Ye. Minashin and V. N. Sharapov, "Developing Methods of Physical Calculation of Nuclear Reactors from the World's First AES to the Present;" ATOMNAYA ENERGIYA, Vol 36, No 6, 1974.

4. Yemel'yanov, I. Ya., M. B. Yegiazarov, V. I. Ryabov et al, "Physical Startup of the RBMK Reactor of the Second Unit of the Leningrad AES imeni V. I. Lenin," ATOMNAYA ENERGIYA, Vol 40, No 2, 1976.

5. Gorodkov, S. S., "Novyy metod rascheta geterogennykh reaktorov" [A New Method of Calculating Heterogeneous Reactors], Preprint IAE-2251, Moscow, 1973.

6. Gorodkov, S. S., "Instruktsiya po pol'zovaniyu programmoy rascheta geterogennykh reaktorov QUAMHER" [Instructions on the Use of the QUAMHER Program for Calculation of Heterogeneous Reactors], Preprint IAE-2294, Moscow, 1974.

7. Batov, V. V., Yu. I. Koryakin, V. I. Pushkarev et al, "The Economics of the Transition Period of the Reactors of Nuclear Power Plants," ATOMNAYA ENERGIYA, Vol 26, No 3, 1969.

8. Batov, V. V., Yu. I. Koryakin, V. I. Pushkarev et al, "Selecting the Optimum Operating Modes of Fuel Charging," in "Nuclear Energy Costs and Economic Development, Proceedings of a Symposium, Istanbul," 20-24 Oct 1969.

9. Yemel'yanov, I. Ya., A. D. Zhurnov, V. V. Pushkarev et al, "Forming the Initial Charge in a Large Channel-Type Reactor," in "Opyt ekspluatatsii AES i puti dal'neyshego razvitiya atomnoy energetiki" [The Experience of Operating Nuclear Power Plants and Methods for Further Development of Nuclear Power Engineering], Obninsk, FEI, Vol 1, 1974.

10. Palmedo, P. F., "A Semi-empirical Description of Detailed Thermal Flux Distribution," NUCLEAR SCIENCE AND ENGINEERING, Vol 21, 1965.

DESIGN OF A REACTOR PLANT

Moscow KANAL'NYY YADERNYY ENERGETICHESKIY REAKTOR in Russian 1980 (signed to press 27 Mar 80) pp 48-79

[Chapter 3 from the book "Channel-Type Nuclear Power Reactor", by Nikolay Antonovich Dollezhal' and Ivan Yakovlevich Yemel'yanov, Scientific Research and Design Institute of Power Engineering, Atomizdat, 2,550 copies, 208 pages]

3.1. The Reactor

The channel-type boiling-water RBMK reactor (Figure 3.1) with graphite moderator and water coolant is designed to generate saturated steam at pressure of 70 kgf/cm^2 (approximately 7 MPa). The main structural part of the reactor--the core--is formed on the basis of calculation and theoretical investigations considered in the previous chapter, where the core structures and its components are also described. The core is located in a concrete shaft measuring 21 X 21 meters and 25 meters deep. The cylindrical graphite stacking 5 consists of blocks with axial cylindrical openings assembled into columns in which fuel and special channels are installed and is located in a sealed cavity (the reactor space) formed by the cylindrical vessel and plates of the upper and lower assembled steel sections. The reactor space is filled with a mixture of helium (approximately 40 percent by mass) and nitrogen to prevent oxidation of the graphite and to improve heat transfer from the graphite to the fuel channels; leakage of helium is limited by filling the assembled steel sections and the spaces surrounding the cylindrical vessel with nitrogen under pressure exceeding the pressure of the helium-nitrogen mixture by 20-120 mm Hg (approximately 0.2-1.2 kPa).

The reactor has upper 8, lower 3 and side 4 biological shielding which reduces the radiation intensity during operation and all power levels to permissible values corresponding to sanitary standards in the USSR. The fuel channels (1,693) are installed in pipe conduit welded into the assembled steel sections.

The coolant is circulated in the reactor circuit by the following scheme. The coolant--water at temperature of 270°C--is distributed from the pressure vessel of the main circulating pumps by regulating valves and by individual pipelines 2 through the fuel channels. Rising upward and flowing around the fuel elements, the water is heated to saturation temperature, is partially evaporated (the average steam content is approximately 15 percent) and is fed to the separator drums

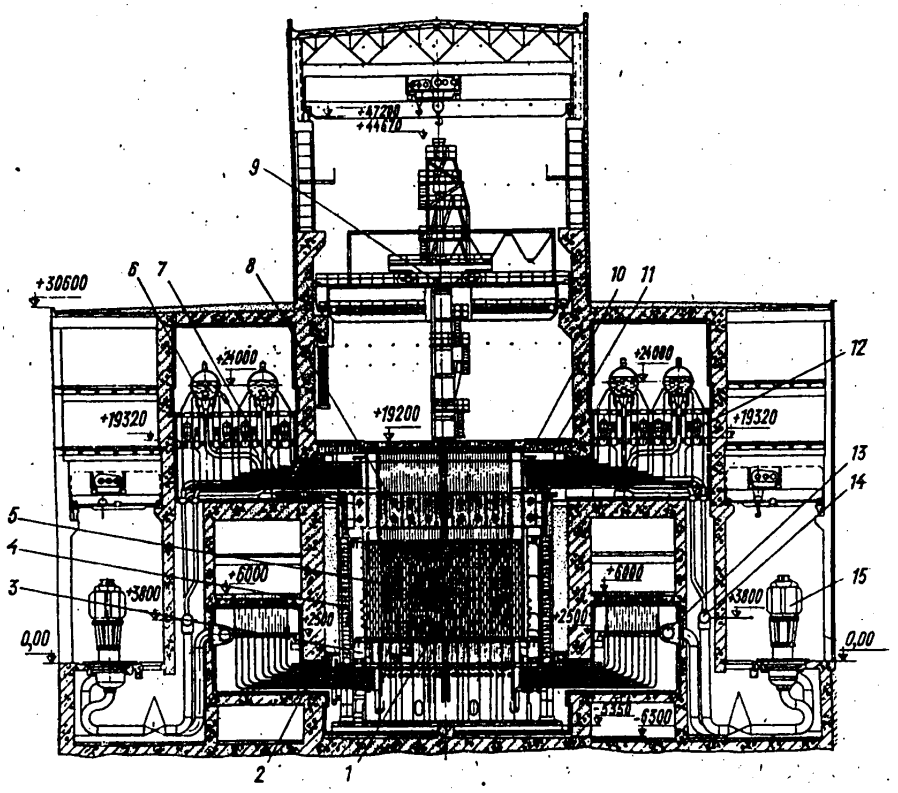

Figure 3.1. Overall View of RBMK Reactor

6 through pipelines 7 in the form of a steam-water mixture. After separation the steam is sent to turbines at a flow rate of 5,400 t/hr at temperature of 284°C and pressure of 70 kgf/cm^2. The condensate from the turbines, passing through the regenerative heaters, is mixed with water from the separators and is fed through the intake water collectors 14 to the main circulating pumps (GTsN) 15, by which it is fed to the fuel channels.

The nuclear fuel is recharged continuously during operation of the reactor by means of a loading-unloading machine (RZM) 9. The fuel recharging intensity at nominal reactor power comprises 1-2 fuel assemblies per day during steady operating mode; the maximum RZM productivity is five assemblies per day. The possibility of conducting partial one-time recharging of assemblies without the RZM on a shutdown reactor is provided.

The reactor is equipped with fuel monitoring systems which issue information about its operation as a whole and about the operation of individual fuel channels and also the necessary signals to the SUZ and emergency signalling system:

the physical energy release monitoring system through the height and radius of the reactor;

the system for monitoring the integrity of the fuel channels;

the system for monitoring the seal of the fuel jackets in each fuel channel (KGO) 12;

the system for monitoring the water flow rate in the fuel channels;

the system for monitoring the temperature of the graphite and of the assembled steel sections.

The information received from these systems is processed by an automated energy unit monitoring system.

The main reactor characteristics are presented below:

Reactor power, kW:	
thermal	$3.14 \cdot 10^5$
electrical	$1 \cdot 10^6$
Coolant flow rate through reactor, t/hr	$37.5 \cdot 10^3$
Steam productivity, t/hr	5,468
Steam pressure in separator, kgf/cm^2	70
Pressure in group pressure vessels, kgf/cm^2	82.7
Average steam content at reactor output, percent	14.5
Coolant temperature, °C:	
at input	270
at output	284
Maximum channel output with regard to 10 percent power misalignment, kW	2,987.6
Coolant flow rate in maximum output channel, t/hr	27.95
Maximum steam content at channel output, percent	20.1
Minimum reserve to critical power	1.25
Height of core, mm	7,000
Diameter of core, mm	11,800
Spacing of fuel lattice, mm	250 X 250
Number of fuel channels	1,693
Fuel enrichment, percent U-235	1.8
Average extent of burnup through reactor, GW·day/t	18.5
Maximum graphite temperature at separate points, °C	750
Maximum surface temperature of zirconium pipe of fuel channel, °C	325
Planned operating life of reactor, years	30

Assembled steel sections of the reactor. The forces due to the weight of the internal assemblies, assemblies and piping of the reactor is transmitted to the concrete and the inner cavity of the reactor is also sealed by means of welded assembled steel sections (see Figure 3.1) that at the same time perform the role of biological shielding. The upper cover 10 serves as the floor of the central room and at the same time of biological shielding of the room against the radiation

of the upper piping of the reactor. The design of the lower part 11 of the covering 10 is made in the form of metal ducts filled with iron shot and serpentinite.

The graphite stacking is surrounded by water biological shielding located in the side assembled steel section. The latter is made in the form of a cylindrical tank of circular cross section with outer diameter of 19 meters and inner diameter of 16.6 meters. The reservoir is separated inside into 16 vertical airtight compartments filled with water that also remove heat from the graphite stacking. The cooling water is fed to the compartments from below and is removed from the top. The channels of the starting and operating ionization chambers, drain pipes and thermocouples sleeves for measuring the water temperature in the compartments are located in the side structures. The installation space between the outer surface of the side structure and the surrounding walls of the concrete shaft is filled with sand.

The upper and lower assembled steel sections belong to the more complex and crucial assemblies. The upper section 8 (see Figure 3.1) is a cylindrical shell 17 meters in diameter and 3 meters high. The bottoms of the shell (the upper and lower slabs) are welded to it along the periphery by airtight seams and are welded to each other by vertical stiffening ribs. Openings are bored in the slabs after reinforcing assembly and welding of the structure during installation according to the location of the precisely repeated openings in the graphite stacking for the fuel channels. Channel pipes for the fuel channels and the channels for the control and monitoring system are installed in the openings and welded and the space inside the formed reservoir between the pipes is filled with serpentinite. The airtightness of the structure and the quality of welding should meet the reqirements of helium density. The upper assembled steel section is installed on 16 roller supports mounted on an annular projection in the upper part of the side steel section and receives the force from the weight of the charged fuel channels, the slab floor and the pipelines of the upper piping of the reactor.

The lower assembled steel section 3--the footing for the graphite stacking--has the shape of a tubular drum 14.5 meters in diameter and 2 meters high. The structure is loaded by the graphite stacking installed on it and by the pipelines of the lower piping of the reactor. Its inner cavity is filled with serpentinite and nitrogen. The number and arrangement of the lower channel pipes for the fuel channels, welded into the upper and lower bottoms of the assembled steel section, are the same as in the upper steel section. After the channel pipes have been welded into the assembled steel section, its inner cavity is tested with a mixture of air and helium to pressure of 1.25 kgf/cm^2 (approximately 0.125 MPa).

The main assembled steel support section 1 (see Figure 3.1) in the reactor is loaded more since it transmits the weight of the lower assembled steel section, the graphite stacking and the weight of the lower water pipelines to the laying part of the foundation plate of the building. At the same time its design solution is distinguished by simplicity and originality. The design is two plates with stiffening ribs 5.3 meters high perpendicular to each other that intersect through the center of the reactor. The plates are welded along the axes of symmetry (in the reactor plane) to the bottom assembled steel section.

Anticorrosion coatings are applied during installation to all the assembled steel sections of the reactor operating in a gaseous medium with the presence of water vapor.

The assembled steel section of the upper covering 10 in the central room has a passage for installation of the fuel and special channels. The diameter of the passage exceeds that of the graphite stacking. The passage is covered by replacable flooring consisting of individual slabs. The flooring plays the role of biological shielding of the central room against radiation of the upper piping of the reactor and the fuel assembly when it is removed from the fuel channel and also serves as heat insulation of the central room.

The slab flooring consists of upper and lower slabs and blocks resting on three risers. The slabs and blocks of the flooring are assembled steel sections filled with concrete-barium-serpentinite cement stone (ZhBSTsK).

The space between the upper and lower slabs and blocks of the flooring is used to lead in the cables of the SUZ servodrives, the energy release monitoring sensors and thermocouples. Air that then passes through the ventilation duct is pumped into the room of the upper piping of the reactor from the central room through gaps of the plate flooring. The pumped air cools the plate flooring and eliminates the possibility that radioactive discharges will enter the central room from the upper piping of the reactor.

Water is delivered and distributed through the reactor channels from group collectors of the lower water piping through pressure-regulating valves and flow meters. To service, monitor and repair these assemblies, they are mounted in the passages below the floor of the room for controlling the regulating valves in the room of the distributing group collectors. The passages are covered with slabs of concrete biological shielding through which rods from the regulating valves are passed into the upper room.

The graphite stacking. The graphite stacking (Figure 3.2) is assembled on the lower structure inside the reactor space. It is a vertical cylinder assembled from columns (2,488) consisting of graphite blocks. Each block is a parallelepiped in shape with cross-section of 250 X 250 mm and 200, 300, 500 and 600 mm high. The main blocks are 600 mm high while the shortened blocks are installed only in the upper and lower end reflectors to displace the joints of the blocks of adjacent columns through the height of the reactor. The overall dimensions of the core (the graphite moderator) are presented below, the thickness of the end reflectors is 500 mm and the thickness of the side reflector is an average of 1,000 mm. The mass of the stacking is 1,700 tons. Graphite that meets special requirements in nuclear purity and density is used to manufacture the blocks. There are openings 114 mm in diameter along the axis of the block that form channels in the columns for the fuel channels and the control and monitoring channels. Graphite rods 6 are installed in the openings (channels) of the columns of the side reflector instead of the channels.

Each graphite column is installed on a steel support slab 5 which in turn rests on a support 4 welded to the upper slab of the lower assembled steel section. The columns are attached and centered in the upper part through sleeve pipes 9 welded into the upper assembled steel section by means of shielding slabs 7 and connecting pipes 8. The shielding and support slabs are essentially identical in design. Manufactured of steel, besides performing the functions of intermediate components for attaching the columns, they provide thermal shielding of the slabs of the

upper and lower assembled steel sections and are part of the biological shielding of the reactor.

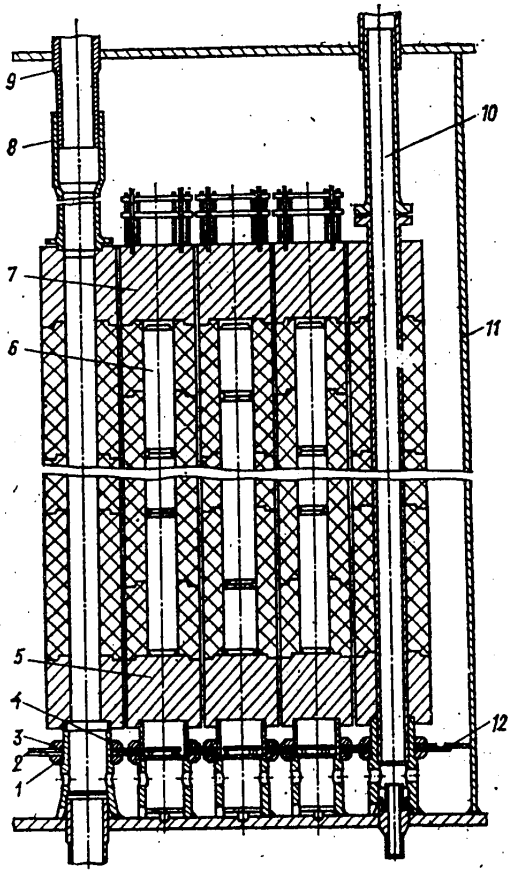

Figure 3.2. Graphite Shielding

A diaphragm 2 designed first to create some resistance to the flow of the helium-nitrogen mixture fed through the lower assembled steel section to direct it through the openings in the support housings into the gap between valves and the stacking blocks and second to reduce the heat transfer by radiation from the support slabs to the upper slab of the lower assembled steel section, is attached to the supports by washers 1 and 3. The diaphragm is made in the form of individual sheets of 08Kh18N10T steel 5 mm thick. The gap between the diaphragm and the inner surface of the housing of the stacking 11 is closed with a ring 12.

The graphite stacking is secured against displacements in the radial direction by rods 10 located in the peripheral columns of the side reflector. The rod is welded below to the support and is movably connected above to the sleeve pipe welded into the lower slab of the upper assembled steel section. The upper joint provides

freedom to temperature shifts of the rod. At the same time the rod is a reflector cooling channel. It is manufactured from pipe with outer diameter of 110 mm and wall thickness of 5 mm. The material is 08Kh18N10T steel.

All the enumerated assemblies are under intensive neutron irradiation and elevated temperatures during reactor operation: thus, for example, the temperature of the support structures reaches 350°C in the region of the upper lattice of the lower assembled steel section and 440°C on the lower support slabs and the maximum graphite temperature (calculated) is 750°C.

The temperature conditions of the graphite stacking. The heat from the stacking is removed to the fuel channels (partially to the SUZ channels), due to which its temperature mode is determined by heat transfer from the graphite blocks to the fuel channels. Gas with an average mass composition of 40 percent helium plus 60 percent nitrogen was used to ensure heat transfer and to maintain the temperature of the stacking in the range of 700-750°C. Sleeves 8 (see Figure 3.3)--solid contact split graphite rings 20 mm high, which were arranged along the height of the channel tightly against each other such that each alternating ring has direct contact along the lateral surface with either a pipe or with the inner surface of a block and also with each other along the ends, are placed for this purpose on the fuel channels. The minimum channel-sleeve and sleeve-block clearances were determined from the condition of the impermissibility of the channel becoming clogged in the stacking due to its radiation-thermal shrinkage during operation of the reactor. A total maximum reduction of the tolerances on the order of 1.5-2 mm was adopted on the basis of operation of uranium-graphite reactors and also data on irradiation of the reactor graphite, which ensures operation of the reactor for a long time.

The graphite temperature initially increases during operation of the reactor due to an increase of the end clearances between the graphite blocks and then decreases due to the prevailing reduction of the radial clearances. A stable temperature of the stacking is established for approximately 5 years and in this case the temperature in the corners of the blocks will be 660°C. The highest temperature of 740°C (760°C in the corners of the block) is reached during the initial period of operation. The temperature of the outer surface of the fuel channel pipe under the solid contact rings does not exceed 325°C. This course of arguments is supported by data obtained during operation of RBMK reactors at the Leningrad, Kursk and Chernobyl'skaya AES.

3.2. The Fuel Channel

One of the main assemblies that determines the economy and reliability of reactor operation is the fuel channel. It is designed for location of TVS with nuclear fuel and to create a coolant flow. The main heat engineering parameters of the fuel channel at 100 percent reactor power are presented in Section 3.1. The integral neutron flux ($E_n > 0.7$ MeV) reaches $3 \cdot 10^{19}$ neutrons/cm^2 during the calculated service life of the channel.

The reactor fuel channel is shown in Figure 3.3. The channel housing is a welded structure whose middle part consists of a pipe 9 with outer diameter of 88 mm and wall thickness of 4 mm manufactured from Zr + 2.5 percent Nb alloy, while the

upper 3 and lower 11 end parts welded to it are made of corrosion-resistant pipes (08Kh18N10T steel) of various diameters. Selection of a zirconium-niobium alloy for the middle part of the channel in the reactor core was determined by the fact that this alloy has satisfactory mechanical and corrosion properties ($\sigma_v \geq 25$ kgf/mm^2 (approximately 250 MPa), $\sigma_{0.2} \geq 17$ kgf/mm^2 (approximately 170 MPa) and δ is 17 percent) with relatively small thermal neutron absorption cross-section (α_a = = $(0.2\text{-}0.3)\cdot 10^{29}$ m^2). The middle part of the channel housing is joined to the end parts by specially developed steel-zirconium adapters.

The channel housing in the reactor is arranged in sleeve pipes welded to the upper 2 and lower 10 assembled steel section. It is movably attached in the upper part by a support fillet and by argon-arc welding of "tendril" seam 4. The lower part of the housing is connected by welding to the sleeve pipe of the assembled steel section through the bellows compensator assembly 12, which permits compensation of the difference in the temperature expansion of the fuel channel and the assembled steel sections of the reactor and also makes it possible to create reliable airtightness of the gas cavity. Moreover, a stuffing-box seal 13 is installed below the bellows compensator in case the bellows fails. The service life of the channel housing is calculated at 25-30 years and if necessary it is replaced in shutdown equipment by means of a special unit which remotely cuts the "tendril" seam between the sleeve and channel inside the upper sleeve and after the channel has been replaced also remotely welds this seam and checks the quality by X-ray flaw detection. The lower seam between the bellows compensator and the channel is cut and welded by a special automatic welding machine.

The fuel assembly is installed inside the channel on a suspension 5 which holds it in the reactor core and provides replacement of the spent assembly by means of an RZM without shutting down the reactor.

A plug cap 7 installed in a housing 6 and which seals the channel with a gasket is located on the upper end of the suspension. A solid steel plug 1, which is the biological shielding is installed between the assembly and the locking plug.

The steel-zirconium joint. Development of a strong and vacuum tight welded steel-zirconium joint for the fuel channels of the RBMK reactor was begun in 1965. Several steel-zirconium joints developed and used both in the USSR and abroad were known by this time. Methods of connecting steel and zirconium parts by contact-reactive soldering, explosive welding, joint molding and so on were known. However, all these methods could not be used for connecting the pipes of the fuel channel of the RBMK reactor. The joints produced by these methods were designed to operate at lower parameters, had lower requirements on retention of airtightness and were made with steels having lower level of permissible stresses at operating temperatures. Therefore, a joint design, the basis of which was the diffusion welding method, was adopted for the RBMK reactor (Figure 3.4).

The inner part of the reducer coupling is made of a zirconium alloy and the outer part, the enclosing part, is made of stainless austenitic steel. The design of the adaptor coupling was developed with regard to achieving a configuration and programmed stress state in the joint that guarantee strength and reliability under operating conditions. The welding technique ensures an optimum diffusion interlayer in

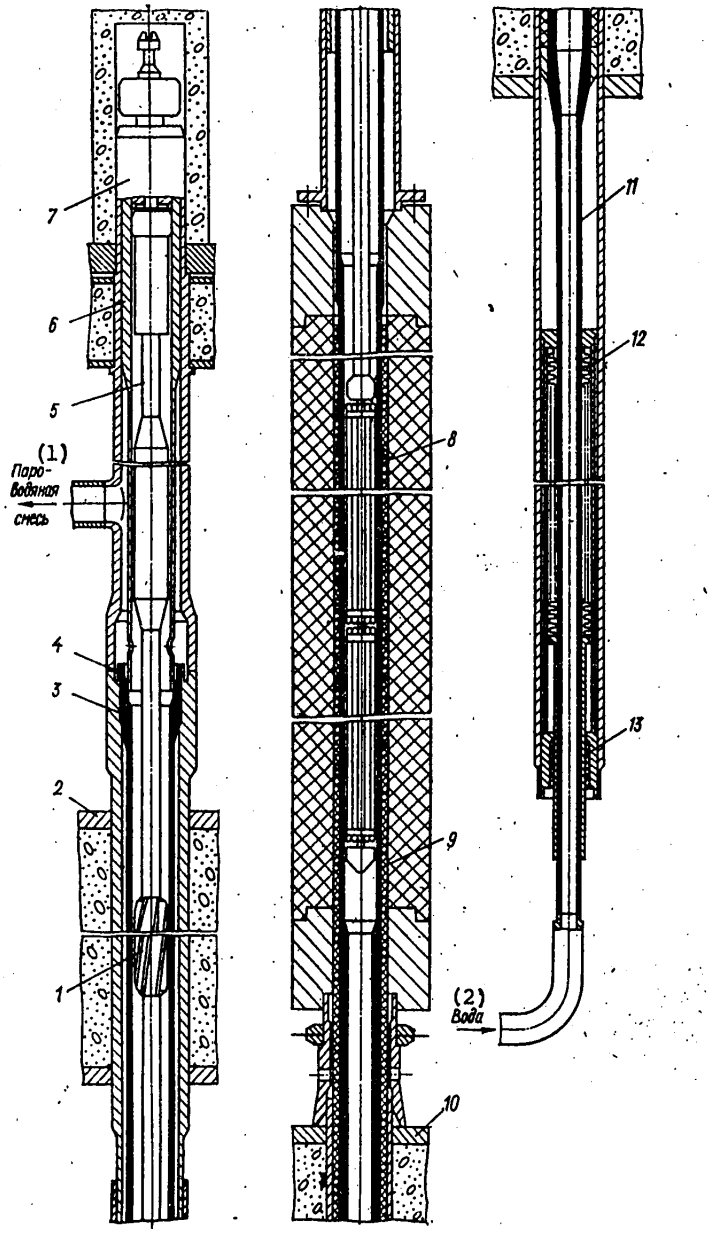

Figure 3.3. Fuel Channel

Key:
1. Steam-water mixture
2. Water

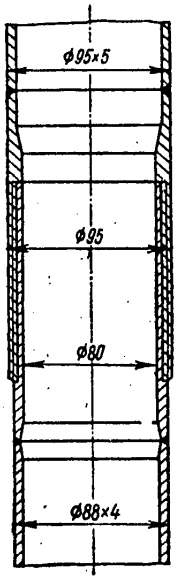

Figure 3.4. Steel-Zirconium Joint

composition and thickness by which high vacuum tightness and corrosion resistance in the steam-water mixture and the gaseous medium in contact with graphite are achieved. The design and technique were developed and the reliability of the steel-zirconium joint was checked with investigation of the stress state at operating temperatures, cyclic strength, corrosion resistance, prolonged corrosive strength and resistance. Bench and reactor tests of the join con r ed their high efficiency during prolonged operation, brief overheating and cyclic thermal loads.

The adapter coupling is welded to a zirconium alloy pipe by electric-arc welding in a vacuum. The developed design and technique of the welded joint provide strength with high degree of flexibility. Thermal-strain hardening conditions and machining of the weld seams and near-seam zones were developed to fulfill high requirements in corrosion resistance. The steel part of the adapter coupling is joined to the steel pipe of the channel by argon-arc welding.

The locking device of the fuel channel. The duct of the RBMK fuel channel is sealed on top by a locking device--plug. With regard to the fact that sealing, unsealing and replacement of the fuel assembly operations should be carried out by an RZM with remote control, the plug has a simple design that provides reliable conducting of machine operations related to its removal--rotation and vertical motion. The requirements to ensure airtightness for the entire service life of the fuel assembly (3-3.5 years) with 30 heat changes during the service life were advanced during development of the locking device; the sealing gasket should be installed and removed by the same RZM operations; the inner duct should have no sharp turns and projections to avoid damage to the surface of the fuel element.

The main working members in the plug (Figure 3.5) are a screw and a holder made of harder steel. During installation of the channel, the RZM works with a special claw on screw 4, which ensures attachment of the plug to the channel housing and consequently ensures sealing. When the TVS is installed into the channel, the suspension housing assembled into a single assembly with the plug, is lowered into the duct housing. The screw is then tightened upward to the maximum, the balls 8 are rolled into the bore of the spacer 10 and do not go beyond the outer diameter of the holder. For sealing, the screw is threaded in the nut by the RZM hook and partially forces the balls from the seats of the holder during sealing by the increased diameter of the spacer into the annular groove of the housing. Upon further rotation of the screw, the balls, being at rest, prevent longitudinal movement of the holder upward and create the possibility of grasping the gasket by the clamping sleeve.

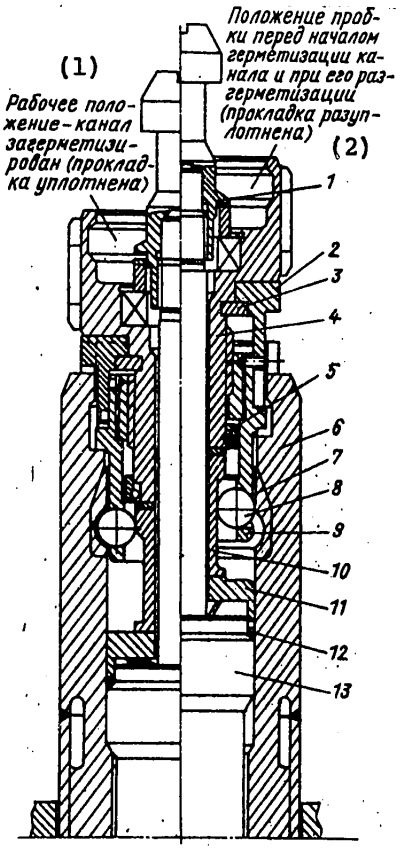

Figure 3.5. Locking Device of Channel: 1--shank; 2--flange; 3--semiring; 4--screw; 5--locking ring; 6--channel housing; 7--surfacing; 8--ball; 9--plug housing; 10--spacer; 11--clamping sleeve; 12--gasket; 13--suspension housing

Key:
1. Working position--channel pressurized (gasket sealed)
2. Position of plug before beginning of channel pressurization and upon unsealing of it (gasket unsealed)

Installation of energy release monitoring sensors (DKE) through the reactor radius is provided in 270 fuel channels. The TVS in these fuel channels are distinguished in design from other TVS by the presence of a sealing sleeve from the pipe passing through the center of the suspension and the fuel assembly designed for installation of the DKE. When installed in the channel, the DKE is sealed in the upper part of the suspension by a metal gasket.

Special channels. Besides fuel channels, special channels in the following quantities are installed in the reactor:

SUZ channels	179
Channels with DKE in height	12
Channels of ionization staring fission chambers (KD)	4
Reflector cooling channels	156
Channels outside the fuel lattice to measure graphite temperature:	
in the plateau zone	8
in the side reflector	4
in the support and upper shielding slabs	8
Channels outside the fuel lattice for ionization chambers:	
working	20
starting	4

The SUZ channels, channels with energy release monitoring sensors in height and channels of the ionization fission chambers (KD) do not differ from each other. The design of these channels and their loops is identical and is shown in Figure 3.6.

The SUZ, KD and DKE channels (in height) are attached to the upper sleeve pipe by means of a locking fillet and "tendril" weld 3 located on the outside. There are bellows 2 in the upper sleeves that compensate for the considerable temperature lengthening of the channels, determined by the temperature drop between the upper assembled steel sections and the cold sleeve pipes. Unlike the fuel channels, lens compensators 6 are installed on the lower sleeve pipes of the special channels. The upper and lower parts of the special channels are made of corrosion-resistant steel, while the middle part is made of zirconium-niobi alloy. The middle part is joined to the upper and lower parts of the ch nel by steel-zirconium adapters similar to those of the fuel channels.

The SUZ channels 1 have heads 4 designed to attach the actuating mechanisms and to deliver cooling water to the channel. The SUZ actuating mechanisms 5 are attached to the heads of the SUZ channels, while sealing sleeves are attached to the heads of the DKE and KD channels, also on gaskets. The sleeves in the DKE channels are designed for installation of sensors and are made of SAV-1 aluminum alloy and the sleeves in the KD channels are designed for installation of the suspensions of the ionization fission chambers and are made of corrosion-resistant steel. A permanent throttle valve 7 whose designation is to create resistance to water flow through the channel that provides reliable filling of it with water, is installed in the lower part of the special SUZ, DKE and KD channels.

The reflector cooling channel (Figure 3.7) is designed for cooling the side reflector of stacking 4, the upper assembled steel section of the rods for attaching

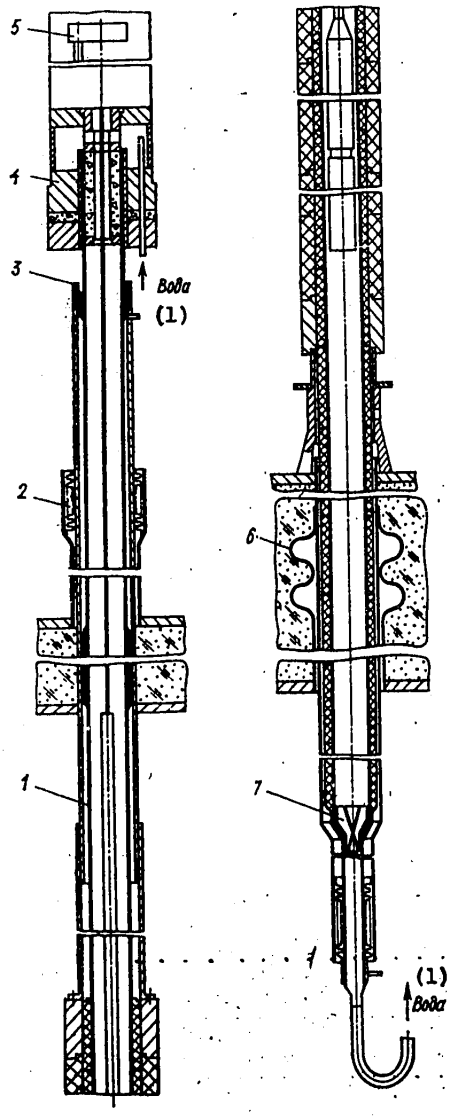

Figure 3.6. SUZ Channel

Key:
1. water

the side reflector 5 and also to reduce the thermal flux to the housing and compensators which form the inner airtight cavity of the reactor. The channel is structurally made in the form of a Field pipe of corrosion-resistant steel. Water enters the channel from the top through the central pipe and is removed through the space between pipes, rising upward.

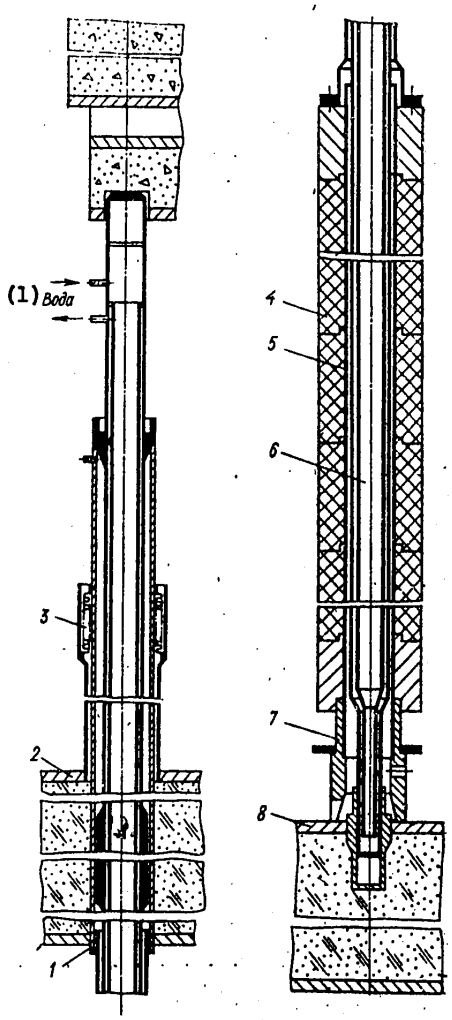

Figure 3.7. Reflector Cooling Channel: 1--loop sleeve; 2--upper assembled steel section; 3--bellows compensator; 4--side reflector; 5--rod for attaching side reflector; 6--Field pipe; 7--sleeve; 8--lower assembled steel section

Key:
1. Water

3.3. The Reactor Pipelines

The reactor pipelines provide circulation of coolant in the channels and assembled steel sections and also circulation of gaseous media in the reactor and the reactor space. The distributing lines contain pipelines and collectors, their suspensions

and supports, fittings with drives and production monitoring devices. The pipelines are divided into lower and upper according to conditions of installation and location. The first group includes water pipelines to deliver water to the fuel channels and drain pipelines of the SUZ channels. The second group includes water-steam pipelines that remove the steam-water mixture from the reactor, pipelines that deliver water to the SUZ channels, pipelines that deliver and drain water of the reflector cooling channels and also pulsed pipes of the system for monitoring the integrity of the fuel channels (KTsTK).

The water and steam-water distributing pipes are part of the multiple forced circulation (MPTs) loop in which the coolant is transported in the following manner: water from the two delivery collectors of the main circulating pumps (GTsN) enters 44 group collectors (22 each on each side of the reactor). The water is delivered from the group collectors through a locking-control valve and spherical flow meter through an individual pipeline to each fuel channel. The coolant-steam-water mixture--is fed through the upper sleeve in the fuel channel into the pipeline through which it is fed directly into a separator. The diameter of the water distributing pipelines is equal to 57 mm and the wall thickness is 3.5 mm. Guide, movable and fixed supports and suspensions are provided to ensure the efficiency of the pipelines. The pipelines of the steam-water distributing pipes 76 mm in diameter and with wall thickness of 4 mm are separated alternately on both sides of the reactor, symmetrically with respect to the axial plane. The rows are arranged in layout within the upper assembled steel section with spacing of 250 mm and are arranged in the separator room with variable spacing of 250, 500 and 1,000 mm. The corresponding connecting pipes of the separators are arranged along the length of the separator with spacing of 250 mm.

Water is fed to the SUZ channels and the reflector cooling channels through individual pipelines from a common delivery collector. The pipelines of the SUZ channels are separated in bundles along the corresponding rows of the sleeves and are connected to the channel heads by tendril welding. Water is removed from the SUZ channels through pipelines located under the lower assembled steel section into a drain collector. Locking-regulating valves and flow meters are installed on each pipeline that delivers water to the SUZ, DKE and KD channels. The valves have manual control. An individual throttle washer or locking-control fitting that serves to distribute the flow rate through the channels during adjustment is installed at the inlet to the housing of each flow meter of the reflector cooling channels.

The impulse pipes of the KTsTK system are designed to remove the gaseous mixture from the reactor space in the region of each cell to check the tightness of the channel. The helium-nitrogen mixture is pumped out to the purification system through the impulse pipes during normal operation. Detection of water in the gaseous mixture being pumped out indicates a leak from the fuel channel.

Besides the considered distributing pipelines, there are additional pipe systems on the bottom and top of the reactor, for example, pipelines for delivery and removal of nitrogen to the different zones of the reactor and the assembled steel sections, for delivery of the helium-nitrogen mixture (discharge of the steam-gaseous mixture), for delivery and removal of water from the side assembled steel sections and different drain pipes.

3.4. Flow Regulators

All uranium-graphite reactors have devices which are used to maintain the flow rate of the working medium at a specific level or to regulate the flow rate in the required range. These devices, namely the shutoff-regulating valves, are installed in the first loop of the RBMK reactor, at the inlet to each fuel channel, and are designed to regulate the coolant flow to achieve a specific steam content. The fluid flow rate through the object of regulation is usually varied by the throttle valve method in nuclear and power plants.

The shutoff-regulating valve (Figure 3.8) provides the necessary regulation and possibility of preliminary monitoring of the water flow rate through the fuel channel in all operating modes of the reactor and also cutoff of the fuel channel from the group collector during repair of the channel or pipes of the water distributing lines. The valves are installed in the room of the water distributing lines on the group collectors and are connected by rods to the indicators and control levers located behind the concrete cover. Water enters the valve cavity from the group collector, passes through the throttle valve device and the flow meter and pipe of the water distributing line to the fuel channel. Regulation is accomplished by changing the gap between the end piece and the seat of the throttle valve. The valve should provide continuous reliable operation for 50,000 hours (Table 3.1).

Table 3.1. Characteristics of Regulating Valve

Parameter	Unit of Measure	Calculated Value	Experimental Value
Flow rate with full-scale parameters	t/hr	30.6-12.0	25.4-12.3
	m^3/hr	39.7-15.6	39.2-16.0
Pressure drop	kgf/cm^2	6.2-13.9	7.6-14.0
Travel of shutoff member	mm	9.6- 3.6	7.7- 3.7
Area of narrow cross-section of seat	cm^2	2.5- 0.9	2.0- 0.9
Throttling gap	mm	2.3- 0.9	1.9- 0.9
Coolant flow rate	m/s	44.1-48.1	47.5-50.4
Dynamic head in narrow cross section	kgf/cm^2	7.7- 9.0	8.3-10.1
Reserve to boiling	kgf/cm^2	18.0- 9.0	15.8- 7.6
Maximum cold (hot) water flow rate	m/s	70(80)	70(80)

3.5. Selecting the Structural Materials and the Water Chemical Regime

The main construction materials used in an AES with RBMK reactor are stainless and perlite steels, zirconium alloys and MNZh-5-1 copper-nickel alloy. Stainless steel 08Kh18N10T is one of the main construction materials of the MPTs loop (pipelines, plating of the separator housing and part of the fuel channel). The total stainless steel surface in the MPTs loop comprises approximately 25,000 m^2. Steel of this type is used to manufacture the housings and pipe bundles of the low-pressure heaters.

Perlite steels are used for the pipelines of the condensate-feed channel, the condenser housings, the heating steam pipelines and the saturated steam pipelines. The total surface of perlite steels comprises approximately 5,000 m^2. Perlite steel is used in the MPTs loop for large shutoff fittings.

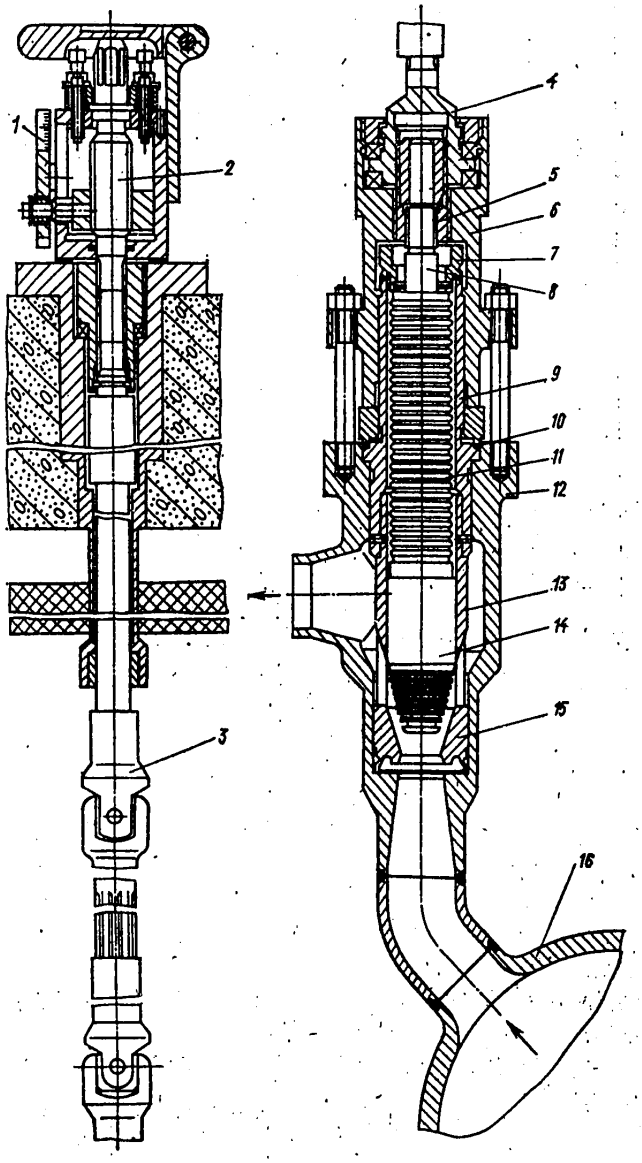

Figure 3.8. Shutoff-Regulating Valve: 1--indicator; 2--indicator screw; 3--drive; 4--drive shank; 5--threaded sleeve; 6--connector; 7--ring; 8--shaft; 9--sleeve; 10--gasket; 11--bellows; 12--housing; 13--throttle valve; 14--end piece; 15--throttle valve seat; 16--group collector

The fuel channels, SUZ channels and fuel element jackets are made of zirconium alloys. The total surface area of zirconium alloys is 13,500 m^2. The pipe bundles of the turbine condensors are made of copper alloys.

The distinguishing feature of the water regime of a boiling-water reactor is increased oxygen concentration in the coolant, caused by radiolysis of water in the core. Consequently, the materials for the MPTs loop are selected with regard to this circumstance.

Neutron irradiation essentially has no effect on corrosion of 08Kh18N10T steel. Steel corrosion is not intensified under shutdown conditions. It may be subjected to corrosion cracking with the simultaneous presence of chlorine ions and oxygen or another oxidant in the medium and with the presence of tensile stresses in the metal. Cracking was not observed in stressed metal in a medium containing only one of these agents [1]. There were no cases of corrosion cracking of the metal (at σ = 33 kgf/mm^2 (330 MPa) during 10,000 hours of testing) in water containing 0.1-0.3 mg/kg of oxygen and 0.1 mg/kg of the chlorine ion at 285°C and in saturated steam containing up to 20-40 mg/kg of oxygen.

Corrosion cracking of 08Kh18N10T steel is observed with chloride concentration on the surface. Concentration of the chlorine ion on the surface of steel in saturated steam containing up to 30-40 mg/kg of oxygen, at which corrosion cracking of steel is observed after 6,000 hours, comprises $1 \cdot 10^{-3}$ mg/cm^2. There may be a phase interface of the medium in the separator at the possible location of chlorine ion concentration under operating conditions of an AES with the RBMK reactor. However, compressive stresses are prevalent at the interface.

An estimate of the operating life of stainless austenitic steel under the operating conditions of a boiling-water reactor, carried out according to the functions from [2], indicate that there should be no danger of corrosion cracking in the MPTs loop during 25-30 years of operation if normal water regime is observed. The danger of corrosion cracking determined by chlorine-ion concentration on the outer surface of MPTs pipelines due to possible leaks from the outside is prevented by electrochemical shielding made in the form of an aluminum coating with AS-8A organosilicate material.

The assembled steel sections of the reactor of perlite steel are made with the same coating. Extensive use of perlite steels both in the MPTs loop and in the condensate-feed channel is still limited since additional purification of the coolant is required, especially after shutdown modes. The feasibility of replacing stainless steel by perlite steel can be solved from the results of prolonged operation.

The high corrosion resistance of the zirconium-niobium alloys used in RBMK reactors in water and steam at 285°C is explained by their capability of passivation as a result of protective oxide films forming [3]. Zr + 1 percent Nb alloy is used for the fuel jackets and ZR + 2.5 percent Nb is used for the fuel channels. The oxygen contained in the water affects these alloys at 285°C.

Reactor radiation is a specific factor whose effect should be taken into account when estimating the resistance of zirconium alloys. It was established experimentally and confirmed theoretically that the rate of the anode process and

consequently the rate of corrosion of Zr + 2.5 percent Nb alloy increases by only 5-10 percent under reactor irradiation conditions. The rate of corrosion of Zr + + 2.5 percent Nb alloy does not exceed 0.024 g/(m^2·day) during 8,000 hours of testing. The intensity of removal of corrosion products to the coolant comprises 1-5 percent of the corrosion rate. The efficiency of zirconium-niobium alloys in the components of the fuel channel, welded joints and adapter is determined by prolonged laboratory and industrial tests [4-10].

Stable operation of RBMK reactors confirms the correctness of selecting materials and corrosion rates of structural materials for the MPTs loop. Taking the selection of construction materials in an AES with RBMK reactor and also the characteristic features of the corrosion behavior of these materials into account, a correctionless water regime was selected and calculated with provision of high purity in the main water loops without any correcting additions and the minimum possible oxygen content in the coolant.

It should be noted that steady oxygen concentration due to removal of radiolysis products and the difficulty of recombination processes has not been established during radiolysis of water in boiling-water nuclear reactors of the RBMK type operating in a single-loop AES circuit. The final products of water, hydrogen and oxygen radiolysis are removed by the steam-water mixture to a separator. They are delivered together with steam from the separator to the turbine condenser where they are removed from the loop.

The radiation-chemical reactions of water in the reactor determines the stochiametric yield of hydrogen and oxygen of approximately 0.6 molecules/100 eV and 0.3 molecules/100 eV, respectively. In this case the oxygen concentration in the saturated steam of the separator comprises approximately 10 mg/kg and that in the water of the MPTs loop during steady operating modes comprises 0.03-0.05 mg/kg. Suppression of radiolysis by special hydrogen additives or hydrogen-containing compounds for boiling-water reactors operating in the single-loop AES circuit is not required.

Table 3.2. Design Standards of Coolant Quality of AES with RBMK Reactor

Indicator	Water of MPTs Circuit	Feed Water After Condensate Purification
pH value	6.5-7.2	7±0.2
Specific electric conductivity, μcm/cm	1.0	0.1
Concentration, mg/kg:		
of chlorine ions	0.1*	0.004
of iron**	0.2	0.01
of copper	0.05	0.002
of oxygen	Not regulated	0.05
salts of hardness, μg-eqv/kg	15	0.5

*A Concentration of 0.15 mg/kg is permitted briefly up to one day.

**Up to 1 mg/kg during transient and starting modes.

If the quality of the reactor water is normalized, it had the purpose of providing minimum rate of corrosion of the construction materials and also minimum deposits on the fuel elements. The standards for the quality of the feed water were determined with regard to the coefficient of concentration by evaporation of the reactor water, the corrosion rate of the materials of the condensate-feed channel and the possibility of the condensate purification. The standards adopted for the design stage are presented in Table 3.2 for the RBMK reactor.

The standards are refined and corrected during operation. Thus, upon conversion to automatic monitoring of pH, the normal range of this indicator was expanded to 6.5-8.0 for reactor water and the standards are made more rigid for the corrosion products of iron, copper and hardness salts. Many years of operating AES with the RBMK reactor showed that the real water regime is considerably better than the planned regime. The indicators of the water of the MPTs loop are presented below:

Specific electric conductivity, μCm/cm	0.4-0.6
Content, mg/kg:	
of chlorine ions	≤0.05
of iron	10
of copper	7-10
of hardness salts, μg-eqv/kv	1.0

Sources of entry of contaminants into the coolant were considered when selecting the means of maintaining the water regime and measures to control this were determined with regard to the physicochemical characteristics of their behavior in the AES loop. All contaminants of the coolant of a single-loop boiling-water AES can essentially be divided into three main groups: saline, finely dispersed (corrosion byproducts) and gaseous. The entry of saline impurities during operation of a plant should be expected as a result of selection of cooling water in the turbine condensers and also with the feed water.

Corrosion byproducts enter the coolant from the entire surface of the loop in all operating modes of the AES and the corrosion byproducts should be removed from the coolant due to their relatively low solubility and capability of precipitation.

The main source of entry of gaseous impurities is radiolysis of water in the reactor core. High purity of water with low specific electric conductivity (less than 1 μCm/cm) is provided by desalinization of it on ion-exchange filters. Therefore, the entire flow of the turbine condensate, the heating steam condensate of the regenerative turbine heaters and also the additive chemically desalinized water pass through condensate purification. It operates by the series-connection scheme of the mechanical and mixed ion-exchange filters. The condition of 100 percent condensate purification of all flows comprising the feed water is strictly observed in this case. It is especially important to observe this condition with highly mineralized (sea) cooling water of the turbine condensers. A mixture of 1:1 KU-2-8chs and AV-17-8chs ion exchangers is used as the load of the ion-exchange filter. Special attention is devoted to the condensate density, which permits operation with influxes of cooling water less than 0.0001 percent.

Since the dissolved impurities in the feed water are concentrated in the MPTs loop in proportion to the coefficient of concentration by evaporation, purging of part

of the reactor water with replacement of it by cleaner water is required to maintain the given standards. There is intraloop purification in the RBMK reactor that operates by the series-connection scheme of alluvial mechanical and ion-exchange filters with mixed load. Water for purification is collected from the GTsN head and is delivered to the feed water line at its inlet to the separators. When estimating the amount of purging water, the required flow rate to maintain each indicator of the reactor water within normal limits was calculated. An equation was derived in which the number of corrosion byproducts settling in the loop was taken into account when calculating the amount of scavenging water. The water is contaminated most by iron corrosion byproducts and a scavenging water flow rate of 180 t/hr (productivity of intraloop purification) was selected according to the content.

Water is purified of oxygen in the turbine condensers and in a deaerator. Moreover, there is blowoff of the noncondensed gases, including oxygen, from the housings of the regenerative turbine heaters. These measures ensure an oxygen content of not more than 0.05 mg/kg in the water after condensate purification and of not more than 0.03 mg/kg in the feed water after the deaerator.

The water regime of the SUZ loop with complete filling of the channels with water is determined by the corrosion resistance of the main construction material--aluminum alloy, for which the pH should be in the range of 5.5-6.5. This pH in the loop is created by radiation-chemical reaction of nitrate-ion formation from nitrogen and oxygen that enter the water as a result of air being dissolved in it in the open tanks of the loop. There is a purification system consisting of a mechanical filter and ion-exchange filter with mixed load of KU-2-8chs and AV-17-8chs to maintain the salt impurities and corrosion byproducts within normal limits. A purification productivity of 10 t/hr is sufficient to maintain water quality better than provided by the standards (Table 3.3). The results of operation confirm the correctness of selecting construction materials, the water-chemical regime of the plant and also the feasibility of combining the system of indicator monitoring of the materials with inspections of the equipment upon evaluation of the resistance of the materials.

Table 3.3. Norms and Actual Indicators of Water Quality of SUZ Loop

Indicator	Normalized Value	Actual Value
pH	5.5-6.5	5.9-6.3
Content, mg/kg:		
of chlorine ions	0.050	0.01
of iron	0.100	0.06-0.03
of aluminum	0.100	0.03-0.01

The water quality of the RBMK reactor is monitored by automatic devices with flow-through sensors and by laboratory methods of analyzing water samples. The automatic devices monitor the content of the most important indicators of the water regime, measurement of which introduces greater and nonspecific errors without automatic devices with flow-through sensors. These indicators should include the specific electric conductivity of the water measured by a type AK-310 conductometer and pH measured by the potentiometric method using a type pH-201 device. The set

of the device includes flow-through sensors and secondary devices with constant recording of the indicators.

The chlorine ion concentration is measured by the potentiometric method using the LTI-TsKTI laboratory device, and also the argentometric and nephelometric methods of analysis. The trilometric method with reverse titration is used to measure the hardness salt concentration. Low concentrations of hardness salts (less than 1 µg-eqv/kg) are determined by the simulator scale. The concentration of iron corrosion byproducts is recorded by the orthophenathroline method, while determination of the copper content is based on its reaction with lead diethyldithiocarbonate. The basis of the method of determining silicon dioxide is formation of complex silicomolybdenum acid. The content of radiolytic products of water-oxygen and oxygen decomposition is measured by means of chromatographs whose operating principle is based on chromatographic separation of gases from water.

3.6. Thermal and Hydraulic Characteristics

3.6.1. The Determining Heat Engineering Parameters.

The main heat engineering factors that determine the efficiency of a uranium-graphite boiling-water reactor are the temperature of the nuclear fuel, the graphite temperature of the stacking and the reserve to critical output of the fuel channel in which a heat transfer crisis begins. Moreover, hydrodynamic stability of the reactor is required.

An excess of permissible fuel temperature or the occurrence of a heat transfer crisis may lead to failure of an individual fuel assembly, but after it is replaced the reactor efficiency is restored. If there is an RZM, then the defective assembly can be replaced in an operating reactor without reducing its power. However, despite the possibility of rather rapid restoration of reactor efficiency, failure of a fuel assembly is qualified as a reactor failure since it leads to removal of the assembly and to deterioration of the radiation situation at the AES. The absence of catastrophic consequences of emergencies related to failure of individual TVS provides the possibility during design of a reactor and also during operation to be oriented toward proability-statistical methods of determining the maximum fuel temperature and the reserve to critical output of the fuel channel.

The probability-statistical method takes into account the random nature of the coefficients related to the error of manufacturing the core elements, the accuracy of measuring the parameters that affect the determining factors, the accuracy of maintaining operating modes and so on. This approach permits one to substantiate the considerably lower reserves to permissible values of parameters than those which the limiting method yields and is now employed extensively in the practice of reactor construction. The state of the cores of RBMK reactors during operation is also monitored on the basis of probability-statistical methods.

If failure of individual fuel elements and of fuel assemblies is permitted when determining the reserves to critical output and maximum fuel temperature, one must proceed from the condition of providing its efficiency during the entire operating period of the reactor when calculating the permissible temperature of the graphite stacking. Failure of the stacking means failure of the reactor for a prolonged

period. For this reason the maximum graphite temperature is calculated and it is determined during operation by using the limiting method when all the parameters affecting the temperature conditions of the stacking deviate in the unfavorable direction toward the maximum possible values.

The maximum permissible temperature of the graphite stacking is assigned on the basis of existing experience of operating uranium-graphite reactors and depends on the composition of the gas filling the stacking and the amount of water entering the stacking from nonpressurized channels. The composition of the filler gas and the amount of water and water vapor in the stacking are measured continuously during reactor operation and the value of the maximum permissible temperature is corrected as a function of the operating conditions. The condition that the maximum graphite temperature should not exceed the threshold temperature at which oxidation of the graphite in the presence of water vapor in the stacking is no longer linearly dependent on temperature but proceeds more intensively, in all operating modes of the reactor was adopted in practice. The experience of operating existing uranium-graphite reactors shows that the efficiency of the graphite stacking during the entire operating period of the reactor is reliably provided if this condition is observed.

3.6.2. Hydraulics of the Circulating Loop and Heat Transfer in the Reactor Core

The hydraulic characteristics of the circulating loop of a uranium-graphite boiling-water reactor consist of the following hydraulic characteristics: the fuel channel (including delivery and drain pipelines), the cutoff-regulating valve at the inlet to the channel and the drain channel (drain pipelines, collectors and circulating pumps of the fittings).

The hydraulic characteristics of the fuel channel of the RBMK reactor were determined on a full-scale simulator bench with thermal output of 6 MW. The heater pipes on the bench were remotely controlled by lattices whose design was similar to that of the spacer components of the reactor. The results were obtained over a wide range of variation of the regime parameters. The method of calculating the coefficient of frictional drag of the heated bundle of rods located in the two-phase coolant flow was developed along with this.

Additional experiments were conducted on special benches to determine the coefficient of hydraulic drag of the spacer lattices, as a result of which the dependence of the coefficient of hydraulic drag of the lattices on Reynolds number was determined; no effect of the mass steam content of the coolant on the hydraulic drag coefficient was found. The frictional drag on the heated bundle of rods was determined during two-phase flow of the coolant with regard to the pressure losses on the spacer lattices, to acceleration of the flow and to overcome the levelling drop. The experimental data obtained in this manner were then compared to the results of calculations by different methods. Processing of the experimental and calculated material made it possible to select the method for calculating the coefficient of frictional drag of the heated bundle of rods washed by a two-phase flow having the least error at flow parameters close to the working parameters of the reactor [11]. The pressure loss to friction is determined by this method from the equation:

$$-\frac{dP}{dz}=\frac{G^2}{2gS^2\gamma'}\frac{\lambda}{d_r}\psi\left[1+x\left(\frac{\gamma'}{\gamma''}-1\right)\right],$$

where dP/dz is the pressure loss related to unit of length, G is the mass flow rate of the coolant, $g = 9.81\ m/s^2$ is the free fall acceleration, S is the cross-sectional area for passage of the coolant, γ' and γ'' are the water and water vapor density in the saturation line, $d_g = 4S/P$ is the hydraulic cross-sectional diameter for passage of the coolant, P is the wetted cross-sectional perimeter, x is the mass steam content, ψ is the relative coefficient of hydraulic drag determined from the empirical relation:

$$\psi = 1 + 0{,}57\left(\frac{1}{0{,}2+\frac{w_0}{\sqrt{gd_r}}\frac{\gamma''}{\gamma'}} - 5{,}2x^2\right)x^{0{,}125}(1-x)^2;$$

$w_0 = G/(\gamma' S)$ is the flow rate of the circulating coolant; the friction coefficient of a smooth bundle of rods is calculated by the formula

$$\lambda = [1{,}82\ \lg(\mathrm{Re}\,\chi) - 1{,}64]^{-2},$$

where

$$\chi = \frac{2\varepsilon}{(1-\varepsilon)^3}\left(\frac{\varepsilon}{2} - \frac{3}{2} - \frac{\ln\varepsilon}{1-\varepsilon}\right);$$

ε is the relative density of the bundle.

A comparative graph of the experimental values of pressure drops on the heated part of a full-scale bench and of data found by calculation using the optimal method is presented in Figure 3.9. The true volumetric steam content used in the calculations is:

$$\varphi = \left(1 + \frac{1-x}{x}\frac{\gamma''}{\gamma'}K\right)^{-1}.$$

The phase slippage coefficient is

$$K = 1 + \frac{0{,}6 + 1{,}5\beta^3}{\sqrt[4]{w_0/(gd_r)}}\left(1 - \frac{P}{225}\right),$$

where β is the volumetric steam content, and

$$\beta = \left(1 + \frac{1-x}{x}\frac{\gamma''}{\gamma'}\right)^{-1}.$$

The results of comparing the calculated and experimental data (see Figure 3.9) made it possible to conclude that the use of the given method is possible for calculating

the hydraulic characteristics of the steam-generating fuel channel of the RBMK reactor.

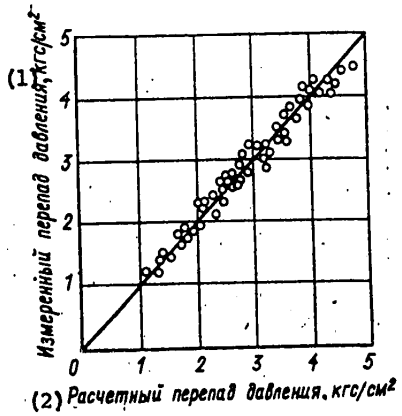

Figure 3.9. Comparison of Calculated and Experimental Data of Pressure Drops on Heated Part of Full Scale Model of Channel

Key:
1. Measured pressure drop, kgf/cm^2
2. Calculated pressure drop, kgf/cm^2

Cold tests of a large series of shutoff-regulating valves were conducted at the design stage of the RBMK reactor, as a result of which it was established that the design of the valves provides the identity of their hydraulic characteristics in the form $Q/\sqrt{\Delta P_{kl}} = f(h)$, where Q is the volumetric flow rate, ΔP_{kl} is the pressure drop in the valve and h is the degree of opening. The calculated and experimental data obtained on the reactor of the first unit of the Leningrad AES for the hydraulics of the fuel channels with inlet sections are compared in Figure 3.10. The results of comparison show satisfactory agreement of calculation and experimemt.

The hydraulic characteristics of the descending loop, the intake delivery collectors and the distributing collectors and fittings were determined with regard to bench and model tests of the corresponding equipment.

The critical output of the fuel channel of a uranium-graphite boiling-water reactor was calculated by the function determined as a result of analysis and processing of experimental results and by the heat transfer crisis in the bundles of heated rods, obtained on bench models and on a full-scale bench of the reactor channel. The experiments were conducted on benches with different configuration of the bundles with coolant parameters close to the working parameters of the reactor. A function similar to that recommended in [12] was selected as the calculating function to determine the conditions for the occurrence of a heat transfer crisis in the fuel channels at the design stage of the RBMK reactor. The mean square error of the calculating formula comprised 8.7 percent with respect to the experimental data available at the same time. This correlation is used in programs for monitoring the state of the cores of existing RBMK reactors. The critical output of each channel is calculated by the formula $N_{kr} = A - Bt_{vkh}$, where t_{vkh} is the water

temperature at the inlet to the channel; coefficients A and B are functions of the water flow rate through the channel and the steam pressure in the separators. The parameters required to calculate N_{kr} are measured by a standard heat engineering monitoring system and are entered automatically into the plant computer.

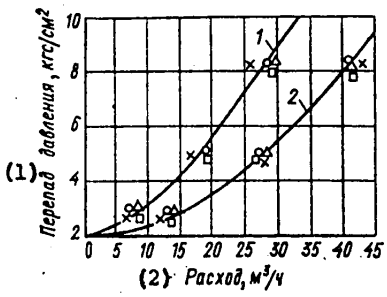

Figure 3.10. Comparison of Calculated Pressure Drops in Fuel Channel to Experimental Data Found on Reactor of First Unit of Leningrad AES: 1--with completely open shutoff-regulating valve (h = 24 mm); 2--with closed shutoff-regulating valve (h = = 8 mm); solid line--calculation; symbols--experimental data for different channels

Key:
1. Pressure drop, kgf/cm^2
2. Flow rate, m^3/hr

Further experiments to investigate the phenomenon of the heat transfer crisis in the channels of a uranium-graphite boiling-water reactor were conducted toward refining the calculating formula. Analysis and processing of the accumulated experimental material made it possible to optimize the coefficients of the formula, which in turn made it possible to increase the calculated value of the critical output of the fuel channels by 5-7 percent. Despite the relatively small increase of the calculated critical power, refinement of the function to determine N_{kr} is reasible since it has a positive effect on the operating and engineering and economic indicators of the reactor. The formula now recommended to calculate N_{kr} in the fuel channels of RBMK reactors has the form:

$$N_{кр}=\frac{4{,}28\cdot10^{6}d_{об}^{0{,}88}(\rho w\cdot10^{-3})^{0{,}57}+4{,}07d_{об}\rho_{w}\cdot\Delta h}{6{,}64\cdot10^{3}d_{об}^{0{,}57}(\rho w\cdot10^{-3})^{0{,}18}+39{,}4L}F,$$

where N_{kr} is the critical output of the channel, kW, $d_{ob} = 4S/P_{ob}$ is the heated diameter of the channel, meters, P_{ob} is the heated perimeter of the through cross-section, w is the mass flow rate, $kg/(s\cdot m^2)$, h is subcooling at the inlet, kcal/kg, L is the length of the channel, meters, and F is the heat transfer surface area in the channel, m^2.

The formula for calculating the value of N_{kr} should be further refined toward taking into account the effect of the nonuniformity of the energy release field

through the height of the core on the heat transfer crisis. As indicated by preliminary analyses, this will make it possible to increase the calculated value of N_{kr} by an additional 5-7 percent. Consideration of the nonuniformity of energy release through the height of uranium-graphite boiling-water RBMK reactors presents no difficulties since a system for monitoring the energy release field through the height of the core is provided.

3.6.3. The Heat Engineering Characteristics of a Reactor at Steady Power Levels

The reserves to critical power and the temperature mode of the fuel assembly fuel and the graphite stacking of the RBMK reactor is monitored during operation and steady power levels by a special Prizma program using the plant computer. The readings of the physical monitoring system, based on intrareactor measurements of the neutron flux through the radius and height of the core, are used to calculate the energy release distribution through the core. Besides the readings of the physical monitoring system, the data that characterize the composition of the core, energy generation of each fuel assembly, the position of the control rods, the distribution of water flow rates through the fuel channels measured by a special monitoring system, the readings of thermocouples located in different zones of the graphite stacking and that measure the graphite temperature and also the readings of the coolant pressure and temperature sensors are entered into the computer.

As a result of calculations by the Prizma program carried out periodically by the computer upon instructions of the operator, he obtains information on a digital printer in the form of a cartogram of the core in which the type of charge of the core, the position of the control rods, the grid for arrangement of intrareactor sensors, power distribution, water flow rates and reserves to critical power for each fuel channel are indicated. The plant computer also calculates the maximum fuel and graphite temperature and indicates the numbers of the channels in which these temperatures occur, the total thermal power of the reactor, the steam content at the output from each fuel channel and other parameters required to monitor and control the reactor.

When the reactor is operating at steady power levels and also during a rise or fall of power, the operator simultaneously with monitoring and control of the energy release field controls the distribution of water flow rates through the fuel channels of the core. Distribution of flow rates is established on the basis of calculating the distribution of reserves to critical power K_z through the fuel channels by the Prizma program: the permissible value of $K_z \geq 1$, and the probability of a heat transfer crisis in the fuel channel comprises 0.0013 at $K_z = 1$. This value has now been checked by the practice of operating existing RBMK reactors, but it can be subsequently corrected toward an increase as statistical material is accomulated.

The need for simultaneous control of the energy release field and distribution of the water flow rate through the fuel channels of a uranium-graphite boiling-water reactor is determined by the large degree of nuclear fuel burnup and the possibility of recharging the fuel in an operating reactor. In this case the burned-up and "fresh" TVS are operated simultaneously. As a result the core structure is complicated with comparatively large nonuniformity of the energy release fields through the reactor radius and it becomes impossible to use the traditional equalization of energy release fields with fixed radial profiling of water flow rates.

Consequently, profiling of the energy release fields and of the water flow rates by algorithms that take into account the real specific conditions occurring during reactor operation is required for effective operation of a uranium-graphite boiling-water reactor.

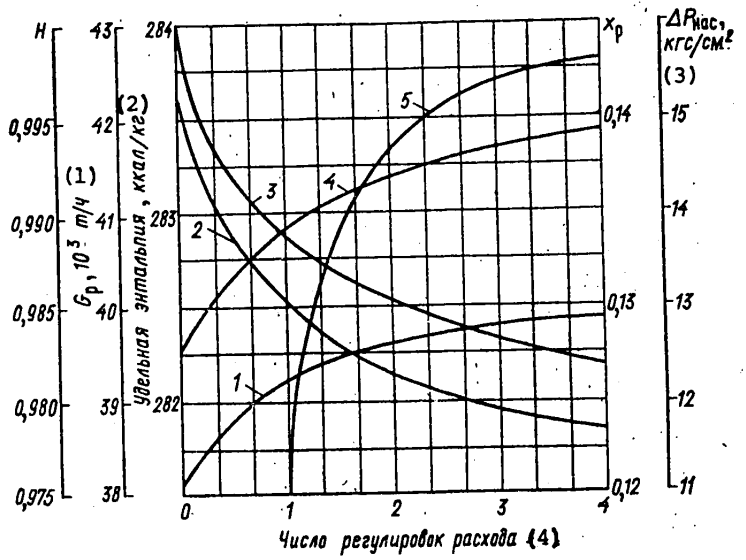

Figure 3.11. Dependence of Main Parameters of RBMK Reactor on Number of Regulations of Flow Rate Through Each Channel: 1--pressure head of GTsN ΔP_{nas}; 2--flow rate through reactor G_r; 3--conditional enthalpy at entrance to reactor; 4--steam content at output from reactor x_r; 5--heat engineering reliability H

Key:
1. Tons/hour
2. Specific enthalpy, kcal/kg
3. kgf/cm^2
4. Number of flow rate regulations

Regulation of the water flow rates through the fuel channels during a nuclear fuel run makes it possible to provide adequate reserves to the heat transfer crisis in the channels thermal-stressed to the maximum with acceptable general water flow rate through the reactor. The calculated dependence of the main parameters of the RBMK reactor operating in the continuous fuel recharging mode on the number of regulations of water flow rate through each channel is presented in Figure 3.11. It is shown in the figure that the probability of at least one of the reactor channels entering the heat transfer crisis mode (R = 1 - H) decreases initially with an increase of the number of regulations and then the value of R becomes stabilized with an increase in the number of regulations above 3. The optimum number of regulations of water flow rate through each channel found in this manner, equal to 2-3 regulations during the run, is acceptable in the continuous fuel recharging mode.

The nonuniformity of the energy release fields can be comparatively high during transition from the initial charge of the core to a charge corresponding to the continuous fuel recharging mode, which leads to the need to increase either the number of regulations of the water flow rate through each channel or the total water flow rate through the reactor (within the capability of the circulating pumps). The main parameters of the RBMK reactor of the first unit of the Leningrad AES during operation and nominal power in the transient core charging mode are presented below:

Electrical output of unit, MW	1,000
Thermal output of reactor, MW	3,130
Number of channels with TVS	1,478
Number of channels with DP	215
Output of most heat-stressed channel, kW	3,010
Maximum linear thermal flux, kW/m	41
Minimum reserve to critical power	1.01
Maximum temperature of graphite stacking, °C	570
Water flow rate through reactor, t/hr	42,000
Mean mass steam content, percent	13
Water temperature at inlet to reactor, °C	270
Steam pressure in separators, kgf/cm^2	69

The water flow rate through the reactor can be regulated by two methods: by changing the degree of opening of the throttle-regulating valves installed at the pressure head of each GTsN and also by changing the degree of opening of the channel shutoff-regulating valves. The throttle-regulating valves are fully opened at nominal power level and the water flow rate through the GTsN is maintained in the range of 6,000-7,000 m^3/hr at power less than 150 MW (electricity) to provide the required reserve to cavitation. Due to the fact that the reactor is started up at reduced productivity of the GTsN, the distribution of water flow rates through the core channels is determined by calculation during this period on an external computer such that an adequate reserve to critical output in each fuel channel is provided when it is brought up to nominal power. When bringing the reactor up to power, the flow rate distribution through the fuel channels is corrected from the results of calculations made by the Prizma program on the plant computer.

The experience of operating existing RBMK reactors showed that the design of the graphite stacking and of the fuel elements at available thermal loads provides maximum graphite and fuel temperatures considerably less than the maximum permissible values. The temperature mode of the stacking depends on how well the thermal contact between the graphite block and the fuel channel pipe, to which heat from the graphite is dissipated, is organized. The developed design of cut graphite rings, from which one is installed with negative allowance on the channel pipe and the other is calculated for negative allowance through the inner opening in the graphite block, provided good heat dissipation from the stacking and the possibility of installation and removal of the channel pipe during the entire reactor operating time. With nitrogen filling the acceptable temperature mode of the graphite at temperatures up to 750°C is provided to outputs of 800-850 MW (electricity). At higher outputs, the stacking is filled with a helium and nitrogen mixture. In this case the maximum graphite temperature comprises approximately 600°C when operating at nominal power.

The value of the maximum fuel temperature determined by calculation using the readings of physical monitoring sensors comprised 1,800-2,000°C at nominal reactor power, which is considerably lower than the melting point of uranium dioxide.

Along with monitoring the reserves to critical power and the temperature mode of the graphite and fuel, selective monitoring of the fuel jacket temperatures is provided in the RBMK reactor under conditions of possible scale formation and deposits of corrosion byproducts on the heat-transfer surfaces. Reference thermometer assemblies supplied with thermocouples located at different points along the height and radius of the fuel assembly are installed for this purpose in the reactor core. The temperature mode of the fuel jackets both in an operating reactor and during repair operations is monitored and studied from the readings of the thermocouples.

3.7. Investigating the Strength of the Equipment and Pipelines

Complex engineering problems related to providing the strength of the equipment and pipelines must be solved during design of an AES [13]. This complexity is determined on the one hand by the use of new materials not having wide distribution in ordinary machine building and not adequately studied, for example, zirconium-based alloys. On the other hand, the conditions of inserting parts in atomic reactors and the related systems differ considerably from those encountered in the practice of operating thermoelectric power plants. This refers primarily to the effect of neutron irradiation on material, as a result of which the plasticity of the material decreases, it becomes embrittled and creep processes are intensified.

The possibility of structures failing due to damage during prolonged static and cyclic loading and extreme deformations accumulated during creep and brittle failure initiated from the zones of different defects, should be considered when designing structures operating under various load conditions and in different operating modes [14]. The problems of creep are of important significance for such components as fuel channel pipes manufactured from zirconium alloys. The criteria of cyclic strength determine the efficiency of the structural zones in which conditions of repeated elastoplastic deformation are realized such as the zones of openings, transfer of fluids, threads, joining of connecting pipes to vessels and so on. Materials become brittle due to the effect of irradiation and thermal and deformation aging and brittle failure of the structures is possible if there are defects in them that exceed specific critical dimensions.

Since the components and assemblies of the MPTs loop are subject during operation to the effect of a wideband spectrum of disturbing high-frequency dynamic forces occurring due to the effect of the flow of the working medium, problems of providing vibration strength acquire special timeliness.

The steam-water mixture at the output from the fuel channel contains a large amount of oxygen (8-10 mg/liter), which requires that problems of corrosion-mechanical strength receive special consideration. Contact of the coolant with the fuel channel pipes leads to separation of oxygen due to the corrosive metal-water reaction and to absorption of it in the zirconium alloys with formation of brittle inclusions--plates of zirconium hydride.

The indicated features of the behavior of material from which the components of the equipment and pipelines of the MPTs loop are manufactured and the operating conditons predetermine the need for investigations to ensure the strength of the equipment and pipelines of AES with RBMK reactors. According to the "Standards for Calculation of Reactor Components, Steam Generators, Vessels and Pipelines of Atomic Power Plants, Experimental and Research Nuclear Reactors and Plants for Strength" [151, all the components of the reactor plant were calculated. The steady modes, the heating-cooling modes, hydraulic tests, disruptions of normal operating conditions and emergency situations related to consequences caused by a hypothetical emergency at an AES, were considered as the main calculated modes. Each mode was characterized by the value and rate of variation of pressure and temperature of the coolant in time and the number of repeat cycles during the service life of the reactor.

Thermal calculations showed that no significant temperature gradients occur in the equipment and pipeline both in the steady and transient modes. Temperature stresses occur mainly in the zones where materials of different structural classes as joined (steel-zirconium, carbon steel-austenitic steel). The stresses determined by calculation were compared to the permissible stresses for the corresponding categories of stresses. This detailed differentiation of stresses permits reliable estimation of the strength, but requires the application of special methods of calculating the stress state. Programs for numerical calculation on a computer were usually the basis of these methods.

The analysis showed that all the components of the reactor unit meet the requirements of normal calculation for strength and at the same time revealed the structural assemblies whose stress state required experimental confirmation. Experimental investigations were carried out using models of optically sensitive materials, plexiglass, metal and also direct measurement of deformations (tensometric measurement) on operating AES during starting-adjusting operations.

Thus, tensometric measurements of descent pipelines, the large-diameter pipes of the GTsN framing, the intake, delivery and distributing collectors, the pipes of the steam-water distributing lines, the fuel channels, separators and assembled steel sections were made during adjustment, startup and operation of the first units of the Leningrad and Chernobyl' AES. The analysis of the given tensometric measurements confirmed the conclusions of strength calculations on the nature of stress distribution and its values.

Vibration parameters were measured simultaneously with tensometric measurements to investigate the characteristics of the vibration strength of structures. Checkpoints of the measurements were selected on the basis of the results of preliminary analysis of the behavior of the structures--at points where pipelines were joined and at fixed supports in the middle part of pipeline runs. It turned out that vibrational stresses in the investigated structural components are very low and do not exceed 1.2 kgf/cm^2 (approximately 12 MPa) in transient operating modes and 0.5 kgf/cm^2 (approximately 5 MPa) in steady operating modes of the reactor. No significant vibrations of the fuel channels and also of the TVS located in them were found.

The reactor unit is operated under conditions of a combination of steady and transient modes. The number of cyclically repeated modes, the range of pressure and temperature variation and the rate of variation directly determine the fatigue resistance of the structures. The method of cyclic strength calculation was regulated by standards for strength calculation. The experimental investigations mainly concerned problems which are not reflected in existing standards. For example, a great deal of attention was devoted to problems of the cyclic strength of a diffusion steel-zirconium welded joint since significant cyclically variable temperature stresses that exceed the yield point of the material occur in it under operating conditions.

The zirconium-niobium alloy used to manufacture the components of the fuel channel is characterized by high plasticity in the initial state, but plasticity may decrease during operation due to hydrogenation and neutron irradiation. The corresponding investigations were conducted to study the effect of the indicated factors on the fatigue strength, fatigue curves were found and it was shown that the given operating life of the fuel channels is provided by the number of transient modes. Similar tests and estimates were also made for welded zirconium-zirconium joints. Direct experiments on cyclic loading by internal pressure and temperature of full-scale mockups of fuel channels under bench conditions confirmed the correctness of the conclusions made.

A number of pipelines of the MPTs loop of corrosion-resistant chrome-nickel 08Kh18N10T steel was protected by an anticorrosion aluminum coating that forms a brittle interlayer of intermetallic compounds whose thickness increases during operation in the contact zone with the base metal. The coefficients of a decrease of fatigue strength, caused by the effect of this interlayer, were determined in special experiments which were used in making the strength calculations.

The possibility of developing the permissible standards for quality control of the production flaws in fuel channel pipes and pipelines of the delivery and intake channels of the GTsN were investigated. Data on the kinetics of fatigue cracks in Zr + 2.5 percent Nb alloy, steel of mark 22K and the welded joints of these materials were used for this purpose. The analyses showed that there is no basis to doubt that the given service life of the components of the MPTs loop will be provided if the possible development of defects due to cyclic loading under operating conditions is taken into account.

The use of Zr + 2.5 percent Nb alloy as the material of the central part of the fuel channel pipe required that an extensive complex of experimental work be carried out to analyze its creep strength and ultimate strength. The investigations were conducted both under laboratory and under reactor conditions. The extreme creep of fuel channel pipes may lead, on the one hand, to selection of gaps between the pipes and stacking of the reactor and on the other hand, to exhaustion of the plastic limit of the material with subsequent failure. It is known that irradiation intensifies creep processes at relatively low stresses and temperatures up to 325°C and the rate of creep is directly proportional to the influence of fast neutrons. The anisotropy of the properties of zirconium alloys may lead to the fact that the lengths of the fuel channel pipes may be increased under operating conditions. All these circumstances were taken into account when estimating the creep strength of the pipes. The analysis conducted with specific assumptions

resulting in a strength reserve showed that the maximum increase of the fuel channel pipe diameter over a period of 25 years of operation will not exceed the permissible increase.

It was established upon study of the variation of the ultimate plasticity of Zr + 2.5 percent Nb alloy that plasticity characterized by relative elongation of a specimen during failure is increased over time. Deformations on the order of 5-10 percent were achieved without failure in fuel channel pipes during experiments under irradiation conditions. The ultimate strength of zirconium alloys increases upon exposure to radiation and the data of laboratory tests of unirradiated specimens can be used as the strength reserve to estimate the ultimate strength. It follows from theoretical estimates and processing of experimental data using the Larson-Miller parameter that the given operating life of a fuel channel is provided by the criterion of ultimate strength [16]. Calculated estimates and experimental data obtained by foreign authors shows that an increase in the length of the fuel channel is possible, which must be taken into account when designing the system for temperature compensation of the channels.

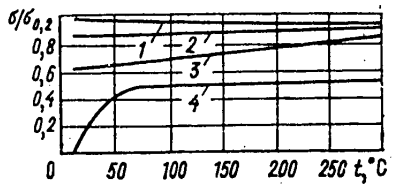

Figure 3.12. Diagram of Failure Strength of Zirconium-Niobium Pipes of Fuel Channels: 1--Effluent $\Phi = 0$, degree of hydrogenation $C_{H_2} = 0.002$ percent; 2--$\Phi = 10^{21}$ neutrons/cm^2, $C_{H_2} = 0.002$ percent; 3--$\Phi = 10^{21}$ neutrons/cm^2, $C_{H_2} = 0.04$ percent; 4--calculated stress in fuel channel

Pipes manufactured from Zr + 2.5 percent Nb alloy become brittle primarily due to the effect of hydrogenation and irradiation. A shift of critical brittleness temperature (KTKh) of Zr + 2.5 percent Nb alloy and of its welded joints due to the effect of hydrogenation even to a relatively low degree (0.02-0.03 percent by mass) encompasses practically the entire temperature range of fuel channel operation. Irradiation also changes the KTKh toward positive temperatures and is greater, the lower the degree of hydrogenation. The maximum value of KTKh comprises about 350°C and does not vary with subsequent increase of the degree of hydrogenation and effluent of neutrons [9]. A high value of KTKh indicates the essential possibility of brittle failure of zirconium pipes and requires that the corresponding analysis of the possibility of this failure be carried out. The critical opening of the crack δ_c was taken as the main characteristic for estimating the brittle failure strength of the material.

Hydrogenation significantly reduces the value of δ_c at temperatures on the order of 20°C and essentially has no effect on δ_c at temperatures above 300°C. Special investigations of specimens cut from pipes of experimental fuel channels of the first unit of the Beloyarskaya AES were conducted to study the effect of irradiation on δ_c. It was determined that irradiation has a significant effect on δ_c

and reduces its value over the entire investigated temperature range (20-300°C). There is no subsequent decrease of δ_c after hydrogenation to 0.04 percent by mass and after neutron flux of 10^{20}-10^{21} neutrons/cm^2.

A diagram for calculating zirconium-niobium pipes for brittle failure strength (Figure 3.12) was constructed on the basis of the data obtained. The nature of stress variation in the fuel channel pipe during operation (curve 4) is shown arbitrarily. Curve 4 lies below the curve of the stresses permissible during operation (curve 3) over the entire range of operating temperatures, which means that brittle failure strength of the fuel channel pipes will be provided.

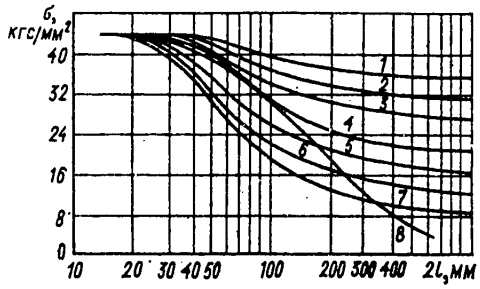

Figure 3.13. Diagram of Failure Strength of Pipelines D_y = 800 mm: 1-7--b/s = 0.3, 0.4, 0.5, 0.6, 0.7, 0.8 and 0.9, respectively (b--extent of defect; s--wall thickness of pipe)

Another important component of the MPTs loop of the RBMK reactor, failure of which is a very serious emergency, are the delivery and intake pipelines with D_y = 800 mm. The investigations permitted construction of the failure diagram of pipelines with D_y = 800 mm, presented in Figure 3.13 [17]. Curves 1-7 were plotted for surface defects of different depth. If a defect exists in the structure and its dimensions and also the stresses in the structure are such that a point with corresponding coordinates is located below curve 8, then only a leak can form in the structure. The plotted diagram was confirmed by the results of testing full-scale straight pipes and elbows with D_y = 800 mm with different surface cuts.

Consideration of the failure diagram permits one to conclude that a leak forms in the pipelines at working pressure of 85-90 kgf/cm^2 (approximately 8.7 MPa) if the defect in it with length of 2l = 470 mm reaches a depth equal to 0.75 of the wall thickness.

The service life and operating conditions of the equipment and pipelines of the reactor unit were selected on the basis of complex calculation-experimental investigations of the strength and efficiency of components of the MPTs loop that encompass study of practically all possible failure sources.

BIBLIOGRAPHY

1. Gerasimov, V. V., A. I. Gromova, V. N. Belous et al, "Corrosion of Structural Materials Under Operating Conditions of the First Circuit of an AES with Boiling-Water Reactors. Stainless and Perlite Steel and Zirconium Alloys," in "Opyt ekspluatatsii AES i puti dal'neyshego razvitiya atomnoy energetiki" [The Experience of Operating Nuclear Power Plants and Methods for Further Development of Atomic Power Engineering], Obninsk, FEI, 1974.

2. Gerasimov, V. V. and V. V. Gerasimova, "Korrozionnoye rastreskivaniye austenitnykh nerzhaveyushchikh staley" [Corrosion Cracking of Austenitic Stainless Steels], Moscow, Metallurgiya, 1976.

3. Gromova, A. I., V. V. Gerasimov, N. A. Kabankova et al, "The Corrosion and Electrochemical Behavior of a Zirconium Alloy with 2.5 Percent Niobium in Water and Steam at High Temperature," ATOMNAYA ENERGIYA, Vol 29, No 5, 1970.

4. Parfenov, B. G., V. V. Gerasimov and G. I. Venediktova, "Korroziya tsirkoniya i ego splavov" [Corrosion of Zirconium and Its Alloys], Moscow, Atomizdat, 1967.

5. Morozova, I. K., A. I. Gromova, V. V. Gerasimov et al, "Vynos i otlozheniya produktov korrozii reaktornykh materialov" [Removal and Deposits of Corrosion Products of Reactor Materials], Moscow, Atomizdat, 1965.

6. Belous, V. N., A. I. Gromova, V. V. Gerasimov et al, "The Corrosion and Electrochemical Behavior of Zirconium Alloy in Water at High Temperature," ZASHCHITA METALLOV, Vol 4, No 6, 1968.

7. Gerasimov, V. V., A. I. Gromova, I. K. Morozova et al, "Deposition of Corrosion Products on the Surface of Zirconium Alloys," ATOMNAYA ENERGIYA, Vol 32, No 1, 1972.

8. Gerasimov, V. V., A. I. Gromova and V. G. Denisov, "Estimating the Corrosion of Zirconium Alloys Under Operating Conditions," ATOMNAYA ENERGIYA, Vol 41, No 1, 1976.

9. Rivkin, Ye. Yu., B. S. Rodchenkov and V. M. Filatov, "Prochnost' splavov tsirkoniya" [The Strength of Zirconium Alloys], Moscow, Atomizdat, 1974.

10. Bulkin, Yu. M., K. K. Polushkin, V. I. Krylova et al, "Design Characteristics and Problems of Efficiency of Fuel Channel Components of the RBMK Reactor," VOPROSY ATOMNOY NAUKI I TEKHNIKI, SERIYA REAKTOROSTROYENIYE, No 2 (9), 1974.

11. Osmachkin, V. S. and V. D. Borisov, "The Hydraulic Drag of Bundles of Fuel Rods in a Boiling Water Flow," Preprint IAE-1957, Moscow, 1970.

12. Macbeth, R. V., "Burn-Out Analysis, Part V: Examination of Published World Data for Rod Bundles," AEEW-R358, 1964.

13. Dollezhal', N. A., O. A. Shatskaya, M. I. Yegorov et al, "Main Problems of the Strength of the Equipment of Atomic Power Plants," "Opyt ekspluatatsii AES i puti dal'neyshego razvitiya atomnoy energetiki," Vol 2, Obninsk, FEI, 1974.

14. Shatskaya, O. A., "Some Problems of Strength in Reactor Construction," VOPROSY ATOMNOY NAUKI I TEKHNIKI, SERIYA FIZIKA I TEKHNIKA YADERNYKH REAKTOROV, No 1 (21), 1978.

15. "Normy rascheta na prochnost' elementov reaktorov, parogeneratorov, sosudov i truboprovodov atomnykh elektrostantsiy, opytnykh i issledovatel'skikh yadernykh reaktorov i ustanovok" [Standards for Strength Calculation of Reactor Components, Steam Generators, Vessels and Pipelines of Nuclear Power Plants and Experimental and Research Nuclear Reactors and Units], Moscow, Metallurgiya, 1973.

16. Rivkin, Ye. Yu., "Problems of the Strength of Fuel Channels of RBMK Reactors," VOPROSY ATOMNOY NAUKI I TEKHNIKI, SERIYA FIZIKA I TEKHNIKA YADERNYKH REAKTOROV, No 1 (21), 1978.

17. Dollezhal', N. A., "Nuclear Power Engineering and the Scientific and Technical Problems of Developing It," ATOMNAYA ENERGIYA, Vol 44, No 3, 1978.

FUEL ASSEMBLIES

Moscow KANAL'NYY YADERNYY ENERGETICHESKIY REAKTOR in Russian 1980 (signed to press 27 Mar 80) pp 95-101

[Chapter 5 from the book "Channel-Type Nuclear Power Reactor", by Nikolay Antonovich Dollezhal' and Ivan Yakovlevich Yemel'yanov, Scientific Research and Design Institute of Power Engineering, Atomizdat, 2,550 copies, 208 pages]

5.1. Operating Conditions and Main Characteristics

High requirements on reliability during the entire service life are placed on the fuel elements and TVS. The complexity of realizing them is aggravated by the fact that the length of the channel is 7,000 mm with relatively small diameter and machine recharging of the assemblies both in a shutdown and in an operating reactor should be provided. The stressful operating conditions of the TVS in reactors of the described type predetermine the need to conduct a large complex of prereactor and reactor tests. The main parameters that characterize the operating conditions of TVS are as follows:

Output of maximum stress channel	3,000-3,200 kW (t)
Coolant flow rate through channel at maximum output	29.5-30.5 t/hr
Maximum mass steam content at output from assemblies	19.6 percent
Parameters of coolant at inlet to assembly:	
pressure	79.6 kgf/cm^2
temperature	265°C
Parameters of coolant at output from assembly:	
pressure	75.3 kgf/cm^2
temperature	289.3°C
maximum flow rate	18.5 m/s
Maximum temperature:	
of outer jacket surface	295°C
of inner jacket surface	323°C
Coefficients of nonuniform heat release:	
through height of assembly	14
through radius of assembly	1.06
Initial enrichment of uranium	1.8-2 percent
Mean uranium burnup plateau through channels	19.5-24.4 GW·day/t of UO_2
Maximum fuel burnup	24-28 GW·day/t of UO_2
Run of assembly with burnup of 24 GW·day/t of UO_2	1,250-1,700 effective days

Service life of assembly with utilization factor of 0.85	1,470 days
Maximum linear output of fuel element	360-385 W/cm
Maximum temperature at center of fuel pellet	2,100°C

The assemblies consist of the following main parts: two TVS that carry the central road, a shank, a cap and rod (Figure 5.1). The assembly, designed to install an energy release monitoring sensor (DKE) through the radius of the reactor, is distinguished by the fact a pipe with steel-zirconium adapter and an end cap is used in it instead of a carrier rod.

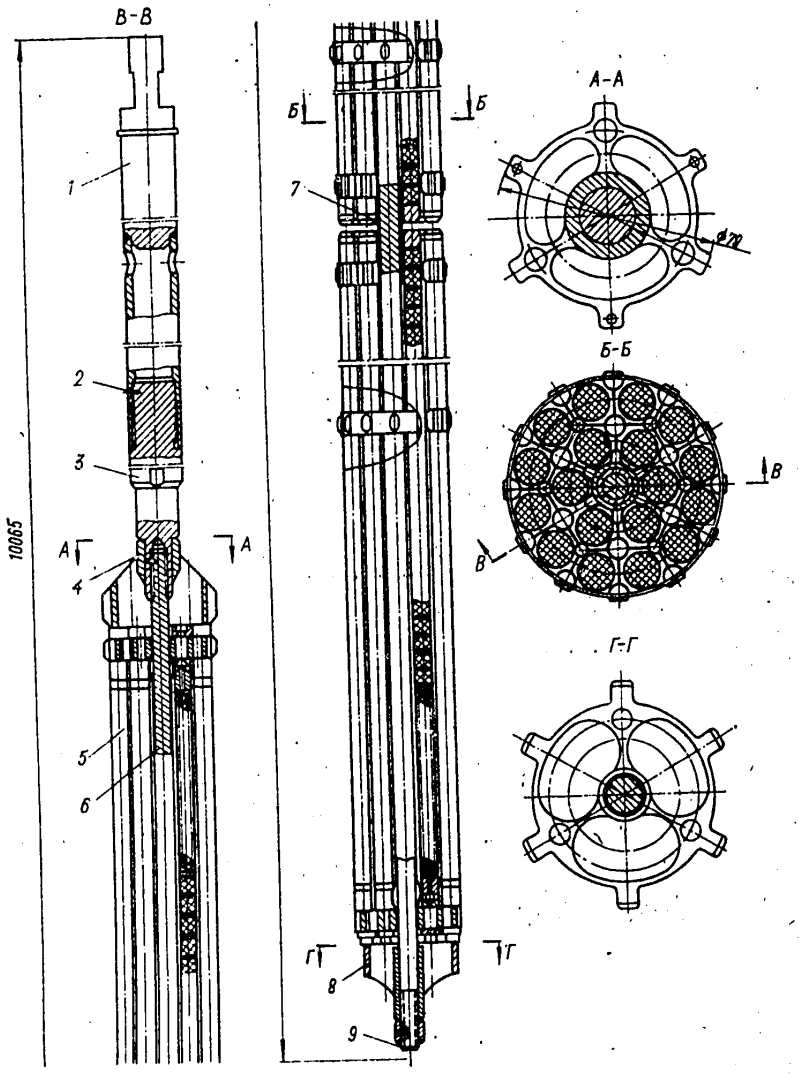

Figure 5.1. Fuel Assembly of RBMK: 1--suspension; 2--pin; 3--adapter; 4--shank; 5--fuel element; 6--carrier rod; 7--sleeve; 8--end cap; 9--nuts

A TVS consists of 18 rod-type fuel elements, a housing and attaching parts; the TVS are interchangeable. The housing is a central pipe on which are installed one end and 10 spacer lattices. The end lattice is attached to the central pipe by beading the pipe and serves to attach the fuel elements by clamping sleeves. The nine spacer lattices are held in the central pipe by means of projections (pressing the protruding end of the central cell into the grooves on the pipe), which permit them to move along the axis for a distance of approximately 3.5 mm upon thermal expansion of the fuel elements. One outer spacer lattice is attached to a key to increase the stiffness against twisting of the bundle.

The spacer lattice is a honeycomb structure and is assembled from the central, six intermediate and 12 peripheral cells and a rim joined to each other by spot welding. Spacer projections are provided on the rim.

The end of the central pipe of the housing has a rectangular cut to half the diameter. The TVS are joined to each other such that the projectionof the pipe of one TVS enters the cut of the other. This provides coaxiality of the fuel elements of two TVS and eliminates rotation of them with respect to each other.

The fuel elements are rigidly attached to the end lattices of the TVS (on the upper and lower boundaries of the core) and the clearance in the center of the core is selected during operation as a result of thermal expansion. The fuel element consists of a jacket with fuel pellets of uranium dioxide, a lower end plug, cylindrical compression spring, sleeve with opening and end cap. The fuel element is sealed by electron beam and argon-arc welding. The inner cavity of the fuel element is filled with an argon and helium mixture.

Reducing the distance between the fuel pellets in the center of the core makes it possible to reduce the spurge of heat release and thus to reduce the temperature of the fuel and the structural material in the zone of the fuel element end plugs. The use of two sections through the height of the core leads to the fact that the fuel elements of each section operate both in the maximum and in the minimum zone of energy release in height. In this case the inner pressure in the fuel elements corresponds to the average fuel temperature through the height.

The geometric and mass characteristics of the fuel assembly are presented below.

Length	10,065 mm
Maximum diameter	79 mm
Length of core:	
maximum	6,954 mm
minimum	6,920 mm
Mass	185 kg
Mass of uranium dioxide in assembly	125-135 kg
Mass of corrosion-resistant steel on length of core	$\leq$ 1.1 kg
Mass of zirconium alloys on length of core	$\leq$ 40 kg

5.2. Results of Main Experimental Work to Analyze the Reliability of the TVS

The majority of problems arising during development of the design was solved by simulation or direct checking. Experimental investigations on electrically heated models were conducted to confirm the heat engineering reliability. Experiments were first conducted on a three-rod bundle and then on bundles with 3, 7 and 19 simulators, but of the shortest length, with simulation of the TVS cell of the RBMK. The purpose of these experiments was to investigate the effect of the number of rods on the occurrence of a heat transfer crisis, which was not found. The tests on a full-scale bench with electrically heated model of a standard assembly with parameters similar to those of the RBMK channel were the final tests.

One of the determining factors of the efficiency of fuel elements is the permissible temperature of the inner surface of the end plug of the fuel element in the center of the core. The temperature distribution in the end plug, fuel and jacket and also the thermal flux density in the region of a heat release surge at the point where the TVS are joined, was deteinined on a computer by the electrical analogy method. Experiments showed that the maximum temperature of the end plug in contact with the fuel does not exceed 520°C and that on the outer surface does not exceed 330°C, while the temperature in the center of the fuel increases slightly within permissible limits for the zirconium alloys used.

Wind tunnel tests were conducted for comparative selection of the designs of the spacer and end lattices. The selected versions were investigated in water and in a steam-water mixture to find the calculating functions of the frictional coefficients in the bundle to determine the local resistance coefficients. The hydrodynamic characteristics of the RBMK TVS were calculated from these data. Confirmation of the calculation results was obtained upon testing on a full-scale bench.

The zirconium alloys used as fuel jackets and other parts of the TVS were investigated for efficiency. Autoclave and dynamic tests of the alloys, welded joints and also the steel-zirconium adapter available in an assembly with DKE were conducted to check the corrosion behavior of the selected alloys during operation in a steam-water mixture. The quality of the coolant, identical to the design quality for the RBMK reactor, was provided during testing. The tests confirmed their suitability for operation in the TVS structure. The materials underwent a final check during reactor tests of the fuel elements and TVS. The results permitted the conclusion that the properties of the selected zirconium alloys are satisfactory and that these properties are retained over a service life of 5 years. A considerable part of the experimental investigations was conducted to check the conformity of the actual efficiency of individual assemblies and of the design as a whole to the requirements placed on them during different operating modes of the TVS.

The program of preliminary strength investigations envisioned the determination of the mechanical properties of the materials used and of the structural strength of the parts and assemblies. The load diagrams corresponded to the assembly operating conditions in the channel and also to the various possible situations during recharging and transport. Thus, cases of seizing or "jamming" of the assembly in the channel during unloading after prolonged operation were considered. In this case the most crucial supporting parts should have a tenfold strength reserve.

The less crucial parts and joints were designed for lower strength reserves. The most dangerous force acting on the assembly in the channel during reactor operation is vibration of the fuel elements and the assembly as a whole, which occurs as a result of pressure fluctuations of the coolant during flow past obstacles of the end part and lattice type.

Different versions of the design were compared from the results of model tests on a two-component vibration table. The vibrational frequency and the dynamic load were selected on the basis of the experience of previous developments and of approximate calculation of the frequency of natural vibrations of the rods and supports along the length. The model to be tested was placed in a steel channel with inner diameter of 80 mm, filled with distilled water. Strain gauges whose readings were recorded wre glued to the fuel element simulators. The quality of the spacer lattice was determined by visual inspection and by measurement of the dimensions before and after the tests and also by the condition of the zirconium fuel jackets under the lattices. Tests of the finally selected lattice design on a vibration table showed their reliability and there was essentially no wear of the fuel jackets. All the joints of the assembly were checked and requirements on their manufacture were developed during the vibrational tests. The effect of vibration of the fuel element core on the wear of the inner surface of the jacket was investigated visually. No significant changes in the jacket were found and the pellets also retained their configuration.

The effect of temperature lengthening on the efficiency of the design was investigated to investigate the mechanical loads on the assembly during startups and shutdowns of the reactor. It is obvious that the fuel element jackets reach a higher temperature when brought to power than the central pipe or the carrier rod. The temperatures should become equalized upon cooling (shutdown). An experiment was conducted on a model in which the central rod was made of steel and the jackets of the fuel element simulators were made of zirconium to determine the effect of thermal fluctuations. The model was cyclically heated and cooled. The difference in the linear expansions of steel and zirconium simulated the difference of the thermal expansions of the fuel elements and the housing. The test results confirmed the reliability of the TVS design.

A number of experimental investigations to check the efficiency of the RBMK TVS was conducted on full-scale models of the assemblies. A special bench was designed and manufactured to analyze the efficiency of the assembly during loading into the reactor channels and removal from them. The bench made it possible to simulate the deformation of the fuel channel, which is possible during installation and operation, and also the different fracture angles at points where individual sections of the channel are welded. The channel was deformed by the clapping sleeves in two mutually perpendicular directions and it was fractured by the flange connectors of the channel. A full-scale model of the assembly was tested and the mass of the assembly corresponded to the real mass. The mockup of the assembly was suspended on a dynamometer and was inserted into the channel at different rates and in this case the mean statistical forces of loading and unloading were determined for each shape and degree of bending of the channel.

The spacer lattices were not damaged during motion of the assembly at rate of 3 m/min if the junctions were tapered with an angle of 60° at the vertex; the rate of

travel of the cassette had to be reduced with smaller acute angle. The beads of the welded seams have no configuration that can be checked; therefore, special requirements were placed on the quality of manufacture of the channel. A rate of travel of the assembly up to 10 m/min could be assumed permissible on the smooth sections of the channel. This was confirmed by loading of full-scale assemblies into the fuel channels of the reactor of the first unit of the Leningrad AES prior to standard charging of the apparatus. The dynamic characteristics of the assembly were also determined on the bench and it was established that the assemblies did not fail even with parts embrittled due to artificial hydrogenation when the assembly dropped into the channel from a height of 0.5 meter and with rigid stopping during travel at a rate of 10 m/min.

A complex check of the efficiency of the assemblies was made on an operating life test bench. A full-scale assembly was placed in a fuel channel simulator. A coolant whose chemical composition and parameters were similar to real conditions was pumped through the channel. Steam was delivered to three chambers along the height of the channel to simulate the steam content. It was delivered through a cermet throttle valve so as to provide quiescent entry into the channel without a transverse shock stream.

The channel was supplied with heat engineering monitoring devices and strain gauges were installed on the three fuel element simulators in the upper TVS to determine the characteristics of fuel element vibration. The inner surface of the channel and the assembly was inspected prior to the beginning of the tests and the dimensions of the assembly were measured. The water and steam flow rates were varied during the tests according to the program and the readings of the strain gauges and assembly vibration sensors were recorded. Thermal cycling by variation of the water temperature at the inlet to the channel (800 cycles) was carried out to test the channel for strength under variable operating conditions. The assembly was tested for 10,000 hours at nominal flow rate and the assemblies were inspected every 500 hours. The vibrational frequencies and stresses in the fuel elements were measured in 16 modes. Operating life tests confirmed the efficiency of the assembly.

The transportability of the assembly was checked simultaneously with tests of the container designed for this purpose. One fully charged container was transported by rail for a distance of more than 5,000 km. The assemblies and containers were then inspected; they passed the test.

The final check of the efficiency of individual assemblies and of the design of the fuel assembly as a whole was conducted during reactor tests. They were conducted on several loop installations. The efficiency of full-size fuel elements was confirmed: the strength of individual assemblies of the fuel assembly, the hydrodynamic characteristics and their variation in time, the possibility of providing reliable heat removal during the entire service life and the behavior of the TVS under variable operating conditions were finally checked. The water conditions during the tests were close to the standard water regime adopted for the RBMK reactor or to an ammonia regime to check the possibility of the fuel elements operating in this mode. Several hundred shutdowns and startups with different rate of power variation were conducted during the testing of the TVS.

The results of testing full-scale TVS confirm the data obtained during mass tests of the fuel elements. The average fuel burnup exceeded the given value and comprised 19,200 MW·day/t. The behavior of the material of the fuel jackets also met the requirements placed on it. The values of elongations of fuel elements of given design, occurring during operation in the reactor, were refined. They comprise no more than 0.20 percent of the initial length during the given run. In this case a clearance of 20 mm existing between the ends of the fuel elements at the junction of two TVS was not fully selected during the entire operating period of the assemblies. The hydrodynamic characteristics were measured repeatedly during tests of full-scale assemblies, which confirmed the correctness of selecting the calculating formulas to determine the hydraulic drag in the channel of the RBMK reactor. They also made it possible to study the growth dynamics of hydraulic drag in time due to deposits of corrosion products on the fuel element surfaces. This growth was insignificant.

The condition of the TVS and also of the pipes of the fuel channels was studied carefully after testing, as a result of which it was established that the assemblies and parts of the RBMK fuel assemblies have the required efficiency. No disruptions of configuration, no wear of the fuel element jackets and no failures of parts were found. The dangerous action of the assembly on the pipes of the fuel channels were also not established.

The efficiency of the RBMK TVS was confirmed as a result of a complex of prereactor and reactor tests. Conducing an extensive check of the design, having principal distinguishing features, made it possible to guarantee that the required characteristics would be achieved during the given service life in plants with uranium-graphite channel-type reactors.

CONTROL DEVICES

Moscow KANAL'NYY YADERNYY ENERGETICHESKIY REAKTOR in Russian 1980 (signed to press 27 Mar 80) pp 119-123, 131-138

[Excerpts from Chapter 6 from the book "Channel-Type Nuclear Power Reactor", by Nikolay Antonovich Dollezhal' and Ivan Yakovlevich Yemel'yanov, Scientific Research and Design Institute of Power Engineering, Atomizdat, 2,550 copies, 208 pages]

[Excerpts] 6.1.8. Regulation of Energy Release Distribution

The operator monitors the energy release distribution, the reserve coefficient to maximum permissible power (by the boiling crisis) and the maximum permissible power (by the linear load), the water flow rates through the channels and the general loop heat engineering parameters such as pressure, flow rates of the circulation and feed water, levels in the separators and so on, during operation of the reactor in the power range of outputs.

Operational monitoring of the energy release distribution is accomplished by signals of deviations from the given settings of DKE currents, side ionization chambers, intrareactor LAZ chambers and if the LAR is shut down, of the LAR chamber. The settings for these systems are calculated periodically by the Prizma program and are entered manually into the systems on the operator's instructions.

Reactor power is monitored from the readings of automatic recorders that record the total DKE(r) current and of the side ionization chambers. The reactor power produced by the SFKRE(r) is compared in the impressions of the Skala system to the results obtained from readings of the heat engineering devices. Detailed information may be issued to the operator both in the form of cartograms and in the form of abbreviated summaries with indication of regions with the least values of K_{zi}^{min} for detailed analysis of the reactor's condition. Operational control of the remaining heat engineering parameters is maintained from signals onto a mimic panel.

The operator's regulating actions during operation of the reactor are reduced mainly to variation of the position of the SUZ rods and regulation of the water flow rates through the channels and settings. It is regulated by an automatic regulator during runup of power while the energy release distribution is regulated manually. Reactor power can be maintained and the energy release distribution can

be stabilized by the LAR system after runup to steady modes. At the same time the operator continues to slowly correct the energy release distribution.

Manual regulation of the energy release distribution is accomplished by alternate movement of the RR and SP rods and includes elimination of radial-azimuth and local axial misalignments. Misalignments developed only by the first axial harmonic are eliminated in the height distributions. The remaining harmonics are very stable and their presence is taken into account during long-term variation of energy release distribution related to recharging of the TVS, DP and so on. In this case the radial surge in the presence of a surge in the bottom half of the reactor is eliminated by introducing a rod from below in the given region or by identical introduction of RR and USP rods in the given region in the upper and lower parts of the reactor, respectively, or by introducing RR or USP rods separately if their ends are located near the center of the core in height, since their travel does not create a height misalignment in this case.

Thus, analyzing the foregoing, it is easy to see that the complex of monitoring and regulating system is essentially hierarchical structures. The monitoring structure has independent subsystems in its base. The computer of the centralized Skala monitoring system with the Prizma program, which calculates and carries out logical analysis of all the incoming information, mutual tie-in of systems and issuance of recommendations on adjustment of them, is located at the top of the monitoring structure. The control structure also has practically independent subsystems in its base. The reactor operator, who performs direct control functions and provides correct interaction of the control subsystems along with performing more complex functions (by the logic and amount of information to be processed), is located at the top of the control structure.

The adopted structures provide reliable, efficient and safe operation of RBMK reactors. Runup to nominal power was first accomplished in 1974; a fragment of the computer printout of the channel parameters during these runups is presented in Figure 6.8.

6.2. Reactor Power Control System

The methods and means of control outlined in section 6.1 reflect the problems of regulating the energy release distribution through the core. Moreover this regulation is required to achieve high power. A system in which ionization chambers located in channels behind the reflector were used as detectors is provided to monitor and control the total reactor power in all modes, i.e., from the subcritical state to the nominal state. This system also reduces the power or completely stops the chain reaction if situations occur that do not permit the process to continue at a given level (emergency situations).

Schematic diagrams of control, logic elements and shaping signals for control of actuating mechanisms and of control mechanisms themselves are included in the given system as components. The energy release field and the total power level are regulated by absorbing rods that are a unified structure.

The block diagram. All the absorbing rods have individual drives and are moved by signals which are shaped in the logic control circuit. The rods are

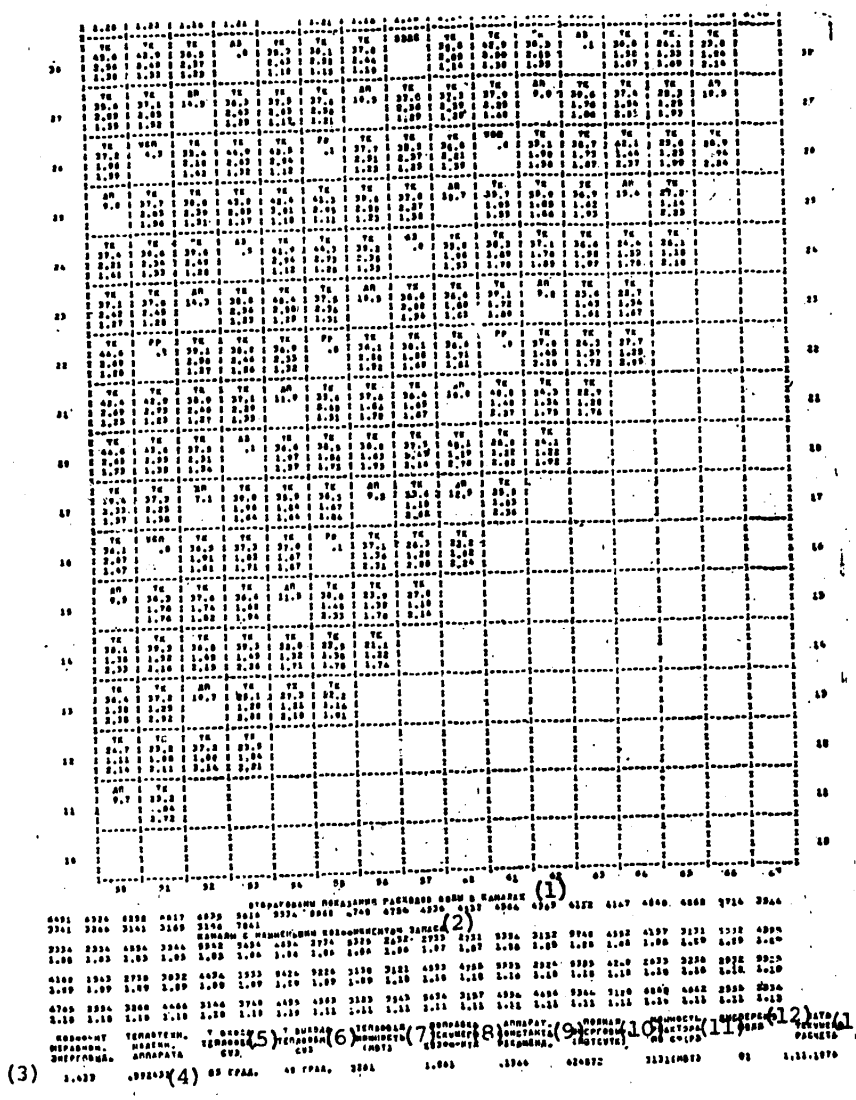

Figure 6.8. Cartogram of Production Parameters of Reactor at Power of 1,000 MW (electricity)

Key:

1. Readings of water flow rates in channels rejected
2. Channels with lowest reserve coefficient
3. Nonuniform energy release coefficient
4. Heat engineering reliability of apparatus
5. Thermal input of heat transfer SUZ

[Key continued on following page]

[Key continued from preceding page]:

6. Thermal output of heat engineering SUZ
7. Thermal output (MW)
8. Correction of current coefficient
9. Apparatus of recommended constant
10. Total energy release (MW per day)
11. Reactor power through [translator's note: one word illegible]
12. Field dispersion
13. Date of current calculation

distributed by groups: automatic regulation of total power, manual remote or automatic regulation of energy release distribution, emergency reduction of total power level or complete stopping of the chain reaction. The design of a rod with displacer is presented in Figure 6.9 and represents sleeves of molded boron carbide enclosed in airtight cavities. The rods are moved by servodrives installed directly in the reactor channels [11]. The neutron flux is monitored from deeply subcritical to nominal power level. A block diagram of the power control is presented in Figure 6.10; no energy release monitoring detectors are included in it. The range of the monitoring detectors are presented below:

Automatic recorder with KNK-53M	10^{-2}--100 percent
M135 device in circuit of operating AR with KNK-53M	10^{-3}--100 percent
M135 device in ARmm circuit with KNK-53M	$7 \cdot 10^{-5}$--7 percent
AZS with KNK-56 in lead	$2 \cdot 10^{-7}$--2 percent
ISS with KNT-31	10^{-10}--$4 \cdot 10^{-7}$ percent

The neutron flux in starting modes and at low power levels in monitored by three independent measuring channels by KNT-31 fission chambers located in the side reflector. The neutron flux density in logarithmic scale and the runup period of the reactor are measured by the secondary electronic devices operating from the fission chamber. After values that exceed the maximum permissible values have been reached by the neutron flux for the fission chambers, the latter are removed from the core. The neutron flux is monitored at intermediate power levels by signals from the KNK-56 highly sensitive starting current ionization chambers located in the tank of the side water shielding. The chambers are surrounded with lead shields to reduce the effect of the γ-background. The neutron flux density and the runup period are determined by the signals of these chambers and the emergency shielding of the reactor during the runup period is also triggered by these signals. The KNK-56 starting ionization chambers are used as sensors of the automatic power control apparatus and also as shielding against an excess of power at low levels.

One automatic medium-power regulator having four channels for measuring the currents of the ionization chambers and acting on the four control rods moving synchronously in the core operates at power levels of 0.25-6 percent. A special electrical system is used to synchronize the travel of the control rods.

Two automatic medium-power regulators, one of which is put into operation and the other of which is in a "hot" reserve state, are used in the range of 6-100

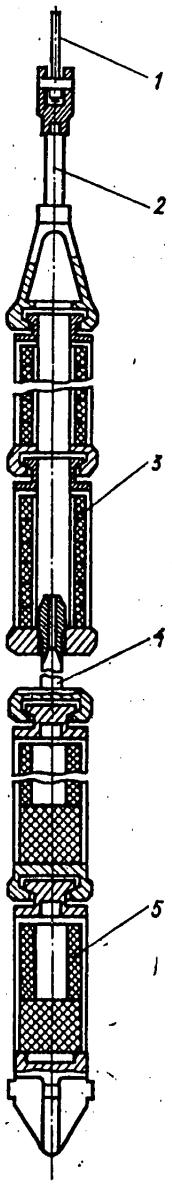

Figure 6.9. Absorbing Rod: 1--cable; 2--rod; 3--absorbing section; 4--telescopic extension; 5--displacer section

percent. A reserve regulator is put into operation automatically if the operating regulator is cut off when malfunctions appear in the apparatus. All the automatic power regulators are made by the same type structure: each has four measuring and four actuating channels and maintains efficiency if any of the measuring or actuating channels fail.

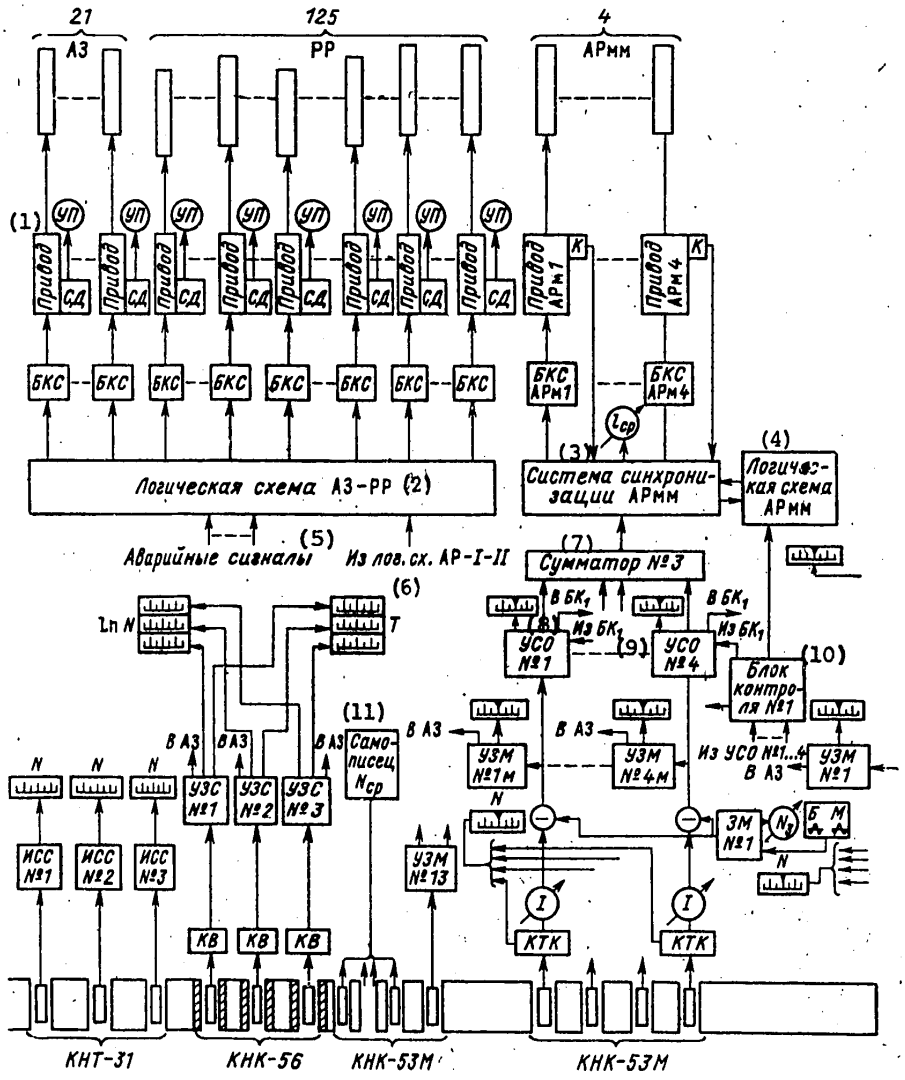

Figure 6.10. Block Diagram of Control and Shielding System: AZ and RR--emergency shielding and manual control rods (the figures are the number of them); ARmm--low-power automatic control rods; AR-I and AR-II--rods of automatic regulators Nos. 1 and 2; USP--shortened absorbing rods (the numbers of these rods are shown); UP--rod position indicator; SD--rod position signal sensor; BKS--signal monitoring unit; lnN, N, T--indicator devices for measuring the current power in logarithmic and linear

[Continued on following page]

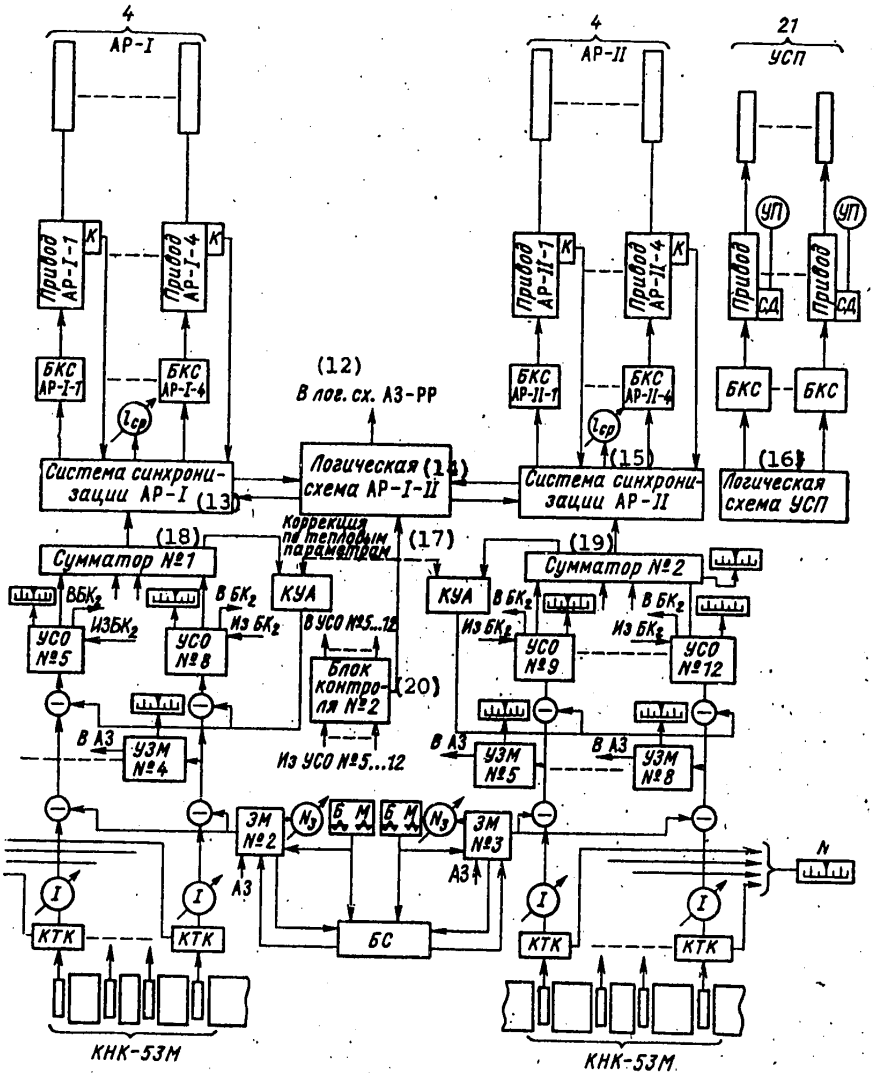

Figure 6.10 [Continued]

scales and for measuring the period, respectively; ISS--counter signal amplifier; KNT-31, KNK-56 and KNK-53M--ionization chambers; UZS--rate of power rise signal amplifier; KV--portable stage; UZM--signal amplifier of excess power; USO--deviation signal amplifier; ZM--power controller; BS--signalling unit; I--galvinometer; KUA--setting corrector; KTK--chamber current corrector; BK--monitoring unit

[Key on following page]

[Key continued from preceding page]:

1. Drive
2. AZ-RR logic circuit
3. ARmm synchronization system
4. ARmm logic circuit
5. Emergency signals
6. From AR-I-II logic circuits
7. Adder No. 3
8. To
9. From
10. Monitoring unit No. 1
11. N_{sr} automatic recorder
12. To AZ-RR logic circuit
13. AR-I synchronization system
14. AR-I-II logic circuit
15. AR-II synchronization system
16. USP logic circuit
17. Correction by thermal parameters
18. Adder No. 1
19. Adder No. 2
20. Monitoring unit No. 2

There are eight protection channels against excess power in the system and the protection is triggered if signals appear in two channels adjacent to the detectors located around the reactor. If signals appear about impermissible rate of runup or about an excess of established power, all the rods with the exception of the USP rods are switched on for insertion into the core. Travel of the rods is stopped upon the disappearance of the signals that caused their initial motion.

Continuous automatic monitoring of the functional state of the measuring apparatus, including the neutron flux sensors, is provided. The functioning of the actuating channels is also monitored by the value of desynchronization of their mutual position. If a malfunctioning measuring or actuating channel is detected, the malfunctioning channel is switched off. On the whole, the regulator maintains efficiency during failure of one measuring or one actuating channel.

6.4. Dynamic Processes

Development of powerful units of AES leads to the need to design new generation reactors distinguished by significant physical dimensions, high specific energy intensity and high rate of burnup. Quantitative changes of the indicated characteristics inevitably lead to qualitative changes of the dynamic properties of the reactors. The characteristic feature of these reactors is the instability of energy release distribution in the core, which largely determines the operating properties of AES and the requirements on control systems. The RBMK-1000 reactor in which all the characteristics of the dynamics inherent to large reactors were manifested, appeared in the Soviet Union as the first serially produced new generation reactor.

This required transition in the investigations of energy release dynamics from a point model to a three-dimensional model. Transit deformations of the energy release field are determined by the combination of neutron-physical and thermohydraulic processes in the core. The problem of investigating the stability of energy release can be reduced in linear approximation to analysis of the roots of the characteristic equation found on the basis of joint solution of equations that describe all the known processes in the core. An approach based on representation of the solution in the form of a series by the eigen-functions of the boundary-value problem (harmonics) is widespread in this case. This approach is more convenient for analytical estimates and provides a clear idea of the deformations when separation of harmonics is possible.

At the same time the use of a digital computer permits one to considerably expand the capabilities of this method during practical solution of problems of dynamics and regulation in those cases when separation of harmonics is impossible. A complex of programs was developed at the design stage for calculating the dynamic characteristics of the energy release field and for determining the boundaries of the zone of stability within different parameters. Specifically, special nomograms were constructed by the complex program for rapid analysis of the dynamic properties of radial-azimuth energy release by the known values of reactivity effects (Figure 6.17). These same nomograms give an idea of the main principles of variation of the dynamic properties of energy release which must be taken into account both during design and during operation of reactors, since significant variations of the physical characteristics of the core occur from the moment of initial charging to runup to the steady recharging mode.

The main results of analyzing the dynamic properties of the energy release field within the core were found even during the period of designing the RBMK and reduced to the following:

the least stable radial-azimuth energy release distribution;

the pattern of deformation development is determined by the shape of the first azimuth harmonic ϕ_{01} with the automatic regulator switched on;

the typical times of deformation of the radial-azimuth field vary in a real range of physical properties of the reactor from hours to tens of minutes. So-called "rapid" instability with time constant on the order of tens of seconds is possible with steam reactivity coefficient of $\alpha_\phi > 5\beta$ and the approach of α_ϕ to this limit should be regarded as impermissible;

energy release distribution through the height of the reactor close to the boundary of instability. The process of transient distortion of the height field developing has the form of fluctuations with a period of approximately 24 hours.

Experiments to determine the effects of reactivity and the characteristics of transient deformations during operation of a reactor at power under normal operating conditions were begun parallel with calculation-theoretical investigations during the period of energy startup of the first unit of the Leningrad AES. The method of experiments to determine the dynamic properties of the field is based on the results of theoretical analysis outlined above [13].

The experiment consists of the fact that operations to maintain the shape of the field are temporarily stopped and the deformation developing during this is recorded with the automatic regulator switched on. The deformation pattern observed in experiment is characterized by development of energy release misalignment through half the reactor, whose profile is determined by the first azimuth harmonic. The azimuth orientation of the misalignment is arbitrary (Figure 6.18). The amplitude of development of misalignment is measured in time by approximately the exponent (Figure 6.19). The index of the degree of this exponent $1/T_{01}$ is the generalized quantitative measure of the field stability in the current state of the reactor.

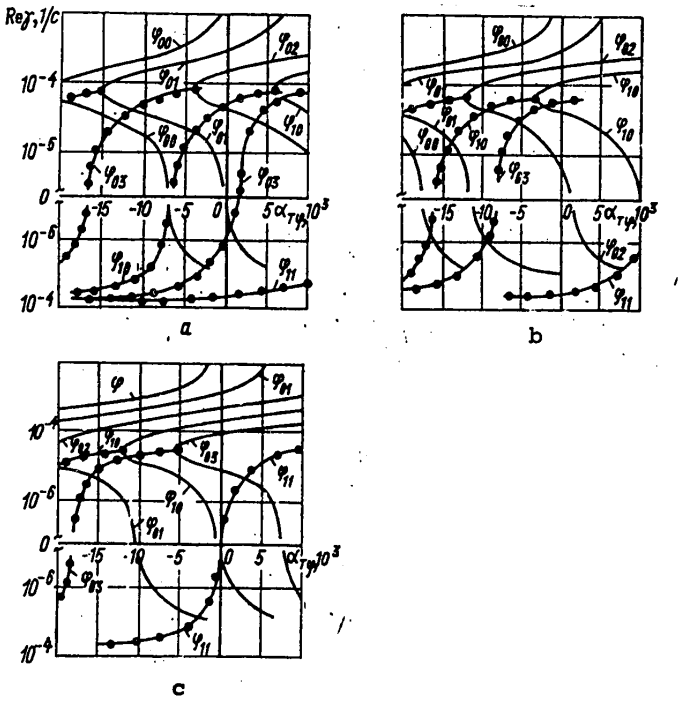

Figure 6.17. Dependence of Active Part of Roots of Characteristic Equation on Total Rapid Power Effect of Reactivity

a--with graphite reactivity coefficient $\varkappa_{gr}$ = 0.01; b--$\varkappa_{gr}$ = = 0.02; c-- $\varkappa_{gr}$ = 0.03; ---- --real roots; -·-·- --complex roots

In August 1974 the value of the rapid power effect of reactivity comprised 4 $4 \cdot 10^{-4}$ β/MW in the first unit of the Leningrad AES. The calculated value of the time constant, corresponding to this reactivity effect, was $T_{01} \approx 1$ hour (Figure 6.20). The time constant determined in experiment by the field dynamics comprised 1.04 hour. Fluctuations of the axial energy release distribution were observed in October-December 1974 in the reactor of the first unit of the Leningrad AES. The characteristics of these fluctuations also corresponded to the calculated values. It should be noted that fluctuations of the axial energy release occurred at a time when the axial field was stable, but the stability reserve was low. According to estimates, the time constant of attenuation of the fluctuations comprised several tens of hours. Under these conditions the changes of the local multiplication factor uncorrelated with the axial deformations related to stabilization of the radial field caused stable fluctuations of energy release through the height of the reactor. An algorithm for volumetric control of the reactor was developed and put into operation to eliminate this phenomenon.

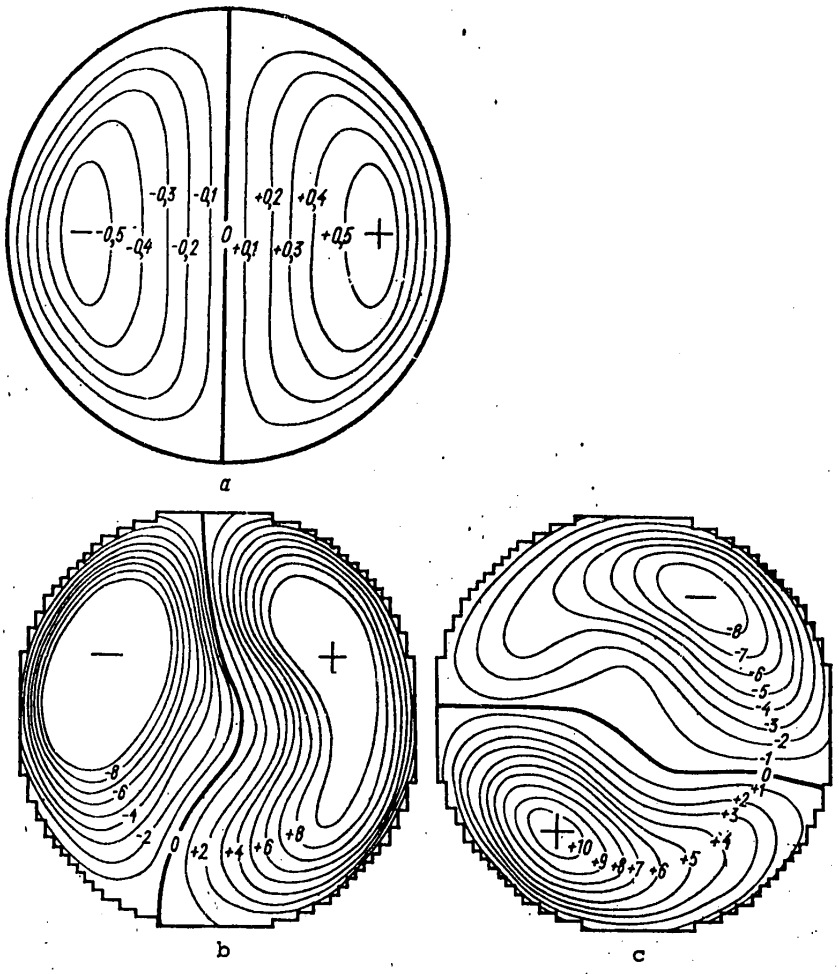

Figure 6.18. Deviations of Field From Initial State in Experiments on Dynamics: a--lines of equal values of first azimuth harmonic ϕ_{01} (r, ν) = J_1 ($\alpha_1 r/R_0$)·sin ν (where α_1 is the first root of the Bessel function, R_0 is the extrapolated radius of the reactor, r and ν are the polar coordinates); b and c--lines of equal deviations of the energy release field, percent, in two experiments

The experiments and analysis of the field deformations under normal conditions proved the reliability of the results of calculations by the developed method. Calculation of the field dynamics now acquires important significance when selecting the composition of the core of RBMK-1500 and RMBKP-2400 reactors. Experiments conducted by the outlined method became a standard means of analyzing the field stability in all operating RBMK-1000 reactors.

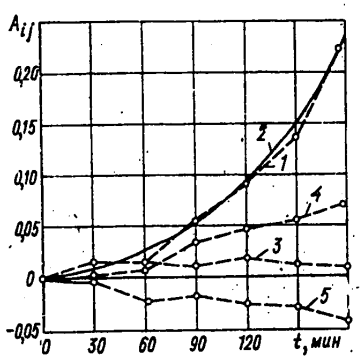

Figure 6.19. Variation of Harmonic Amplitudes: 1--first azimuth harmonic $R_{01} \cos \nu$; 2--approximation by exponent; 3--first azimuth harmonic $R_{01} \sin \nu$; 4 and 5--second azimuth harmonics $R_{02} \cos \nu$ and $R_{02} \sin \nu$, respectively

Further scientific and methodical developments of the problems of analyzing the dynamics of energy release are directed toward determination and refinement of the main principles of the effect of the steady form of the field, nonlinear factors, the dependence of reactivity effects on coordinates, the effect of the control process on field dynamics and development on this basis of more improved methods and programs for calculating the dynamic characteristics of energy release within the reactor.

Optimization of dynamic characteristics. Investigation of the dynamics of RBMK reactors and analysis of foreign data show that instability of energy release in the core is an inherent property of large power reactors. However, this instability is manifested differently depending on the specific physical, thermodynamic and geometric characteristics of the reactor. The shape and time of development of deformations may vary over a wide range (from tens of seconds to tens of hours) as a function of these characteristics. It is obvious that the simpler the form of deformation and the longer the time of development, the simpler organization of control is.

The experience of operating the Leningrad AES showed that the instability of azimuth distribution with time constant of more than 30 minutes essentially has no effect on reactor control and is not even perceived by the operating personnel as an instability. Moreover, special experiments were required to prove the instability. At the same time deformations of the height field with period of 25-30 hours had an appreciable effect on reactor control and required development of special control algorithms. This circumstance is related to the fact that the appearance of axial deformations leads to the need to consider the reactor as a three-dimensional control object and to develop three-dimensional control algorithms. There fore, one of the most important problems of reactor development is optimization of the parameters and structure of the core such that its dynamic properties are most favorable for organization of control or at least significant complications do not develop.

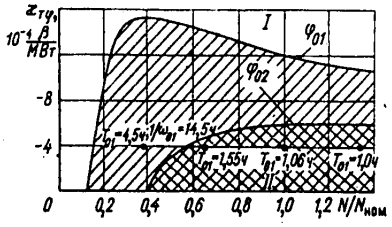

Figure 6.20. Boundary of Stability Zone of Radial-Azimuth Energy Release (ϕ_{01} and ϕ_{02}) in the Plane of a Rapid Power Effect ($\varkappa_{T_\phi}$) and Relative Reactor Power (N/N_{nom}, N_{nom} = 3,200 MW): I and II--stability and instability zones, respectively; the values of the time contsant of development of deformation of the first azimuth harmonic type (01) are shown for $\varkappa_{T_\phi} = -4 \cdot 10^{-4}$ β/MW

The available practical experience of purposeful practical improvement of the dynamics of reactors of the first unit of the Leningrad AES confirmed the effectiveness of this approach. The following methods of active interference in the dynamics of a reactor can now be formulated on the basis of analyzing the dependence of dyanmic energy release properties on the physical and thermothydraulic characteristics:

variation of the U-235 nuclei and graphite ratio in the core due to variation of fuel enrichment, an increase of fuel charge, variation of lattice spacing, the use of graphite with lower effective density and so on;

formation of a specific energy release profile that provides high stability of the reactor;

an increase of the mean effective steam content and temperature of the fuel elements and a decrease of the mean effective graphite temperature in the core.

The possibility of improving the operational properties of reactors by purposeful variation of their dynamic properties was used extensively when working out measures to increase the stability of RBMK-1000 reactors and during design of RBMK-1500 and RBMKP-2400 reactors. As a result the decision to convert to fuel with two-percent enrichment was adopted for all RBMK-1000 reactors. This enrichment was also adopted for RBMK-1500 and RBMKP-2400 reactors.

Characteristics of the effect of the external circuit on reactor operation. The behavior of the production parameters of the external loop, which is dependent both on the output parameters of the reactor and on operation of the main equipment (turbogenerators, deaerators, separator drum, feed assemblies, GTsN and so on) and their control systems, has a significant effect on reactor operation along with the internal processes. Such parameters of the external loop as the pressure and level in the separator drum, delivery water flow rate and flow rate through the MPTs loop act on the reactor by external feedback. It is characterized by its own transfer coefficients and phase distortions which depend to a significant degree

on the quality of operation of the automatic thermal systems that switch on the level and pressure regulators of the separator drum. The task of these automatic systems is to bring the reactor and turbogenerator power, the steam flow rate to the turbine with delivery of feed water into agreement and also to provide normal steam separation conditions in the separator drum.

The dependence of the parameters of the external loop on the operation of its equipment (turbogenerator, GTsN, feed pumps and so on) determines the nature of the effect of this equipment on reactor operation, which must be taken into account when organizing the reactor control system and the mode management algorithms during normal operation and in emergency situations.

Problems related to design of external systems are primarily related in provision of the required operating properties of the reactor unit to selection of the required characteristics of the equipment and optimization of the automatic thermal systems. Thus, based on the dynamics of the transient and emergency modes, requirements on the inertial characteristics of the GTsN were determined that provide reactor safety when supplying its own needs. Investigations of the automatic thermal systems showed that its optimization may significantly improve the quality of the transient processes in the reactor unit by the integral power of the reactor, the pressure and level in the separator drum and may increase the safety and reliability of its operation in transient modes [14].

The essential feature of the external loop is the presence of two circulation loops, each of which has its own production equipment with the corresponding controls systems. A two-loop layout of the circulating loop is in itself a potential source of asymmetrical disturbances of the reactor that stimulate the occurrence of transient azimuth deformations. Therefore, both the space-time behavior of energy release and operation of both loops of the external circuit with its control systems must be simulated during investigations of the dynamic processes in the reactor. This situation is based not only on theroretical investigations but also on the data of the operating experience of AES with RBMK-1000 type reactors.

The role of experimental investigations. A required step of investigations is an experimental check of theoretical propositions which is the basis and stimulus for further development of theory. Data obtained on operating reactors have the greatest value in this case since it is essentially impossible to reproduce real interrelated processes in their combination under bench conditions. Therefore, extensive complex investigations of the dynamics whose task was to confirm the main design solutions and to refine the relationships, principles and characteristics of the processes, were developed from the first days of startup of the pilot unit of the Leningrad AES. The main task in organizing the investigations was to develop methods of conducting and processing the results of experiments which would yield preliminary results with minimum changes of the operating mode of the reactor and AES and observation of all the standards and safety regulations. The significance of experimental investigations is not limited only to a check of the theoretical propositions and confirmation of the design solutions. As indicated by the experience of operating AES, the experimental methods developed and convenient to operate become an essentially standard means of monitoring the dynamic properties of a reactor [15]. The need for this monitoring is determined by the fact that there is considerable evolution of their physical and dynamic

characteristics during reactor operation, related to variation of the isotope composition of the fuel and to the different measures to modernize the charge and components of the core.

Very promising in organization of systematic monitoring of reactor characteristics are statistical methods of investigations, despite the difficulty of introducing them mainly by engineering concepts. These difficulties include the need to record the fluctuations of the production parameters with high resolution and automatic processing of large files of accumulated information. The experience of using statistical methods to diagnose the dynamic state of the RBMK-1000 reactor [15] shows the effectiveness and possibility of practical use of these methods under industrial operating conditions based on standard monitoring-measuring equipment at the plant. It should be noted that statistical methods may be useful to solve a number of problems of reactor diagnostics and equipment operation of AES and may also be a convenient means of special investigations in existing reactors.

Data on the behavior of parameters during random emergency modes are very valuable to deepen the concepts of the principles of processes and to refine the characteristics and also to obtain information about real disruptions in the operation of equipment. The main problem in this case is to organize monitoring and recording of all main parameters upon the occurrence of an emergency with the required resolution both in time and amplitude. The indicated problems can be solved by using special measuring complexes that include digital computers.

It is obvious that planned investigations should be conducted in all operating reactors by unified standard methods (for comparability of results). The methods should be developed and improved in coordinated order in this case.

BIBLIOGRAPHY

1. Yemel'hanov, I. Ya., L. V. Konstantinov and V. V. Postnikov, "System for Monitoring the Energy Release Distribution in the RBMK Reactor," ATOMNAYA ENERGIYA, Vol 34, No 5, 1973.

2. Yemel'yanov, I. Ya., V. N. Vetyukov and L. V. Konstantinov, "Discrete Monitoring of Energy Release Distribution in the Cores of Nuclear Reactors," ATOMNAYA ENERGIYA, Vol 34, No 2, 1973.

3. Alekseyev, V. I., I. Ya. Yemel'yanov and V. P. Lipin, "A Small Triaxial Fission Chamber," ATOMNAYA ENERGIYA, Vol 43, No 1, 1977.

4. Yemel'yanov, I. Ya., M. A. Borisov, Yu. I. Volod'ko et al, "Inertialess Monitoring of the Neutron Flux Level by a Direct Charge Sensor with Silver Emitter," ATOMNAYA ENERGIYA, Vol 27, No 3, 1969.

5. Yemel'yanov, I. Ya., Yu. I. Volod'ko, V. V. Postnikov et al, "Variation of Neutron Detector Sensitivity With Silver Emitters During Prolonged Operation in a Reactor," ATOMNAYA ENERGIYA, Vol 42, No 5, 1977.

6. Yemel'yanov, I. Ya., V. V. Postnikov and G. V. Yurkin, "Calculation Method of Approximating Discrete Measurements of Power Distribution in Power Reactors," ATOMNAYA ENERGIYA, Vol 41, No 5, 1976.

7. Yemel'yanov, I. Ya., V. G. Nazaryan and V. V. Postnikov, "Optimization of Energy Distribution in the Core of a Large Power Reactor," ATOMNAYA ENERGIYA, Vol 44, No 4, 1978.

8. Sveshnikov, A. L., "Prikladnyye metody teroii sluchaynykh funktsiy" [Applied Methods of Random Function Theory], Moscow, Nauka, 1968.

9. Karpov, V. A., V. G. Nazaryan and V. V. Postnikov, "Investigating the Random Component of Thermal Release Distribution in a Nuclear Reactor," ATOMNAYA ENERGIYA, Vol 40, No 6, 1976.

10. Konstantinov, L. V., V. V. Postnikov and V. N. Vetyukov, "Reliability of Evaporative Channels of Reactors of the Beloyarsk AES Type," ATOMNAYA ENERGIYA, Vol 29, No 3, 1971.

11. Yemel'yanov, I. Ya., V. V. Voskoboynikov and B. A. Maslenok, "Osnovy poryektirovaniya mekhanizmov upravleniya yadernykh reaktorov" [Fundamentals of Designing the Control Mechanisms of Nuclear Reactors], Moscow, Atomizdat, 1978.

12. Yemel'yanov, I. Ya., "The Existing State and Prospects for Development of Monitoring and Control Systems of RBMK Type Reactors," VOPROSY ATOMNOY NAUKI I TEKHNIKI, SERIYA FIZIKA I TEKHNIKA YADERNYKH REAKTOROV, No 1 (21), 1978.

13. Aleksakov, A. N., B. A. Vorontsov, I. Ya. Yemel'yanov et al, "Deformation of the Energy Release Field in the RBMK," ATOMNAYA ENERGIYA, Vol 46, No 4, 1979.

14. Belousov, V. V., P. A. Gavrilov, L. N. Podlazov et al, "Selecting the Optimum Automatic Thermal System for RBMK Type Reactors," VOPROSY ATOMNOY NAUKI I TEKHNIKI, SERIYA FIZIKA I TEKHNIKA YADERNYKH REAKTOROV, No 1 (21), 1978.

15. Abakumov, V. Ya., A. N. Aleksakov, B. A. Vorontsov et al, "Some Problems of Monitoring the Dynamic Characteristics of Reactors of the Leningrad AES," in "Atomnyye elektrostantsii" [Atomic Power Plants], No 3, Moscow, Energiya, 1979.

THE RECHARGING MACHINE

Moscow KANAL'NYY YADERNYY ENERGETICHESKIY REAKTOR in Russian 1980 (signed to press 27 Mar 80) pp 182-188

[Chapter 10 from the book "Channel-Type Nuclear Power Reactor", by Nikolay Antonovich Dollezhal' and Ivan Yakovlevich Yemel'yanov, Scientific Research and Design Institute of Power Engineering, Atomizdat, 2,550 copies, 208 pages]

10.1. Configuration and Design

The most important requirement placed on the RBMK reactor is the need for it to operate with minimum shutdowns. Therefore, fuel recharging and elimination of some emergency situations in an operating reactors is provided without reducing its power. This can be carried out only by a special machine that performs the following operations:

recharging the TVS in an operating and cooled reactor;

checking the passage of the fuel channel in caliber that simulates a standard assembly;

sealing of the fuel channel with a plug (production or emergency);

mechanized elimination of some emergency situations.

Fuel recharging in an operating reactor should be carried out at operating parameters of the fuel channels.

The loading-unloading machine (RZM) should perform five operations on recharging the fuel channels in an operating reactor during 24 hours without reducing its power and no fewer than 10 operations of channel recharging on a shutdown reactor.

The working principle of the RZM in an operating reactor includes the following. An RZM filled with condesnate at temperature of 30°C is joined to the channel to be recharged. Pressure equal to the pressure in the fuel channel is established in the pressure vehicle and the channel is unsealed. Condensate is pumped into the channel from the pressure vehicle at flow rate up to 1 m^3/hr. The cold condensate prevents penetration of steam and hot water from the fuel channel to the RZM. After the spent fuel assembly has been removed, the channel is sealed and

the pressure in the pressure vehicle is dropped to atmospheric pressure. The machine is disconnected from the channel and is sent to the point where the spent assemblies are unloaded.

The main parts of the RZM are a crane, container, two replaceable pressure vehicles (one installed on the machine and the other in the repair zone), truss, production equipment, guidance system and control members. An overall view of the RZM is shown in Figure 10.1. The crane which moves theRZM through the central room consists of a gantry 18 with span of 21 meters and a carriage 19 which moves along the gantry. The crane gantry is moved to a distance of 39.6 meters and the carriage by a distance of 12.5 meters along the crane tracks 11 meters from the floor of the central room. The gantry and carriage have two travel speeds each: 9.75 and 1.2 m/min. The low speed is necessary for precise aiming of the RZM and in this case the gantry and carriage are moved in increments of 1 mm. The mass of the gantry is 105.8 tons and that of the carriage is 56.3 tons. A massive steel ring is welded to the carriage and a container 17,which is the biological shielding together with the ring, is attached to its lower end.

The container is a steel cylinder with inner diameter of 770 mm and wall thickness of 500 mm. It consists of six sections with total mass of 200 tons. There is movable biological shielding 13 in the bottom section of the container that closes the gap between the bottom of the container and the floor of the central room at the moment of recharging. A cab and platforms with ladders are attached to the outside of the container. The "active" lower half of the pressure vehicle is located inside the container. A truss 6 with four platforms where the production equipment 2 is located, electrical equipment and monitoring and measuring devices are located is installed on the RZM crane carriage. There are term buckles on the truss--tightening devices by which the pressure vehicle is held in the vertical position. The production equipment is designed to supply the RZM systems with circulation water, turbine condensate and air of the required parameters. Its main parts are feed pumps, bellows type cocks, valves, containers and compressed air tanks. The water pressure, flow rates and levels are measured by means of monitoring and measuring devices.

Two systems for precise aiming of the RZM toward the fuel channel--an optical-television system 12 (main) and contact system (reserve) 18 for loss of visibility in a steaming fuel channel are installed in the lower part of the container. The optical-television system permits visual observation of the image of the end of the fuel channel head through a television set or eyepiece of this system and to join the circumference of the fuel channel head to the sighting cross-hatched circle by small movements of the gantry and carriage. The contact system for guiding the RZM is a pneumoelectromechanical device designed to guide the RZM toward the axis of the channel by direct mechanical contact of the system with the side surface of the fuel channel head. The RZM is controlled from the operator room, which is located behind the end wall of the central room on the side of the reactor. Moreover, a control console for moving the crane is installed in the RZM cab.

The most crucial structure of the RZM is the pressure vehicle, which is a high-pressure vessel inside which are located the actuating mechanisms that perform the following functions:

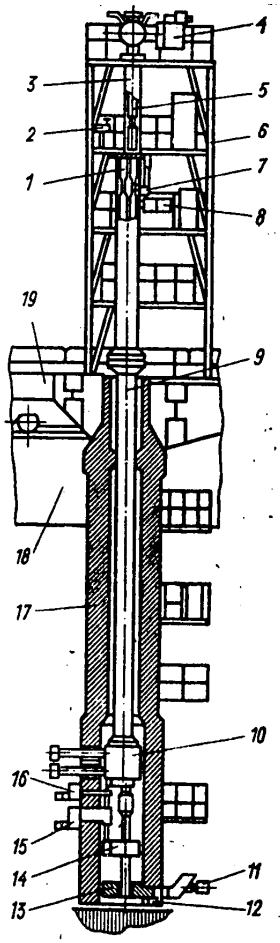

Figure 10.1. Cross-Section of RZM

airtight connection to the fuel channel head;

unsealing and sealing the fuel channel plug;

removal of the spent fuel assembly and suspension from the fuel channel;

checking the fuel channel in caliber;

installing a fresh fuel assembly and suspension into the fuel channel;

inserting the emergency fuel channel plug;

operation of the RZM on the charging and uncharging recesses of the central room.

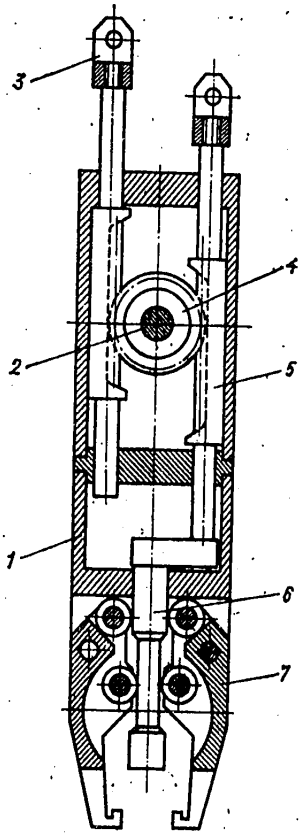

Figure 10.2. Grab With Equalizing Mechanism

All the main parts of the pressure vehicle (upper 3, middle 9, lower 14 and shut-off device 10) are joined to each other by flange joints and sealing gaskets. The upper part of the pressure vehicle includes all the mechanisms related to hoisting and lowering of the suspension and assembly: drive for movement and control of the grab 4. The assembly is raised and lowered by the grab, moved and controlled by means of two chains 5. The grab is moved during joint motion of the chains and is controlled (opened or closed) upon counter motion. Only the grab, chains and guide sprockets are located in the high-pressure zone, while all the drives are located outside the pressure vehicle housing. The rotating shafts are sealed by asbestos-fabric cuffs of the herringbone type.

The grab (Figure 10.2) is made in the form of a precast cylindrical housing 1 in which are installed two gear racks 3 and 5 that interact with pinions 4 located on the shaft of the grab drive mechanism 2. The grab is rigidly connected to the chains by the upper ends of the racks. This version provides uniform load distribution on both chains during hoisting and lowering of the suspension and assembly. A cam 6 that acts on the jaws of the grab 7 is attached to the lower end of one of the racks. The configuration and arrangement of one of the cam profile are selected so as to provide separation or closing of the grab jaws during countermotion of the racks.

The chains are made of channel-type links with bushings and rollers in the joints. Both chains always operate together and their working sections are arranged in a guide pipe while their free sections are located in the chain receptacles. The middle part of the pressure vehicle (see Figure 10.1) is designed for location of fresh and spent assemblies, gauge and plugs. The middle part includes a housing, cartridge 1, chain winding mechanism 7 and cartridge rotation drive 8. The housing of the middle part of the pressure vehicle is structurally made in the form of a vessel (a pipe 600 mm in diameter) which consists of three sections with total length of 16.5 meters. There is a cartridge support with chain winding mechanism and cartridge rotation mechanism in the upper section of the housing.

The pressure vehicle cartridge (a pipe 448 mm in diameter) consists of three sections with total length of 16.5 meters each. Four containers of pipe 140 mm in diameter over the entire length of the cartridge are installed in each section of it. A fresh assembly, gauge and emergency plug are located in the containers. One container is left free to place the assembly removed from the reactor in it.

The shutoff device is designed to open and close the working zone of the pressure vehicle, to cut off the working cavity of the pressure vehicle from that of the fuel channel, for emergency closing of the fuel channel cavity when performing emergency work in the pressure vehicle and to ensure biological shielding of the cavity of the lower part of the pressure vehicle when the assembly is raised into the cartridge. It is two slide valves with parallel disks joined in series in one massive housing which also performs the role of biological shielding. The electromechanical drives of the slide valves are removed together with the bellows type seal beyond the wall of the container through stepped openings in the doors of the third section. The lower part of the pressure vehicle is designed for airtight remote connection of the pressure vehicle cavity to the fuel channel and also for sealing and unsealing the fuel channel. A joining connecting pipe with mechanism for moving it 16 and loops are located in the lower part.

The joining connecting pipe is designed to perform the main function of the lower part of the pressure vehicle--it is joined to the head of the channel, sealed by means of rubber inflation cuffs and acts on the shutoff device of the channel with a special hook 15 (see Figure 10.1), i.e., it seals or unseals it. The mechanism for moving the joining connection pipe moves it vertically by means of two ball-screw reduction gears and two conical and a distributing reduction gear. Sensors that provide remote operation of the mechanism, sensors for limiting the free fall of the joining connecting pipe and for compensating for the thermal fluctuations of the fuel channel and the upper position of the joining connecting pipe are attached to the ball-screw reduction gears.

The loops are designed to deliver turbine condensate, air and electric power to the movable part of the joining connection pipe. The hydraulic loop provides filling of the joining connecting pipe with the turbine condensate, sealing of the rubber inflatable cuffs and removal of leaks from the inflatable rubber cuffs to the pressure sensor. Air is fed through the pneumatic loop to the sensor of the lower position of the grab and connection pipe. Electric power is fed by means of the electric loop to the level meter, sensors of the lower position of the connection pipe and grab and also to the thermocouple. A simplified kinematic diagram of the drives that recharge and unseal the RZM is presented in Figure 10.3.

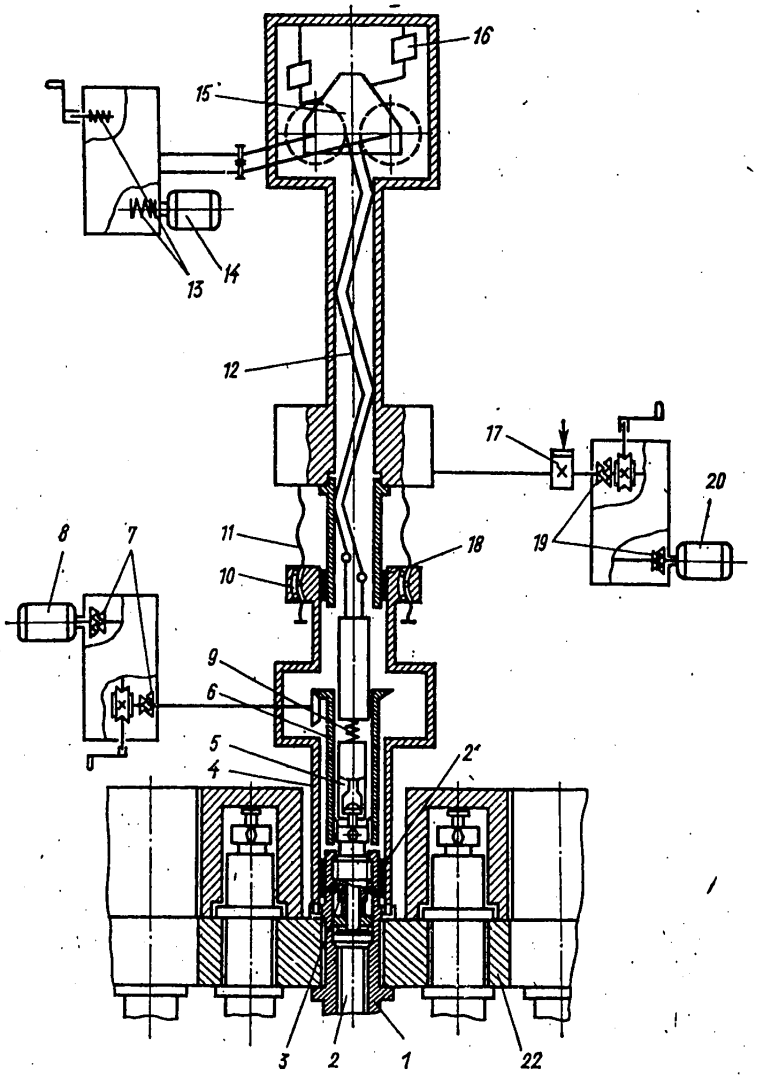

Figure 10.3. Functional Diagram of Drives for Recharging and Unsealing of RZM: 1--fuel channel (TK); 2--shutoff plug of TVS suspension; 3--spherical lock of plug; 4--joining connection pipe (SO); 5--grab; 6--TK sealing key; 7--moment clutches of TK sealing drive; 8--TK sealing drive; 9--damping spring of gram; 10--spherical nuts of TK moving drive; 11--spherical screws that limit the rate of motion of the TK; 12--chains that impart motion; 13--reducer with moment couplings; 14--motor; 15--carriage with sprockets; 16--flexible elements of strain gauges; 17--switch to raise SP 18--bellows seal of SP; 19--moment transfer clutch; 20--TK moving drive; 21--sealing cuffs; 2--concrete blocks

The following machine service zones are provided in the central room.

1. The parking place is a zone in the central room designed for parking the machine during periods between reactor recharges.

2. A simulator bench designed for:

adjustment and checking of the mechanisms of the machine;

filling the pressure vehicle with condensate;

simulation of standard recharging;

loading a fresh assembly into the pressure vehicle;

decontamination of the inner cavity of the pressure vehicle;

replacement of the inflatable cuffs of the joining connection pipe.

The simulator bench has the corresponding equipment to perform these operations.

3. An assembly for receiving the spent assemblies is used to receive the gauge.

4. The repair zone is designed to replace a pressure vehicle that has failed. It is located in the central room in the region of the simulator bench. A fully assembled reserve pressure vehicle is permanently located in the zone.

10.2. Operating Modes

Preparation of the RZM for operation. The machine is put into operation in the following manner. The simulator bench is prepared: the plugs are removed from the seat (seats I and II of the simulator bench) to fill the pressure vehicle with condensate. The gauge and production plug are installed in these seats. The electropneumatic power supply of the machine mechanisms is switched on and it is fed from the parking place to the simulator bench to seat I.

After power has been supplied to the RZM, the valve for filling the feeder tank with condensate from the loop is opened automatically. The machine is joined to seat I on the simulator bench and the gauge is tightened into the dry machine and the machine is then joined to seat II and the production plug is removed from it. The pressure vehicle of the RZM is then filled with condensate in seat II until the level in the filling tank of the joining connection pipe appears. After the pressure vehicle has been filled with condensate, the sealed slide valves are opened, the condensate is dumped from the seat and the joining connection pipe to the piping in the machine is separated from the seat.

Standard recharging. The following procedure is observed when the machine is operating in the standard recharging mode. The RZM with pressure vehicle filled with condensate (t = 30°C) is directed toward seat I or II of the simulator bench in which fresh fuel assemblies are first installed. The joining connection pipe is joined and sealed with the head of the seat. The seat and joining connection

pipe are then filled with condensate from the seat filling system. The slide valves are then opened after this operation, a fresh TVS is screwed into the cartridge of the pressure vehicle and is installed in it. The protective slide valves are closed and the condensate from the joining connection pipe in the seat are dumped into the sewer.

The machine is disconnected from the seat and is sent to the reactor to recharge the fuel channel.

Recharging of the fuel assembly. The operator instructs that a specific fuel channel be prepared for recharging according to the program for recharging the reactor. The protective plug is removed from the channel and the cable of the γ-detector is disconnected from the assembly plug. These operations are performed manually by workers of the central room. The RZM automatically emerges to the coordinate of the channel to be recharged, is joined and the plug of the machine is then sealed to the head of the channel by high pressure. The joining connection pipe is then filled with condensate from the tank, the slide valves are opened, the feed pump is switched on and a pressure of 73-75 kgf/cm^2 is created in the pressure vehicle. The grab is lowered and linked to the head of the assembly. The sealing and unsealing mechanism is switched on and the channel is unsealed.

When the process of unsealing is completed, the hoisting mechanism is switched off and the spent assembly is raised to a height of 7.5 meters to the cooling zone where it is held for 10 minutes. The cold condensate (t = 30°C) begins to be fed into the fuel channel at the moment it is unsealed from the machine (the pump operates to feed condensate constantly to the pressure vehicle until a fresh assembly has been installed in the channel and it has been sealed) at a flow rate up to 0.5-1.0 m^3/hr. After the assembly has been held in the cooling zone, the hoisting mechanism is switched off, the assembly is inserted into the pressure vehicle and is installed in the cartridge. The passage of the channel is checked by the gauge and a fresh assembly is then installed in the reactor. The pump feeding the condensate to the pressure vehicle is switched off after the channel has been sealed and the pressure in the pressure vehicle is dropped to atmospheric pressure. The sealing slide valves are closed, the cavity of the connection pipe is joined to a special blower and the airtightness of the channel head is checked. The condensate is removed by compressed air delivered to the upper part of the joining connection pipe, which forces the condensate into the tank, prior to disconnecting the connection pipe with the channel from the cavity of the joining connection pipe.

The RZM is then unsealed and disconnected from the fuel channel and the machine is sent to the assembly for reception of spent assemblies. The receiving assembly is prepared for unloading the spent assembly from the RZM pressure vehicle into the jacket of the holding tank, which is installed in one of the seats of the receiving assembly, even during operation of the RZM on the reactor. The jacket is filled with condensate. The machine with the spent assembly in the pressure vehicle automatically emerges to the coordinate of the prepared jacket. The machine is joined and sealed to the jacket of the holding tank. The cavity of the joining connecting pipe is filled with condensate from the tank, the slide valves are opened and the spent TVS is removed from the pressure vehicle to the jacket. The slide valves are then closed, the condensate is expelled into the tank from the connection pipe by compressed air and the machine is disconnected from the jacket and is ready for a new recharging cycle.

Recharging a shut-down and cooled reactor. A shut-down and cooled reactor can be recharged by two versions:

1) unloading two spent assemblies with installation of fresh assemblies to replace them;

2) unloading two spent assemblies and fresh assemblies are installed in the reactor without using the RZM by means of devices and transport equipment provided in the central room.

In both versions the production operations of the RZM are simplified in nature since the excess pressure in the reactor is maintained at 2-5 kgf/cm^2 (approximately 0.2-0.5 MPa) or is absent and the condensate is drained to the level of the assembly heads. If there is pressure in the reactor, the RZM is continuously filled with condensate and it is not delivered to the pressure vehicle by the RZM systems. If there is no pressure in the reactor, condensate must be fed to the pressure vehicle constantly when unloading the spent assemblies. The production plug is first removed from the cartridge of the pressure vehicle when unloading two spent assemblies and the gauge is also removed when unloading four assemblies. The time of the recharging cycle for two assemblies is 350 minutes and consequently the RZM is capable of recharging eight fuel channels per day. A total of 267 minutes is expended to unload four assemblies, i.e., the RZM is capable of unloading 20 fuel channels per day.

PROSPECTS FOR DEVELOPMENT OF URANIUM-GRAPHITE CHANNEL-TYPE REACTORS

Moscow KANAL'NYY YADERNYY ENERGETICHESKIY REAKTOR in Russian 1980 (signed to press 27 Mar 80) pp 189-203

[Chapter 11 from the book "Channel-Type Nuclear Power Reactor", by Nikolay Antonovich Dollezhal' and Ivan Yakovlevich Yemel'yanov, Scientific Research and Design Institute of Power Engineering, Atomizdat, 2,550 copies, 208 pages]

11.1. Principles for Improving the Core

Channel-type uranium-graphite power reactors will be improved in their subsequent development in engineering and economic characteristics. These improvements will be made as further design and planning developments are made, experimental investigations are conducted and experience in operating reactors at existing AES is accumulated. As a result capital expenditures per unit of established power of an AES, the cost of generated energy, the number of operating personnel, specific construction volumes and consumption of metal, including stainless steel, the laboriousness and periods of construction and installation work should be reduced and the operating reliability and maneuverability of the energy units with these reactors should be increased. All this can be achieved by increasing the intensity of the core and the extent of nuclear fuel burnup, conversion to the block principle of constructing a reactor, introduction of nuclear superheating of steam with an increase of its initial parameters and with simultaneous improvement of the thermal layout of the unit, improvement of the configuration of the energy block and other improvements in the designs of the basic equipment and of schematic and configuration decisions.

One must also bear in mind in this case the tendency toward an increase of the unit output of units caused by the constant increase of the requirement of the total introduced power of AES. Some promising solutions to improve uranium-graphite power reactors and energy units with these reactors are considered below.

An increase of the unit power is one of the possible methods of improving the economy of AES. This path was reflected in development of RBMK-1500, RBMK-2000 and RBMKP-2400 [1-4] with electrical output of 1,500, 2,000 and 2,400 MW, respectively, with respect to RBMK reactors. The output of the fuel channel has been increased 1.5-fold in the RBMK-1500 reactor compared to the RBMK-1000 reactor due to intensification of the heat transfer, which makes it possible to increase the power of the BRMK-1000 to 1,5000 MW while maintaining the overall dimensions and

design of the reactor. The channel diameter, number of fuel elements in the assembly and lattice spacing have been increased in the RBMK-2000 reactor. This makes it possible to develop a reactor with double output in the dimensions of the RBMK-1000.

Development of a channel with increased output with respect to RBMK reactors opens new opportunities toward improving their engineering and economic characteristics. The experience of operating AES with RBMK-1000 reactors showed that there is some reserve both with respect to the linear loads on the fuel elements and with respect to the maximum channel output (with respect to conditions of heat transfer crisis). On the other hand, it turned out that the stability of energy release distribution decreases as fuel is burned up and as additional absorbers that compensate for the initial excess reactivity are removed from the reactor.

As indicated by calculations and confirmed by experiments, the main factor that determines the deformation of the energy release fields with time constant of the first azimuth harmonic from several to tens of minutes is a positive steam reactivity coefficient α_ϕ. A decrease of its value improves the stability of energy release distribution. An increase of the nuclear fuel to moderator nuclei ratio can be regarded as the most economical and optimum method of reducing the steam coefficient; an increase of enrichment is most economical and optimum for operating reactors. The main characteristics of a reactor with an increase of fuel enrichment for steady continuous recharging mode are presented in Table 11.1.

Conversion to increased fuel enrichment leads to an increase of the extent of burnup, variation of coefficient α_ϕ that improves field stability and to a reduction of nuclear fuel and fuel element consumption. On the other hand, an increase of enrichment and a corresponding increase of the extent of fuel burnup leads to an increase of output of a freshly charged channel, to an increase of the lifetime of the fuel in the reactor and to an increase of linear loads on the fuel element (Table 11.2). The possibility of increasing channel output (up to 1.5-fold) has been confirmed by development and creation of the fuel channel for the RBMK-1500 reactor.

Turning to discussion of the results, it should be noted that the given data should be regarded mainly as comparative rather than as absolute data since the calculations were made for a steady fuel recharging mode. Coefficients of nonuniformity K_r and K_z, found with regard to the experience of operating RBMK-1000 reactors, and the calculated recharging coefficients were used when determining the output of freshly charged channels. $K_r = 1.4$ was adopted for reactors operating on fuel with enrichment of 1.8 percent and the coefficient of nonuniformity by height was $K_z = 1.4$. Based on the experience of operating RBMK-1000 reactors, the mean square error of determination and maintenance of channel output σ_k was assumed equal to 5.2 percent while that of the linear load on that of the fuel element was $\sigma_t = 7.7$ percent.

The data indicate that an increase of fuel enrichment in RBMK-1000 reactors is a realistic method of increasing the effectiveness of fuel utilization. The use of enrichment up to 3.6 percent is possible according to the permissible outputs of channels and linear loads on the fuel element. The problem of increasing channel output and the linear loads on the fuel element up to 1.5-fold has been resolved

Table 11.1. Main Characteristics of Reactors When Using Fuel of Designed (1.8 percent) and Increased Enrichment

Parameter	RBMK-1000					RBMK-1500	
Initial fuel enrichment, percent	1.8	2.0	2.4	3.0	3.6	1.8	2.0
Calculated extent of burnup, GW·day/t	18.5	22.3	28.8	37.6	45.7	17.8	21.6
Isotope composition of unloaded fuel, kg/t:							
U-235	3.9	3.5	2.9	2.5	2.2	4.4	3.8
U-236	2.1	2.5	3.1	4.0	4.8	2.1	2.4
Pu-239	2.2	2.2	2.2	2.1	2.1	2.2	2.2
Pu-240	1.8	2.0	2.3	2.5	2.5	1.8	2.0
Pu-241	0.5	0.5	0.6	0.6	0.7	0.5	0.5
poisons	19.4	23.3	30.1	39.1	47.8	18.6	22.8
Variation of steam reactivity coefficient with respect to design coefficient $\Delta\alpha_{\phi,\beta}$	--	-1.3	-3.5	-6.4	-9.0	-1.5	-2.7
Consumption of enriched uranium at ϕ = 0.8, t/(year·GW (electricity))	50.5	42	32.5	25	20.5	52.4	43.3
Annual need for fuel elements, 10^3 units/(year·GW (electricity)) at ϕ = 0.8	16	13.3	10.2	7.9	6.5	16.5	13.6
Fuel component of electric power cost C_t, kopecks/(kW·hr)	0.252	0.232	0.216	0.208	0.208	0.260	0.240
Fuel component of reduced expenditures z, kop/(kW·hr)	0.370	0.362	0.370	0.405	0.445	0.335	0.325
Constant component of cost C_p, kop/(kW·hr)	0.365	0.365	0.365	0.365	0.365	0.283	0.283
Cost of electric power C = = $C_t + C_p$, kop/(kW·hr)	0.617	0.597	0.581	0.573	0.573	0.543	0.523

FOR OFFICIAL USE ONLY

APPROVED FOR RELEASE: 2007/02/09: CIA-RDP82-00850R000400080004-5

Table 11.2. Output of Fuel Channels and Linear Loads on Fuel Elements as a Function of Charged Fuel Enrichment

Parameter	RBMK-1000				RBMK-1500	
Fuel enrichment, percent	1.8	2.0	2.4	3.0	3.6	1.8	2.0
Output of freshly charged channel with regard to K_r, kW	2,650	2,800	3,150	3,500	3,800	4,050	4,250
Maximum channel output with regard to accuracy of maintaining output ($3\sigma_K$), kW	3,050	3,250	3,650	4,050	4,350	4,680	4,910
Linear load on fuel element in freshly charged channel q_l, W/cm	295	315	350	390	420	455	485
Maximum value of q_l with regard to accuracy of maintaining output ($3\sigma_r$), W/cm	360	385	430	480	520	560	595
Run of TVS, effective days	1,100	1,350	1,730	2,260	2,750	700	860

in the RBMK-1500 reactor [5, 6]. In this case the TVS are equipped with heat transfer intensifiers; the channel design and the delivery and drain pipelines are not changed. TVS without intensifiers can be used with more moderate increase of fuel enrichment in the RBMK-1000. For example, conversion to 2 percent fuel enrichment can be accomplished without any design changes in the TVS.

We also note that the maximum values of output presented in Table 11.2 were obtained on the assumption that the algorithm for equalization of output through the core remains the same as in existing RBMK-1000 reactors. At the same time one can suggest a number of measures, part of which has already been tested experimentally in reactors, that make it possible to expand the capability of equalizing the energy distribution in the core. These measures may include the use of absorbing rods inserted into fresh TVS and removed as channel output decreases, the use of burnup absorbers, optimization of recharging procedures and so on. A specific reserve for equalization is related to the possible increase of the operational reserve of reactivity with some operating modes of the AES in the power system.

An increase of enrichment leads to a decrease of fuel element and natural uranium consumption. The annual consumption of fuel elements upon conversion from version to version decreases by 20-30 percent and if three percent enrichment is used, it decreases by one-half; the U-235 content in the unloaded fuel is reduced to 0.25 percent, i.e., to the spent tailings of enrichment plants, and if enrichment of 3.6 percent is used, it is reduced to 0.2 percent, which resolves the question of the feasibility of extracting the U-235 from the spent fuel. An increase of initial enrichment significantly changes the steam coefficient of reactivity, reducing it compared to enrichment of 1.8 percent and even shifting it in the negative direction, which proves the stability of energy release distribution, but requires special consideration of the transient modes.

If there is no doubt of the variation of parameters of channel output, linear load on the fuel element and variation of the steam coefficient of reactivity α_ϕ considered above with an increase of enrichment, an increase of the extent of burnup to 40-46 GW·day/t of uranium and the calendar lifetime of the fuel elements in the core to 10-12 years when using enrichment of 3-3.6 percent accordingly requires special investigations and confirmation. The prognosis for development of fuel elements with oxide fuel burnup of 45-50 GW·day/t of uranium may be assumed realistic on the example of fuel elements for VVER reactors [7, 8]. A more difficult problem is to provide viability and integrity of the fuel elements for prolonged periods under reactor conditions.

The possibility of increasing channel output 1.5-fold opens up new prospects for RBMK-1000 reactors and ensures a significant improvement of the economic indicators of the fuel cycle due to an increase of fuel enrichment. When fuel with enrichment of 2.4-3.0 percent is used in RBMK-1000 reactors, development and experimental confirmation of the efficiency of fuel elements that permit extent of burnup up to 40 GW·day/t of uranium and that have a guaranteed lifetime of approximately 10 years in the core are required. This is one of the trends toward which extensive experimental-design and research work should be conducted to improve RBMK-1000 reactors [11].

The outlined concepts are based on the assumption that the fuel is uranium dioxide. If favorable results in development of the techniques of other fuel compositions,

for example, silicided, carbide and other fuels, they can be used; calculations indicate their promise.

11.2. Sectional-Block Design of a Reactor

The channel-type reactor as a whole and its individual assemblies are now mainly assembled at the construction site. The components of the reactor in the form of parts or small assembly units are delivered from different plants to the installation site, where they are assembled into a single structure. A large number of spot assembly-welding operations with the necessary monitoring is carried out under installation conditions in this case. It is understandable that the installation conditions are less adaptable for these types of operations than conditions in specialized shops. Therefore, conversion of a large fraction of assembly and welding operations from the installation site to plant conditions would make it possible to increase the quality of reactor manufacture and to improve control and increase its operating reliability. Moreover, this decision will provie a considerable reduction of the periods of installation work in construction of AES and consequently of the total construction period. All this yields a large saving.

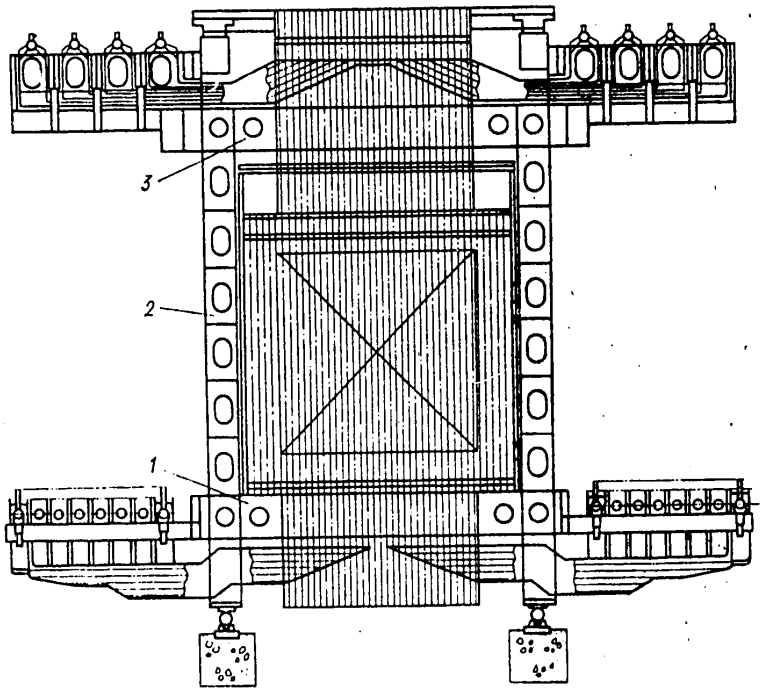

Figure 11.1. Sectional-Block Reactor: 1-3--lower, side and upper blocks, respectively

The reactor is manufactured in a specialized plant shop in the form of individual blocks with all related assemblies and parts. The blocks are joined to each other at the construction site of the AES during installation of equipment, forming a

single structure [9]. This reactor has been called a sectional-block reactor (SBR). The core of an SBR is a rectangle in layout and is divided into individual rectangular sections. The total number of reactor channels is determined by its thermal output and the required number of channels for monitoring and control of its operation. The number of channels in individual sections and consequently the overall dimensions of sections and the number of sections are determined by the capabilities of transporting the reactor blocks from the manufacturing plant to the reactor installation site.

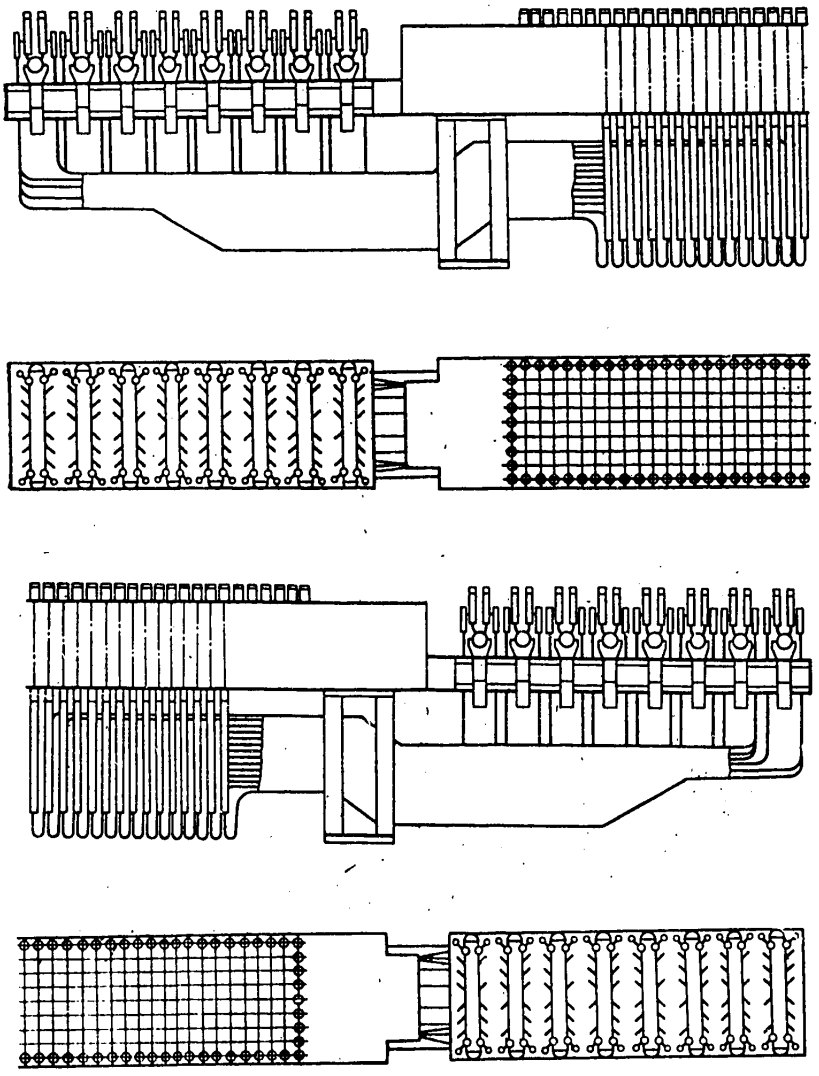

Figure 11.2. Lower Block

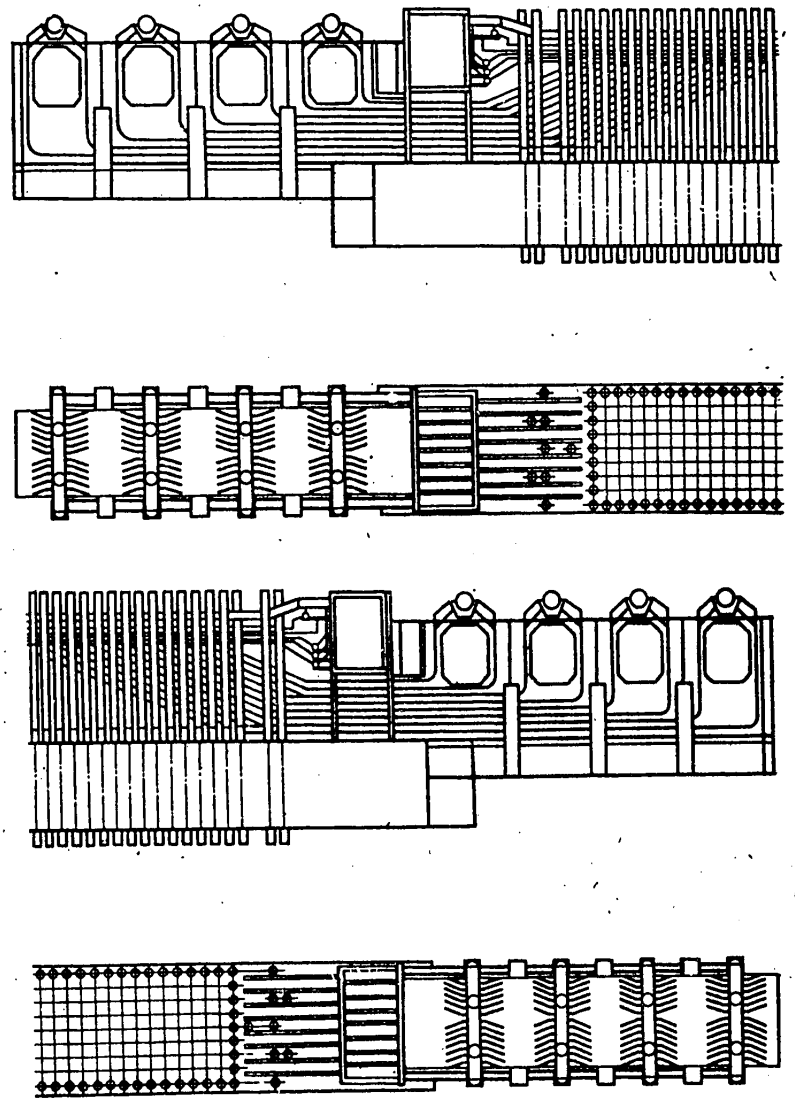

Figure 11.3. Upper Block

An overall view of the reactor is presented in Figure 11.1. Each section is assembled from lower, upper and side blocks. Making the core and consequently the reactor in the shape of a rectangle with constant width permits one to increase the reactor power to the required value by increasing its length by installing a large number of standardized sections. (There is a limit in power in a cylindrical reactor, determined by the maximum possible diameter of the upper plate). In this case development of a new design of the main blocks and rearrangement of the machine-building base are not required to convert to new, increased power. The

central sections are designed for arrangement of the fuel and special channels and the side reflector in them, while the two end sections of the reactor are used to locate the end reflector in them.

The lower and upper blocks (Figures 11.2 and 11.3) are hollow sealed boxes in the form of parallelepipeds with internal longitudinal and transverse ribs to provide stiffness to the structure, welded from sheet steel. The blocks are transported in assembled form from the manufacturing plant to the AES construction site on special rail transporters (Figure 11.4). Transport by water, air or on truck-trains is also possible.

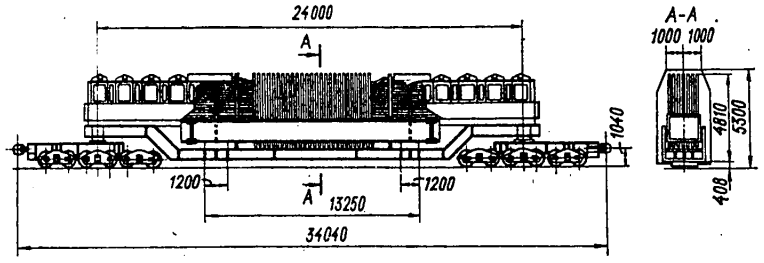

Figure 11.4. Transport of Reactor Block (third-order upper off-gauge load) on Railroad Transporter

The sectional-block design of a uranium-graphite reactor permits an increase in the quality of manufacture and at the same time an increase of operating reliability and also considerably reduces the period of AES construction as a result of conversion of a large part of operations in manufacture of the reactor from the assembly site to specialized plant conditions. All this yields a large saving.

11.3. Steam Superheating in the Core

The turbines at most modern AES operate on saturated steam at pressure of 60-70 kgf/cm^2 (approximately 6-7 MPa) in front of the check valve. These comparatively low steam parameters are explained by the poor efficiency of existing zirconium alloys used as the material of the fuel jackets at elevated temperatures and also of the fuel channel pipes in channel-type RBMK reactors. At the same time the efficiency of the AES is increased, capital expenditures for construction are reduced and the reliability and maneuverability of the turbounits are increased with steam superheating in the core. Thermal discharges into the environment are reduced and the flow rate of the cooling water through the turbine condensers is reduced with an increase of efficiency.

If steam superheating to 450°C at presure of 65 kgf/cm^2 (approximately 6.5 MPa) is provided, then the thermal output of a reactor with superheating will be 11-12 percent less compared to an energy unit with saturated steam of the same pressure and same electrical output. This is a considerable advantage that leads to an appreciable reduction of the nuclear fuel consumption. The specific steam consumption at the indicated superheating parameters are less by approximately a factor of 1.4 than saturated steam consumption of the same pressure. The turbounit is

improved, its reliability is increased and the operating conditions of the steam-inlet and steam-outlet members of turbines are improved due to use of superheated steam and a reduction of its consumption. A reduction of steam consumption also results in a decrease of the number of main circulating pumps and separators in the reactor unit.

All these advantages yield a considerable saving. However, an increase of coolant parameters with introduction of nuclear superheating requires the use of materials efficient at elevated temperatures in the core.

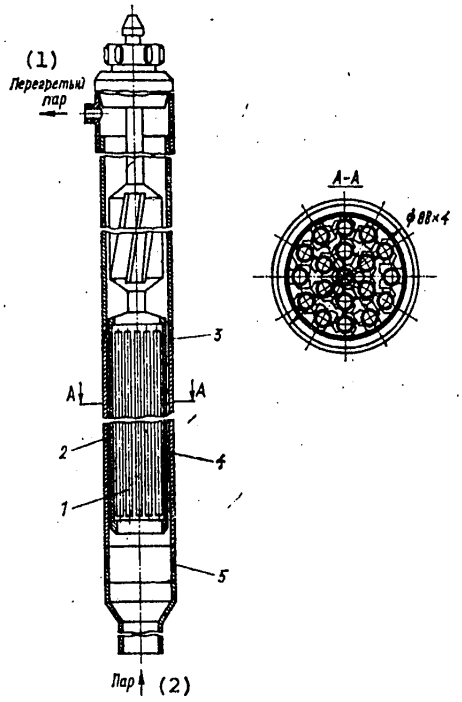

Figure 11.5. Superheating Channel: 1--fuel assembly; 2--TVS housing; 3--upper adapter; 4--zirconium pipe of channel; 5--lower adapter

Key:
1. Superheated steam
2. Steam

Water-graphite reactors of the Beloyarskaya AES in which steam is superheated in the core to 510°C at pressure of 90 kgf/cm^2 (approximately 9 MPa) have been operating for a long time in the Soviet Union [10]. Since the coolant temperature in the superheated channels is considerably higher than that in the evaporation channels, the superheated fuel element jackets should now be made of steel. A zirconium alloy should be used in the structure of superheated channels, as well as in the evaporation channels, to manufacture the channel pipe. The fuel jackets must first be made of steel since their temperature exceeds 600°C. This naturally reduces somewhat the neutron balance in the superheated part of the core.

However, the advantage is comparatively low and the total saving achieved from steam superheating remains significant when steel is used only for the fuel jackets.

The superheated channel (Figure 11.5) is similar in design to the evaporator channel and is a welded tubular structure 18-20 meters long. The channel is made of zirconium pipe with outer diameter of 88 mm and wall thickness of 4 mm within the core. The zirconium pipe is joined at the top and bottom to pipes of corrosion-resistant steel by means of steel-zirconium adapters.

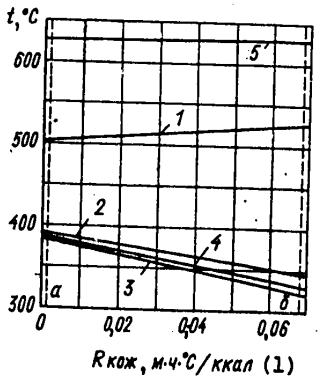

Figure 11.6. Dependence of Steam Temperature and of Superheated Channel Components on Thermal Resistance of Fuel Assembly Housing: 1--steam temperature at assembly output; 2--steam temperature at output from slit between assembly housing and channel pipe; 3--maximum temperature of inner surface of channel pipe in height; 4--maximum temperature of middle cross-section of channel pipe in height; 5--maximum temperature of outer fuel jacket in height; a--with housing in form of 72 X 1 pipe; b--with housing in form of two coaxial pipes 74 X 1 and 69 X 0.4 in diameter

Key:
1. m·hr·°C/kcal

The characteristic feature of a superheated assembly design is the presence of a housing. There is a slit 1-2 mm wide between the outer surface of the housing and the inner surface of the channel pipe. As a result part of the saturated steam entering the channel from below is passed through the slit to cool the zirconium pipe of the channel. The temperature dependence of the steam and superheated channel components on the thermal resistance of the housing for thermal output channels of 2,400 kW with saturated steam temperature of 290°C at the inlet and superheated steam temperature of 470°C at the channel output are shown in Figure 11.6. The results were obtained at steam flow rate through the slit, comprising 25 percent of the total flow rate through the channel equal to 14.5 t/hr.

11.4. The Coolant Loop and Equipment Configuration

The sectional principle of reactor core configuration is feasible and can also be used in the design of the entire reactor unit. With this principle the coolant circuit is separated into several loops identical in output and composition and equipment configuration. There are evaporation and superheated loops in a reactor with superheated steam in the core. The evaporation loop is a circuit of multiple forced circulation, while the superheated loop is an open superheated steam circuit. The equipment of each loop is arranged in individual boxes insulated from adjacent boxes by protective walls, which permits repair operations in them without complete shutdown of the reactor.

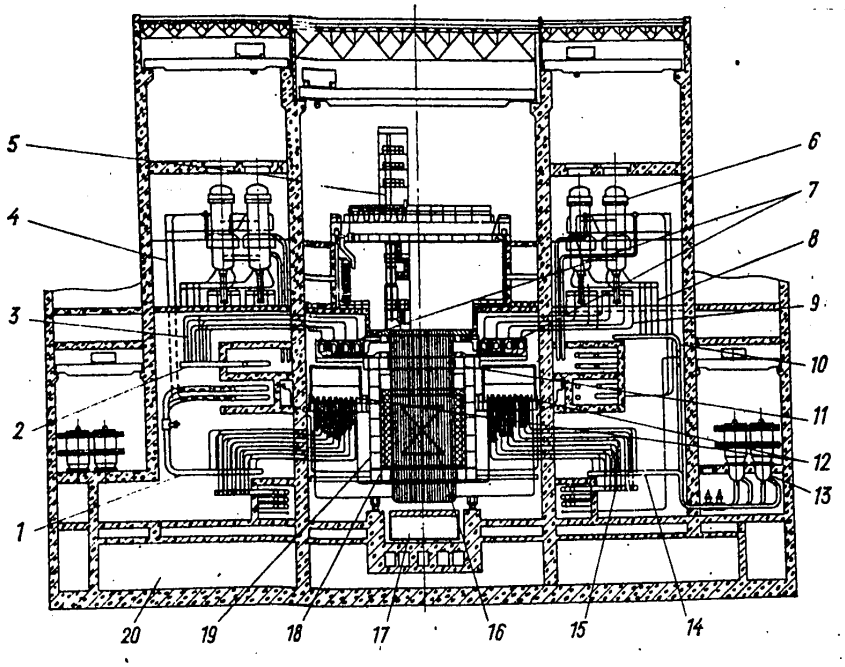

Figure 11.7. Configuration of RBMKP-2400 Reactor Unit (longitudinal section): 1--saturated steam collector; 2--superheated steam collector; 3--superheated steam pipelines; 4--saturated steam pipelines; 5--loading-unloading machine; 6--steam separator; 7--assembled group collectors; 8--separated water pipelines; 9--steam-water mixture pipelines; 10--intake collector; 11--upper block; 12--distributing group collectors; 13--main circulating pump; 14--delivery collector; 15--feed water collector; 16--graphite stacking; 17--lower repair machine; 18--lower block; 19--side blocks; 20--bubbling basin

The multiloop principle of designing a reactor unit provides great advantages. The entire unit seemingly consists of several relatively independent units. Because of this it has high flexibility. The individual loops or several loops can

operate at lower power compared to the remaining loops or can be switched off completely. This capability permits repair operations on the loop with the reactor operating at reduced power both during planned repairs and during repairs caused by disruptions in operation of a given loop. The entire reactor must be shut down in reactor units having no division into individual loops located in protective boxes to carry out any repair work. Therefore, the repairability of a sectional unit is higher than that of a nonsectional unit.

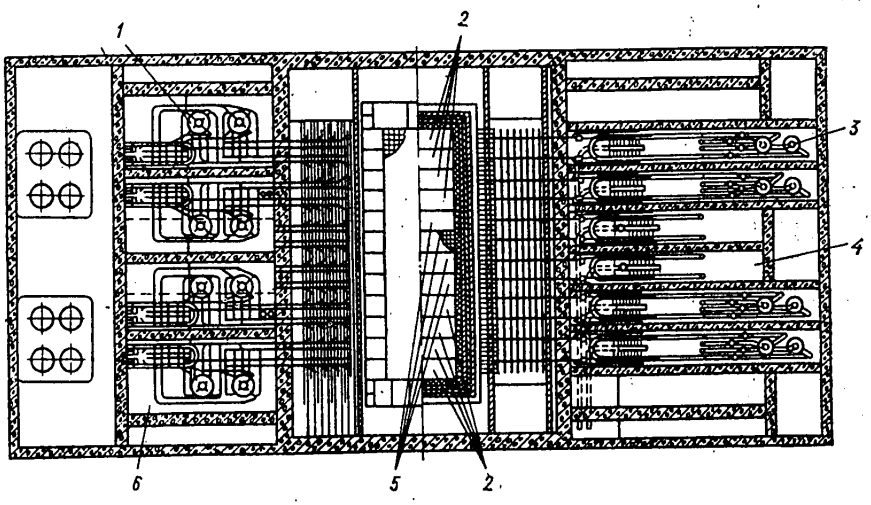

Figure 11.8. Configuration of RBMKP-2400 Reactor Unit (transverse section): 1--steam separator; 2--evaporation sections; 3--main circulating pump; 4--superheated loop box; 5--superheated sections; 6--evaporation loop box

Division of the unit into individual loops sharply increases its safety. The output of each loop is relatively low. The diameters of all the pipelines and the dimensions of equipment are also considerably less than that without separation into loops. Therefore, the consequences of an emergency will be considerably lower if the seal of the circuit is broken due to ruptures of pipelines or equipment failures. Thus, the measures required to ensure the safety of the environment and population and also of plant personnel are easier to fulfill and require lower expenditures.

The sectional-block design of a reactor and the multiloop version of the coolant circuit permit easy variation of output of the power unit by selecting the required number of standardized reactor sections and loops of the coolant circuit. Additional research work is not required and new equipment does not have to be produced in this case, which yields a large saving.

It is known that the unit output of power units will increase constantly. This trend will also be maintained in the future. The problem of increasing the unit outputs is solved comparatively simply with a sectional-block design. The safety

of the power units is not reduced in this case since it is determined by the characteristics of the individual loop rather than by those of the reactor and the circuit as a whole.

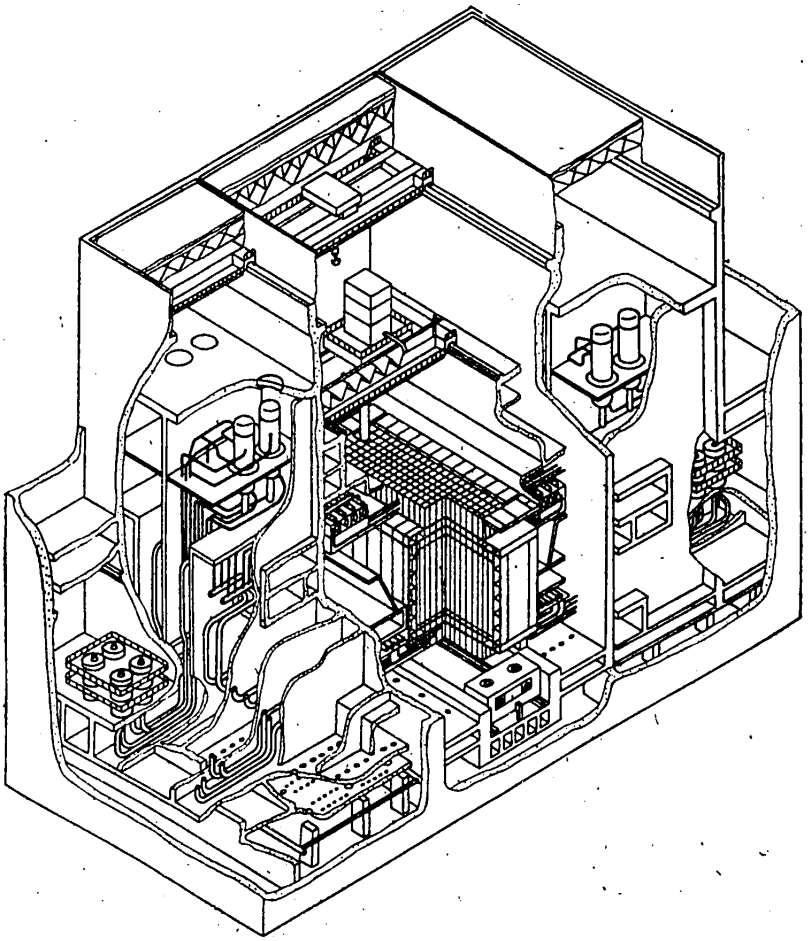

Figure 11.9. RBMKP-2400 Reactor Unit

The configuration of the RBMKP-2400 reactor unit, consisting of a sectional-block reactor with nuclear superheating of steam and multiloop coolant circuit, is presented in Figure 11.7, 11.8 and 11.9.

Channel-type power reactors with boiling-water coolant have achieved considerable development in the Soviet Union. There is considerable positive experience of their reliable operation at existing AES, upong which the first--the Leningrad AES imeni V. I. Lenin--has been operating successfully since 1973 (Figure 11.10). There are also great prospects for a further significant improvement of AES with these types of reactors. A reactor with improved engineering and economic indicators--the RMBKP-2400--has now been developed. A graph of an atomic power plant with RBMKP-2400 type reactor is shown in Figure 11.11.

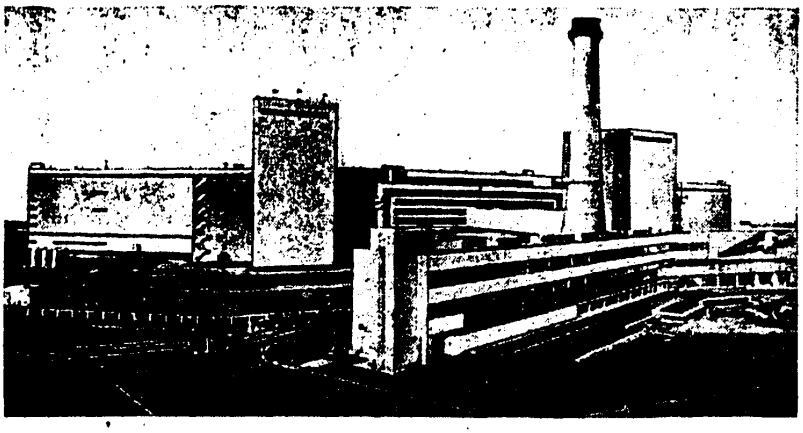

Figure 11.10. Leningradskaya AES imeni V. I. Lenin (first unit)

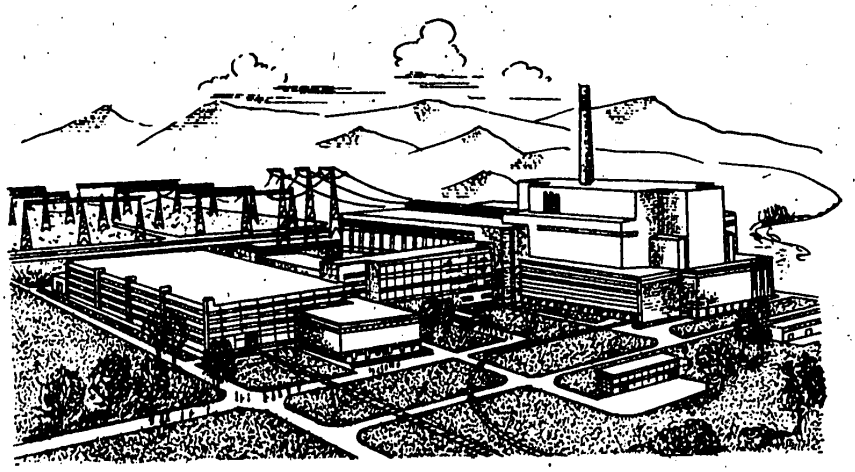

Figure 11.11. Overall View of Planned AES with RBMKP-2400 Reactor

BIBLIOGRAPHY

1. Petros'yants, A. M., "Sovremennyye problemy atomnoy nauki i tekhniki v SSSR" [Modern Problems of Atomic Science and Engineering in the USSR], Moscow, Atomizdat, 1976.

2. "Atom sluzhit sotsializmu" [The Atom Serves Socialism], Moscow, Atomizdat, 1977.

3. Aleksandrov, A. P., Yu. M. Bulkin, I. D. Dmitriyev et al, "Physical and Energy Startup of the First Unit of the Leningrad AES imeni V. I. Lenin," ATOMNAYA ENERGIYA, Vol 37, No 2, 1974.

4. Yemel'yanov, I. Ya., P. A. Gavrilov and B. N. Seliverstov, "Upravleniye i bezopasnost' yadernykh reaktorov" [Control and Safety of Nuclear Reactors], Moscow, Atomizdat, 1975.

5. Dollezhal', N. A. and I. Ya. Yemel'yanov, "The Experience of Developing Large Power Reactors in the USSR," ATOMNAYA ENERGIYA, Vol 40, No 2, 1976.

6. Aleksandrov, A. P. and N. A. Dollezhal', "Development of Channel-Type Uranium-Grahpite Reactors in the USSR," ATOMNAYA ENERGIYA, Vol 43, No 5, 1977.

7. Aden, V. G., Yu. K. Bibilashvilli, A. S. Zaymovskiy et al, "The Fuel Element of the RBMK-1000 Reactor," ATOMNAYA ENERGIYA, Vol 43, No 4, 1977.

8. Tsykanov, V. A. and Ye. F. Davydov, "Radiatsionnaya stoykost' teplovydelya-yushchikh elementov yadernykh reaktorov" [The Radiation Stability of the Fuel Elements of Nuclear Reactors], Moscow, Atomizdat, 1977.

9. Dollezhal', N. A., I. Ya. Yemel'yanov, Yu. M. Bulkin et al, "Channel-Type Sectional-Block Reactor with Nuclear Superheating of Steam with Electrical Output of Two Million kW," in "Opyt ekspluatatsii AES i puti dal'neyshego razvitiya atomnoy energetiki" [The Experience of Operating AES and Methods of Further Improvement of Atomic Power Engineering], Vol 2, Obninsk, FEI, 1974.

10. Dollezhal', N. A., V. M. Malyshev, S. V. Shirokov et al, "Some Results of Operating the Beloyarskaya AES imeni I. V. Kurchatov," ATOMNAYA ENERGIYA, Vol 36, No 6, 1974.

11. Yemel'yanov, I. Ya., A. D. Zhurnov, V. I. Pushkarev and A. P. Sirotkin, "Increasing the Efficiency of Uranium Utilization in the RBMK-1000," ATOMNAYA ENERGIYA, Vol 46, No 3, 1971.

6521
CSO: 8144/0120

- END -